RSC Advances

REVIEW

View Article Online
View Journal | View Issue

Cite this: *RSC Adv.*, 2024, **14**, 33864

Recent progress in therapeutic applications of fluorinated five-membered heterocycles and their benzo-fused systems

Ashraf A. Abbas, [a] Thoraya A. Farghaly [ab] and Kamal M. Dawood *[a]

Received 6th August 2024
Accepted 18th October 2024

DOI: 10.1039/d4ra05697c

rsc.li/rsc-advances

Heterocyclic derivatives grafted with fluorine atom(s) have attracted the attention of scientists due to the unique physicochemical properties of the C–F bond. The inclusion of fluorine atom(s) into organic compounds often increases their lipophilicity and metabolic stability, enhancing their bioavailability and affinity for target proteins. Therefore, it is not surprising to find that more than 20% of the medications on the market contain fluorine, and nearly 300 fluorine-containing drugs have been officially approved for use as medicines. In this review article, we are interested in classifying and describing the reports comprising varied therapeutic activities of the directly fluorinated five-membered heterocycles and their fused systems during the last two decades. These therapeutic activities included antiviral, anti-inflammatory, enzymatic inhibitory, antimalarial, anticoagulant, antipsychotic, antioxidant, antiprotozoal, histamine-H_3 receptor, serotonin receptor, chemokine receptor, prostaglandin-D2 receptor, and PBR

[a]*Department of Chemistry, Faculty of Science, Cairo University, Giza, 12613, Egypt. E-mail: kmdawood@sci.cu.edu.eg; Fax: (+202) 35727556*

[b]*Department of Chemistry, Faculty of Science, Umm Al-Qura University, Makkah, Saudi Arabia*

Ashraf A. Abbas

Professor Ashraf A. Abbas was born in Egypt in September 1968 and he is presently Professor of Organic Chemistry, Department of Chemistry, Faculty of Science, Cairo University, Giza, Egypt since 2009. He graduated from Cairo University in 1990. He received his M.Sc. and PhD degrees in 1994 and 1997, respectively, from Cairo University. He spent six months in the Fakultat fur Chemie, universitat of Konstanz (Germany) on a DAAD fellowship (1996) to finish his PhD thesis and one year at Tokyo Institute of technology (TIT, Japan) as UNESCO fellow (postdoctoral fellowship) from Oct. 2001 to Sept. 2002. He received several research prizes in chemistry; (1) he was awarded the prize of Prof. Dr Mohamed Abdel Salam in chemistry (2001) for young scientists provided by Academy of Scientific Research and Technology (Egypt). (2) He was awarded the Cairo university encouragement prize in Chemistry in 2004. (3) He was awarded the Third Word Academy of Science (TWAS) prize in chemistry for young scientists in 2004 provided by ICTP-Strada, Triesta-Italy, (4) he was awarded the State Award in Chemistry, Egypt, 2005. He has published many papers in the field of synthesis and applications of macrocycles and bis-heterocycle chemistry.

Thoraya A. Farghaly

Thoraya Abd Elreheem Farghaly was born in Cairo, Egypt in 1974. She received her BSc (1996); M.Sc. (2002) and PhD (2005) degrees from University of Cairo. She is Professor of organic chemistry in the Chemistry Department, Faculty of Science, University of Cairo. She works at Umm Al-Qura university from 2014 till now. She joined the scientific school of Prof. A. S. Shawali in 1997 and she has published more than 220 papers in the area of the chemistry of hydrazonoyl halides, heterocyclic chemistry and bioactive heterocyclic compounds.

inhibition activities. In many cases, the activities of fluorinated azoles were almost equal to or exceeded the potency of reference drugs.

1. Introduction

Approximately 85% of bioactive chemicals are expected to consist of heterocyclic moieties, therefore researchers have been motivated to include heterocyclic structures in synthetic medications.[1] Conversely, adding fluorine atom(s) to medications throughout the latter part of the 20th century offered an additional essential method for designing pharmaceuticals.[2–4] Fluorinated drugs have experienced significant growth since the introduction of the first fluorocorticosteroid and fludrocortisone in 1954.[5] Currently, 20% of the drugs on the market are fluorinated, and approximately 30% of fluorinated drugs are considered blockbuster pharmaceuticals.[6] Almost 300 pharmaceuticals containing fluorine have been officially approved for use as medications.[7] The incorporation of the small size highly electronegative fluorine atom(s) into organic molecules was attributed to the unique physicochemical characteristics of the C–F bond,[8] comprising the chemical and physical properties of the entire molecules such as polarity, high bond strength, and little steric hindrance, acidity, basicity, solubility, and hydrogen bonding interactions.[9–13] In addition, the inclusion of fluorine atom(s) in organic compounds often increases their lipophilicity and metabolic stability, enhancing their bioavailability and binding affinity with target proteins.[14–17]

It was reported that fluorine-substituted thrombin inhibitors have C–F…C=O interactions greatly affected the protein–ligand interactions and significantly enhanced the binding affinities. Fluorinated thrombin inhibitors showed binding affinity five times stronger than the nonfluorinated analogues. X-ray structure analysis showed that the F atom is in remarkably close contact with the H–C_α–C=O moiety of Asn98 of thrombin.[18–20] In addition, the close amide-NH···F interaction between fluorine and amide residues in proteins was very predominant and established by X-ray crystallography.[20–22]

The presence of fluorine atom(s) in heterocyclic scaffolds made them more biologically potent compounds where several commercial drugs approved by the FDA were found to possess directly fluorinated heterocyclic ingredients as described in Fig. 1. For example, **Favipiravir** (or Avigan) was approved in 2014 as an antiviral drug used to treat influenza in Japan including A(H1N1), A(H5N1), and the recently emerged A(H7N9) avian virus.[23] In addition, some fluorinated nucleosides were also approved as antiviral drugs, such as **Sofosbuvir** (Sovaldi) for the treatment of hepatitis C, and **Claudine** for the treatment of hepatitis B virus.[24] Furthermore, **Fludarabine** was approved as an immunosuppressant drug.[25] Some fluorine-containing heterocycles were also approved as anti-HIV drugs, such as **Emtricitabine** which was approved by FDA in 2003 as a NRTI (Nucleoside reverse transcriptase inhibitor),[26,27] and **Lenacapavir** (Sunlenca, GS-6207), was approved in 2022, as potent HIV CA (human immunodeficiency virus capsid protein) inhibitor with picomolar-range potency.[28] **Koselugo** (Selumetinib): for treatment of neurofibromatosis type 1, a genetic disorder that causes tumors to grow on nerves.[29] **Rykindo** (Risperidone) was approved by the FDA in 2023 as an antipsychotic drug for the treatment of schizophrenia.[30]

Furthermore, the therapeutic potency of some non-fluorinated heterocycles of potent therapeutic effects was compared with their fluorinated analogues, to confirm the marked influence of replacing a hydrogen atom with a fluorine atom (Fig. 2).[31–33] For example, the anti-viral drugs **Emtricitabine** (**II**) and its 5-fluoro analogue of **Lamivudine** (for treatment of HIV) (**I**) are examples of this effect, where **II** is a more potent HIV-1 inhibitor four-to ten-fold times than **I**.[31,32] The 4-fluorinated indole **IV** is about 50-fold HIV-1 inhibitor than the non-fluorinated indole **III**.[33,34] Similarly, the γ-secretase **VI** had extraordinary potency compared with its analogue **V**.[35]

Thus, medicinal chemists and drug developers are highly fascinated with fluorine-based small molecules in drug discovery and are focusing their efforts on overcoming the challenges associated with the insertion of fluorine atom(s) into small organic molecules. Advancements in technology have made it easier to incorporate fluorine into new small molecules.

Kamal M. Dawood

Kamal M. Dawood graduated from Cairo University, Egypt in 1987, and received his PhD in 1995 from Cairo University. In 1997 he was awarded the UNESCO Fellowship at TIT for one year and in 1999 he was awarded the JSPS Fellowship for two years and in both fellowships he worked with Professor T. Fuchigami at the Tokyo Institute of Technology (TIT) in the field of "Anodic Selective Fluorination of Heterocycles'. Further, he was awarded the Alexander von Humboldt (AvH) Fellowship at Hanover University in 2004–2005 with Prof. A. Kirschning (in the area of polymer-supported palladium-catalyzed cross-coupling reactions) and as AvH three short visits in 2007, 2008 and 2012 with Prof. P. Metz at TU-Dresden (in the field of Metathesis Reactions in Domino Processes). Since May 2007 – to date, he has been appointed as a full Professor of Organic Chemistry, Faculty of Science, Cairo University. He worked as Professor of Organic Chemistry at Chemistry Department, Kuwait University from Sept. 2013 till Aug. 2017. He received many National Awards: Cairo University Award in Chemistry (2002), the State Award in Chemistry (2007), Cairo University Award for Academic Excellence (2012) and Cairo University Merit Award (2017). He has published more than 160 scientific papers, reviews, and book chapters in distinguished international journals. There are about 3900 citations of his work (Scopus h-index 33).

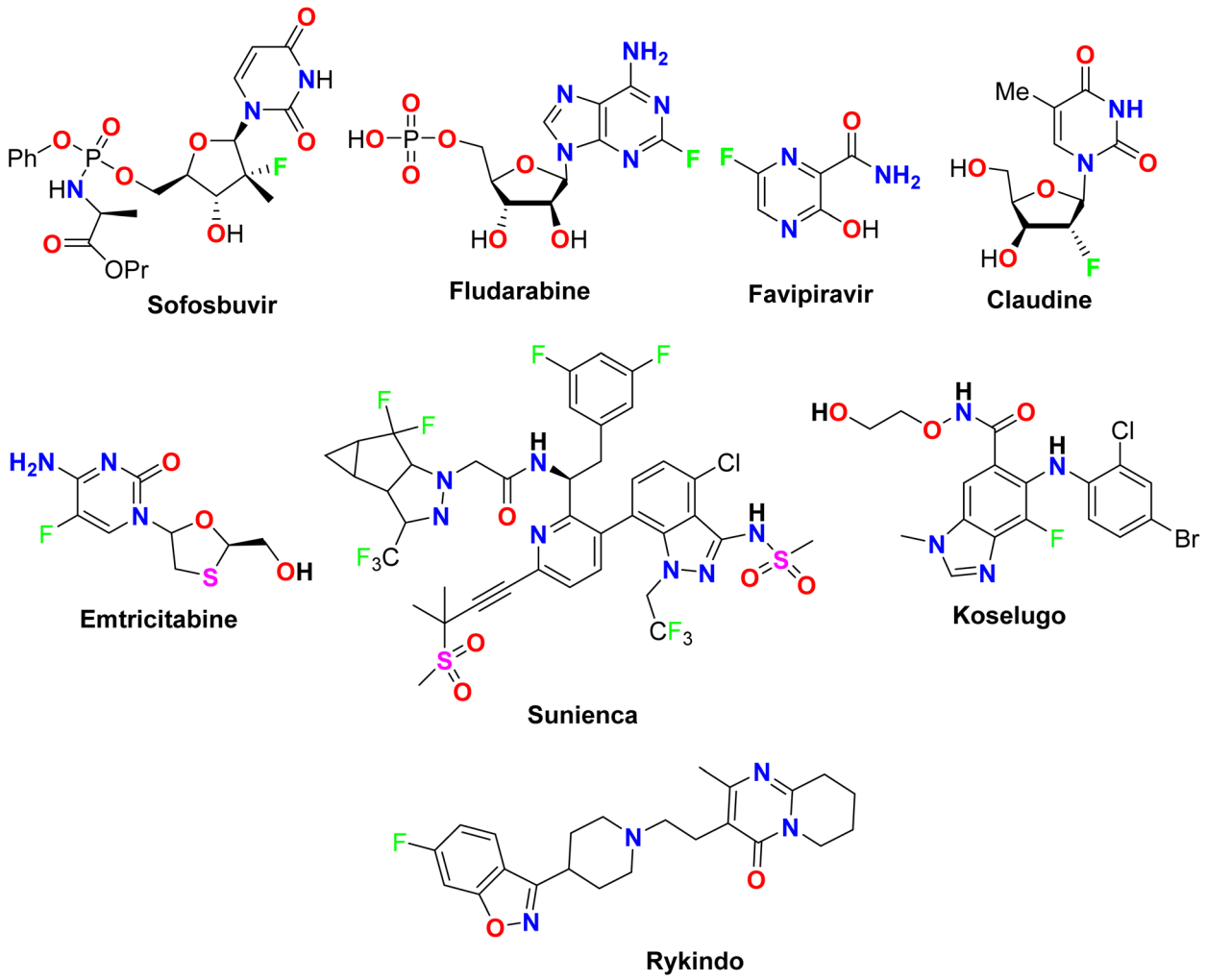

Fig. 1 The structure of some FDA-approved fluorinated medications.

Fluorine atom(s) have been inserted into heterocyclic rings *via* either chemical or electrochemical synthetic routes. Chemical fluorination of heterocyclic systems was reported employing either nucleophilic or electrophilic fluorinating agents such as F_2, SF_4, XeF_2, Et_2NSF_3 (DAST), or *N*-fluoropyridinium triflates.[36–38] On the other hand, the electrochemical fluorination protocol involved the use of the ionic liquids; alkyl ammonium fluoride salts ($Et_3N \cdot nHF$, or $Et_4NF \cdot nHF$ ($n = 3, 4, 5$)) as stable fluoride ion sources.[39–44] The late-stage fluorination of heterocycles was reported as a straightforward promising tool

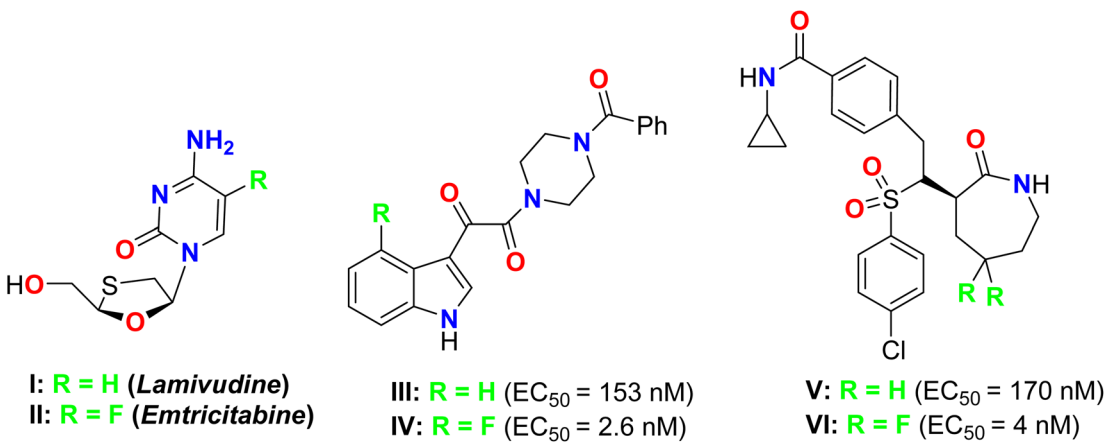

Fig. 2 Some medicinally active fluorinated heterocycles and their non-fluorinated analogues.

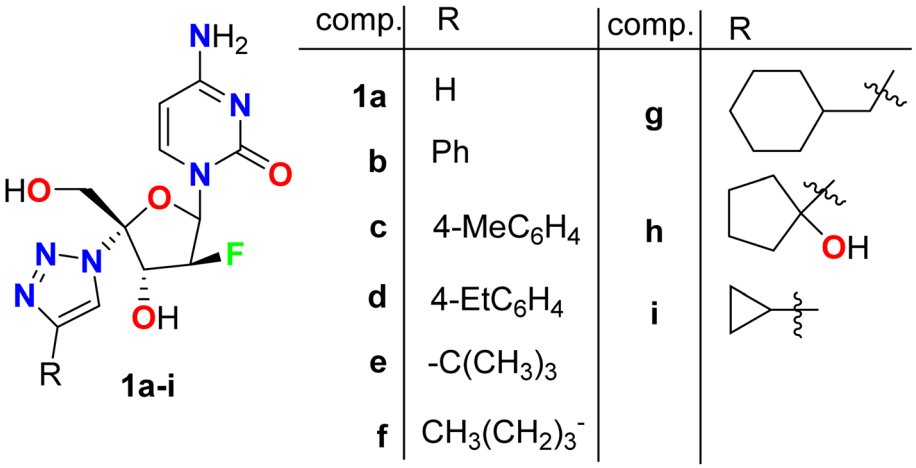

Fig. 3 Structure of triazole-based fluoro-arabinofuranoside derivative **1a–i**.

involving metal-catalysed procedures to enhance the C–F bond formation of small molecules with potential industrial applications.[45]

The aforementioned interesting historical background compiled with our ongoing insightful evaluations of bioactive heterocycles,[46–51] inspired us to focus our attention on the recent reports comprising varied therapeutic activities of the directly fluorinated five-membered heterocycles and their fused systems during the last two decades from 2004 till the end of 2024. The heterocycles incorporating only fluoroaryl or fluoroalkyl groups are not considered in this review article. The current review article is expected to serve as an interesting pool for researchers interested in medicinal chemistry and pharmaceutics for the possibility of synthesis of drug-like small fluorinated molecules.

2. Antiviral activity of fluorinated heterocycles

2.1. Antiviral activity fluorinated furans

A series of triazole-based fluoro-arabinofuranoside molecular hybrids **1a–i** were synthesized screened for their *anti*-HIV-1 activity (Fig. 3). The inhibitory activity (EC_{50}) was determined by an *anti*-HIV (wild-type) replication assay. Most of these fluorinated derivatives demonstrated potent *anti*-HIV-1 activity. Interestingly, compounds **1a**, **1b** and **1e** showed high potent antiviral activity with EC_{50} values of 0.09 μM, 0.083 μM, and 0.08 μM, respectively, with almost equipotent or better activity than Zidovudine reference *anti*-HIV drug (EC_{50} = 0.084 μM). SAR study disclosed that the unsubstituted triazole or the presence of phenyl group at the triazole-C-4 position maintained the potent antiviral activity (compounds **1a** and **1b**), however presence of electron donating substituents at the phenyl ring (**1c** and **1d**) led to a dramatic decrease of *anti*-HIV potency. Among the other derivatives that R was alkyl group, the presence of the bulky *t*-butyl group (compound **1e**) showed the highest antiviral activity, while alkyl substituents resulted in reduced antiviral activity. In addition, the *anti*-HBV activity of compounds **1b**, **1c**, and **1i** was also investigated against the production of HBsAg (HB surface antigen) and HBeAg (HB e antigen) by ELISA assay, and the EC_{50} was determined. Compound **1c** showed high activity against HBsAg production with EC_{50} = 0.01 μM but compound **1b** possessed the most potent activity in inhibition of HBeAg production with EC_{50} = 0.25 μM. Therefore, these fluorinated hybrids were considered to have great potential as new *anti*-HIV drugs.[52]

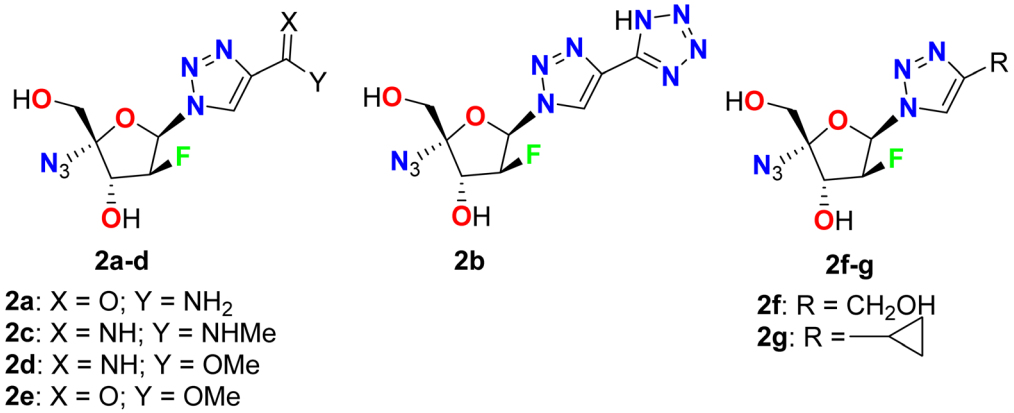

Fig. 4 Structure of 1,2,3-triazole-based fluoro-arabinofuranoside derivatives **2a–g**.

Liu *et al.* described the synthesis and *in vitro anti*-HBV activity of a series of 1,2,3-triazole-based fluoro-arabinofuranoside derivatives **2a–g** in the cellular model (Fig. 4). All the tested compounds showed inhibitory activities comparable to the positive control, lamivudine at 20 μM. The most promising *anti*-HBV activity and low cytotoxicity in the cell model were reported for the amide-substituted candidate **2a**, where this compound retained significant activity against lamivudine-resistant HBV mutants with 45.3% and 21.9% inhibition of HBsAg and HBeAg, compared with Lamivudine (3TC-treated) that showed 47.7% and 22.1% inhibitions, respectively, at 20 μM concentration, on 9 days. On the other hand, both the liver and serum DHBV DNA levels (53.3% and 67.4%, respectively) were decreased markedly upon treatment with **2a**, in duck HBV (DHBV)-infected duck models. SAR study revealed that the high activity of **2a** has relied on the presence of the amide group at the triazole ring that can interact with the viral DNA polymerase through hydrogen bonding between the amide group and dGMP, as well as the π–π stacking interactions between the 1,2,3-triazole planar heterocyclic and the adjacent DNA base. Besides, the azido group participated in a hydrophobic interaction with the side chains of Val84, Phe88, Leu180, and Met204. These developed studies provided strong support for the application of compound **2a** as a potential alternative therapy for the treatment of HBV infection.[53]

Smith *et al.* described a synthetic route to some fluorinated furano-nucleoside hybrids **3–5** and screened their potency as inhibitors of the RNA polymerase encoded by hepatitis C virus (HCV) in the subgenomic replicon assay system using the 2209-23 cell line (Fig. 5). Among the synthesized compounds in this series, the derivatives **4b** and **5** proved their highest antiviral potency in the HCV replicon system with EC_{50} values of 24 nM and 66 nM, respectively. The derivative **4b** exhibited more than a 50-fold enhancement in the antiviral potency when compared to the parent non-fluorinated nucleoside analogue **3**.[54]

Synthesis of the regioisomeric N1- and N3-nucleoside fluorinated furanosyl nucleosides **6a–d** and **7a–d** was reported by Kharitonova *et al.* and their inhibitory activity against the herpes simplex virus type 1 (HSV-1) *in vitro* was performed by the method of cytopathic effect (CPE) inhibition assay (Fig. 6). The cytotoxicity was also studied using the Vero-E6 (African green monkey kidney) cells at the maximal concentration of

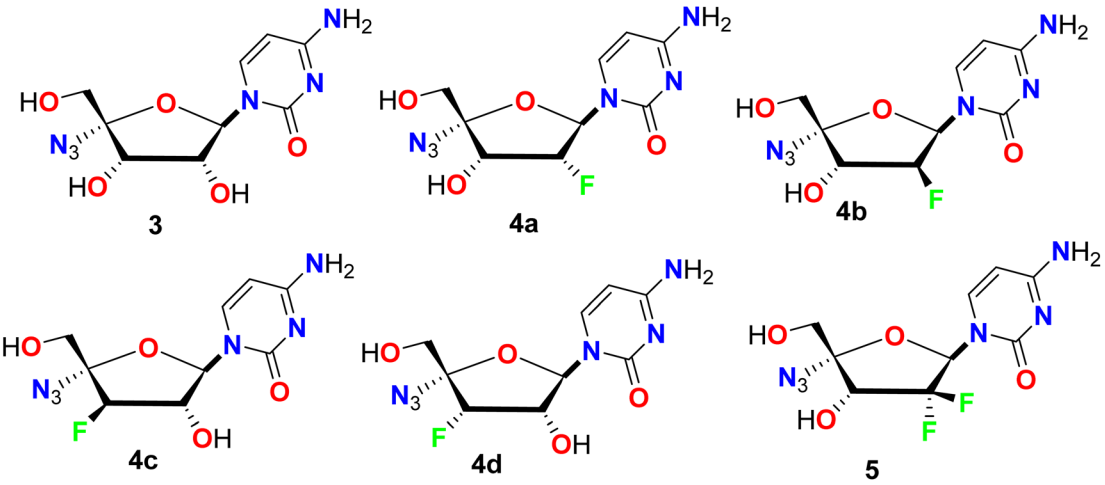

Fig. 5 Structure of fluorinated furano-nucleoside hybrids **3–5**.

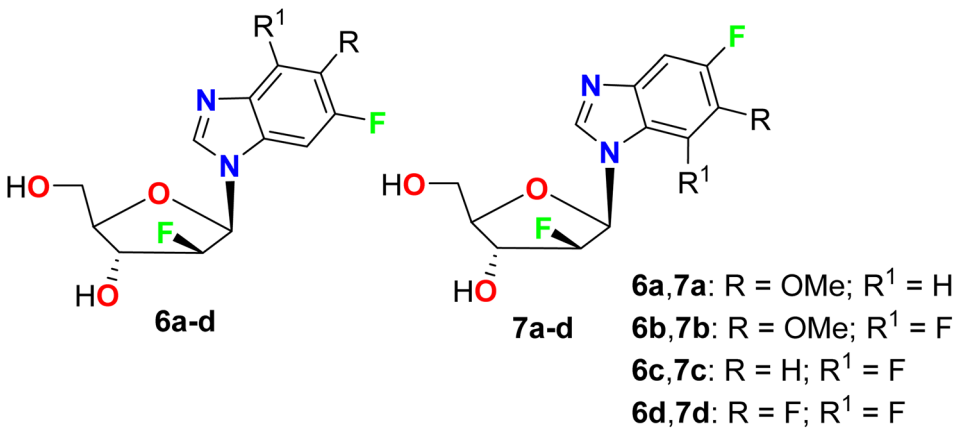

Fig. 6 Structure of fluorinated furanosyl nucleosides **6a–d** and **7a–d**.

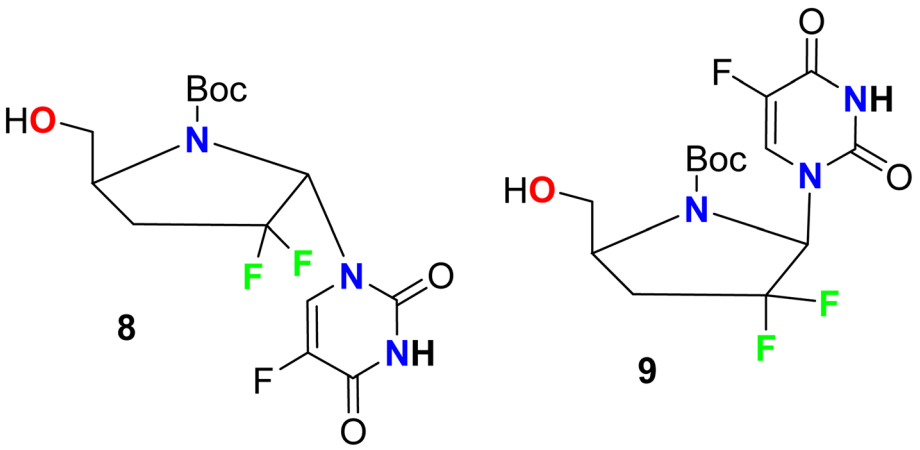

Fig. 7 Structure of fluorinated pyrrole-based hybrids **8** and **9**.

1000 μg mL^{-1} for 72 hours. Compounds **6–7** demonstrated inhibition of the development of virus-induced CPE in a wide concentration range 6–8 times lower than CD_{50}, where compounds mixtures **6a** and **6b** had CD_{50} values of 245 and 487.5 μg mL^{-1}, respectively.[55]

2.2. Antiviral activity fluorinated pyrroles

Ferrero *et al.* reported the synthesis of two fluorinated pyrrole-based hybrids **8** and **9** and their *anti*-HIV-1 activity was investigated (Fig. 7). The bioassay was carried out using AZT (zidovudine) as a reference standard with human peripheral blood mononuclear cell (PBM) protocol. Most of the tested compounds showed moderate activities against $HIV\text{-}1_{LAI}$ compared with AZT and the fluorinated derivatives **8** and **9** showed the best activity in the series with EC_{50} values 36.9 μM and 44.5 μM, respectively, compared with AZT (EC_{50} = 0.0017 μM).[56]

2.3. Antiviral activity fluorinated isoxazoles

A wide range of the fluorinated spiro-isoxazoline derivatives **10a–o** and **11a–k** were synthesized and evaluated for their *in vitro* antiviral activity against human cytomegalovirus (HCMV) (Fig. 8). The viral inhibitory bioassay was carried out, in the presence of GFP (green fluorescent protein, using quantitative

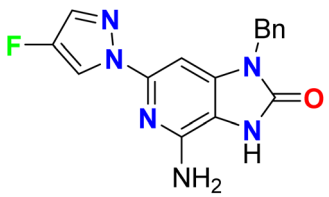

12

Fig. 9 Structure of 4-fluoropyrazole hybrid **12**.

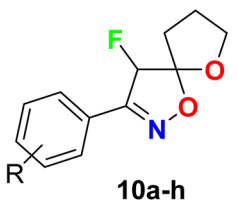

10a-h

R = **a**, H; **b**, 4-Me; **c**, 4-F; **d**, 4-Cl; **e**, 4-Br; **f**, 2,6-$(Cl)_2$; **g**,. 4-CF_3; **h**, 4-NO_2

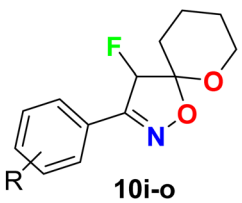

10i-o

R = **i**, H; **j**, 4-F; **k**, 4-Cl; **l**, 4-Br; **m**, 2,6-$(Cl)_2$; **n**,. 4-CF_3; **o**, 4-NO_2

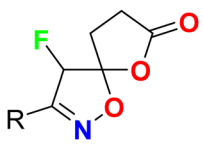

11a-i

R = **a**, Ph; **b**, 4-MeC_6H_4; **c**, 4-FC_6H_4; **d**, 4-ClC_6H_4 **e**, 4-BrC_6H_4; **f**-2,6-$Cl_2C_6H_3$; **g**, 4-$CF_3C_6H_4$; **h**, Me; **i**, $CH_2CH_2CH_3$

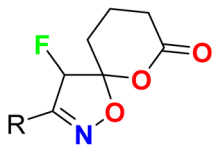

11j,k

R = **j**, 2,6-$Cl_2C_6H_3$; **k**, COOEt

Fig. 8 Structure of fluorinated spiro-isoxazoline derivatives **10a–o** and **11a–k**.

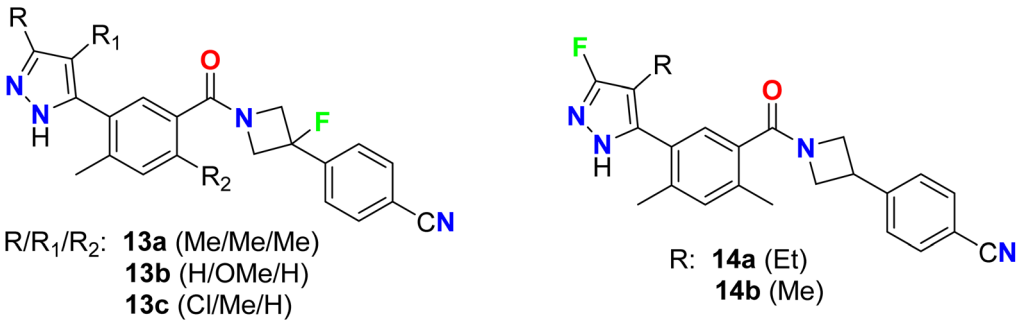

Fig. 10 Structure of 4-fluorinated azetidine-based pyrazole molecular hybrids **13** and **14**.

fluorescence microscopy. Four derivatives **10d**, **10i**, **10n**, and **10o** showed significant *anti*-HCMV properties with IC_{50} values of 9.47 μM, 11.2 mM, 10.47 μM, and 2.54 mM, respectively. Thus, compounds **10d** and **10n** presented significant activity against HCMV with IC_{50} 9.47 μM and 10.47 μM, compared with ganciclovir (reference drug for treatment of HCMV) with IC_{50} = 4.96 μM. The cytotoxicity of the most active compounds **10d** and **10n** on HFF (human foreskin fibroblasts) cells, at the double value of the IC_{50} concentrations, was measured, where the tested compounds exhibited almost 100% cell viability without any significant cytotoxicity.[57]

2.4. Antiviral activity of fluorinated pyrazoles

The 4-fluoropyrazole hybrid **12** was reported as Toll-Like Receptor 7 (TLR-7) modulator for treatment of viral infections (Fig. 9). By PBL/HCV replicon bioassay, compound **12** had selectivity modulated the TLR7 receptor activity over other known Toll-like Receptors with EC_{50} 0.47 μM.[58]

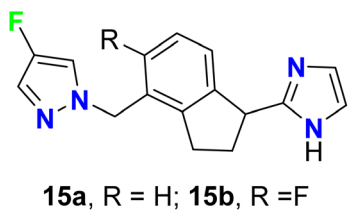

Fig. 11 Structure of imidazole-based 4-fluoropyrazole derivatives **15a–b**.

Some fluorinated azetidine-based pyrazole molecular hybrids **13a–c**, and **14a–b** were designed by Oslob *et al.* and were evaluated for their antiviral activities (Fig. 10). The antiviral activity was assessed using the HCV lb replicon system at ten three-fold dilutions. The fluorinated azetidine derivatives **13a–c** displayed good inhibitory activity against the HCV genotype-lb (HCV-GT-lb) with EC_{50} values of 0.45, 0.74, and 0.23 μM, respectively. However, the fluorinated pyrazole analogue **14a** showed promising inhibitory action with EC_{50} 0.083 μM, 5-fold to 9-fold activity better than the fluorinated azetidine analogues.[59]

Roberts *et al.* described two imidazole-based 4-fluoropyrazole derivatives **15a–b** as potent, partial agonists of the α_{1A} adrenergic receptor (Fig. 11). Compounds **15a–b** showed good selectivity over the α_{1B}, α_{1D}, and α_2 sub-types. Both compounds **15a–b** proved to be selective for α_{1A} receptor over the other α sub-types, where they had EC_{50} values 9 nM and 17 nM, and their intrinsic efficacies (α_{1A} E_{max}) were 83% and 60%, respectively. Furthermore, compound **15b** had the best pharmacological properties with a binding activity α_{1A} K_i = 5 nM.[60]

2.5. Antiviral activity of fluorinated indazoles

Two 5-fluoroindazole derivatives **17a–b** (Fig. 12) were synthesized and examined for their *anti*-HIV activity. The lack of resilience to mutations in the reverse transcriptase (RT) enzyme, for the treatment of HIV, was a main obstacle related to NNRTIs (non-nucleoside reverse transcriptase inhibitors). The two derivatives were assigned as NNRT inhibitors and showed

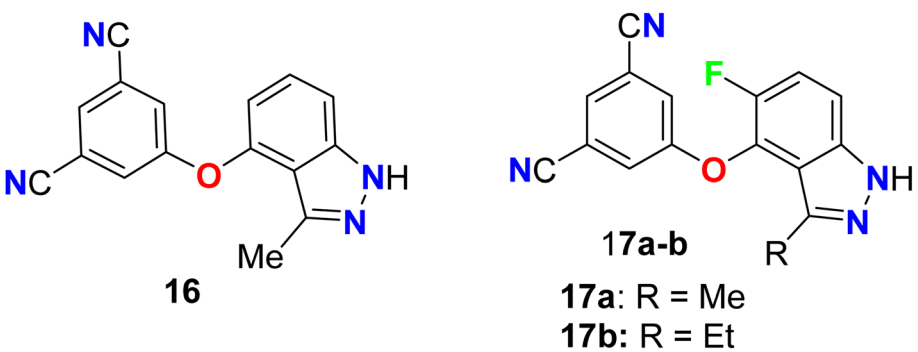

Fig. 12 Structure of 5-fluoroindazole derivatives **17a–b**.

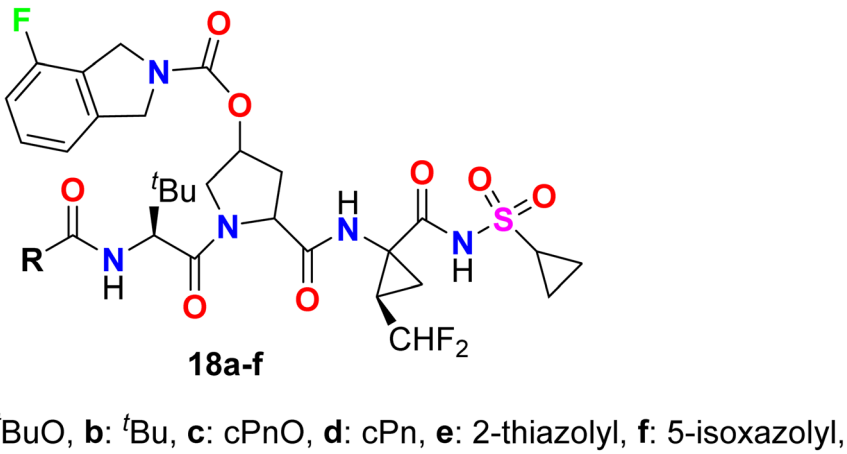

Fig. 13 Structure of 4-fluoroisoindoline derivatives **18a–f**.

excellent metabolic stability and mutant resilience compared with the known inhibitors efavirenz and capravirine. Both compounds showed the presence of fluorine atom in compound **17a–b** greatly improved their potency, against the wild-type reverse transcriptase enzyme, nearly 7-fold and 13-fold (IC values of 50 nM and 25 nM) better than the non-fluorinated derivative **16** (IC_{50} = 332 nM), respectively. Thus, SAR proved the importance of the presence of fluorine atom at position-5 as well the presence of ethyl group at position-3 instead of methyl group. Compounds **17a** and **17b** demonstrated also promising potency against the clinically relevant K103N and Y181C RT mutations, particularly compound **17b** had the best potency against Y181C with an IC_{50} value of 32 nM much better than both efavirenz and capravirine, reference drugs of HIV, with IC_{50} values 40 nM and 61 nM, respectively.[61]

2.6. Antiviral activity of fluorinated isoindolines

The 4-fluoroisoindoline derivatives **18a–f** were invented and synthesized by Gai *et al.* and studied their inhibitory activity against hepatitis C virus (HCV) NS3-NS4A protease (Fig. 13). The activity of reported hybrids as inhibitors of HCV replication (cell-based assay) in replicon-containing Huh-7 cell lines was studied. Most of the invented compounds showed promising activities in both enzyme inhibition and cell-based replicon assays for HCV. The antiviral potency of the invented compounds on HCV replicon RNA levels in Huh-7 cells was calculated by comparing the ratio of HCV/GAPDH in the cells exposed to the compound *versus* cells exposed to the DMSO vehicle (negative control).[62]

2.7. Antiviral activity of fluorinated indoles

Piscitelli *et al.* reported the antiviral activity of some fluorinated indole-carboxamide derivatives **19a–i** against the HIV-1 WT in human T-lymphocyte (CEM) (Fig. 14). All the examined compounds demonstrated high potent inhibition of the HIV-1 replication in human T-lymphocyte (CEM) cells at low concentrations and were weakly cytostatic. The antiviral activity of the fluorinated derivatives **19a–e** was highly potent with EC_{50} values ranging between 2.0–4.6 nM against the HIV-1 WT. The other fluoro derivatives **19f–i** showed also good antiviral activity with

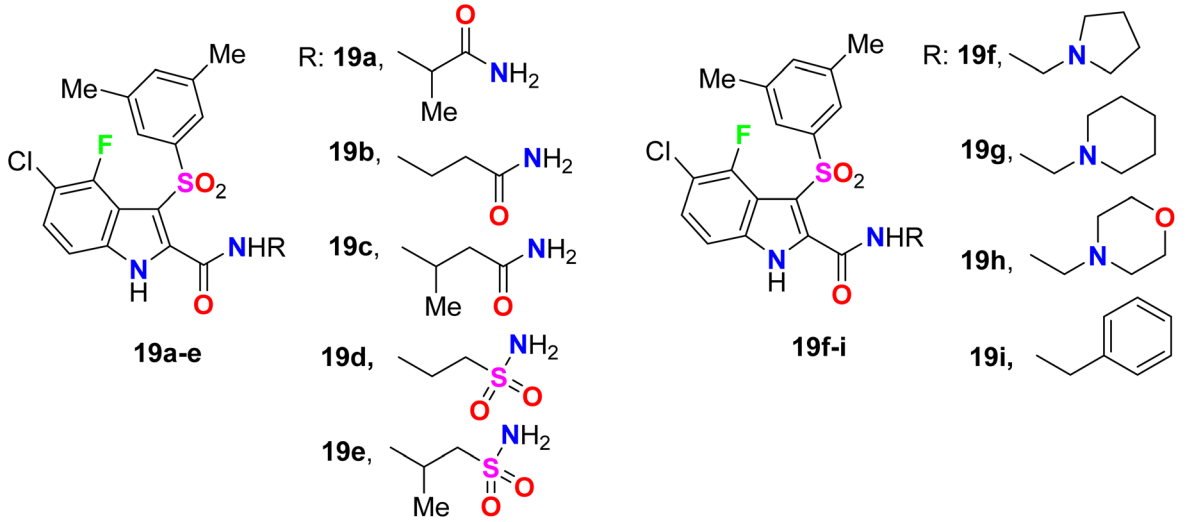

Fig. 14 Structure of fluorinated indole-carboxamide derivatives **19a–i**.

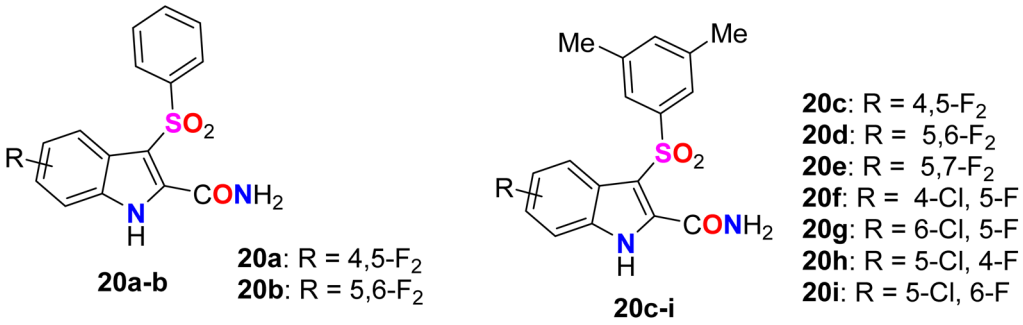

Fig. 15 Structure of benzenesulfonyl fluorinated-indolecarboxamide derivatives 20a–i.

EC_{50} values ranged between 2.5–5.8 nM against the HIV-1 WT when compared to efavirenz standard (ED_{50} = 1.5 nM).[63,64]

A series of benzenesulfonyl fluorinated-indolecarboxamide derivatives **20a–i** were synthesized and their inhibitory activity against wild-type HIV-1 non-nucleoside reverse transcriptase (NNRT) was evaluated in MT-4 and C8166 cells using MTT assay (Fig. 15). Compounds **20a–i** were found to possess potent activity against HIV-1 WT without any cytotoxicity up to 20

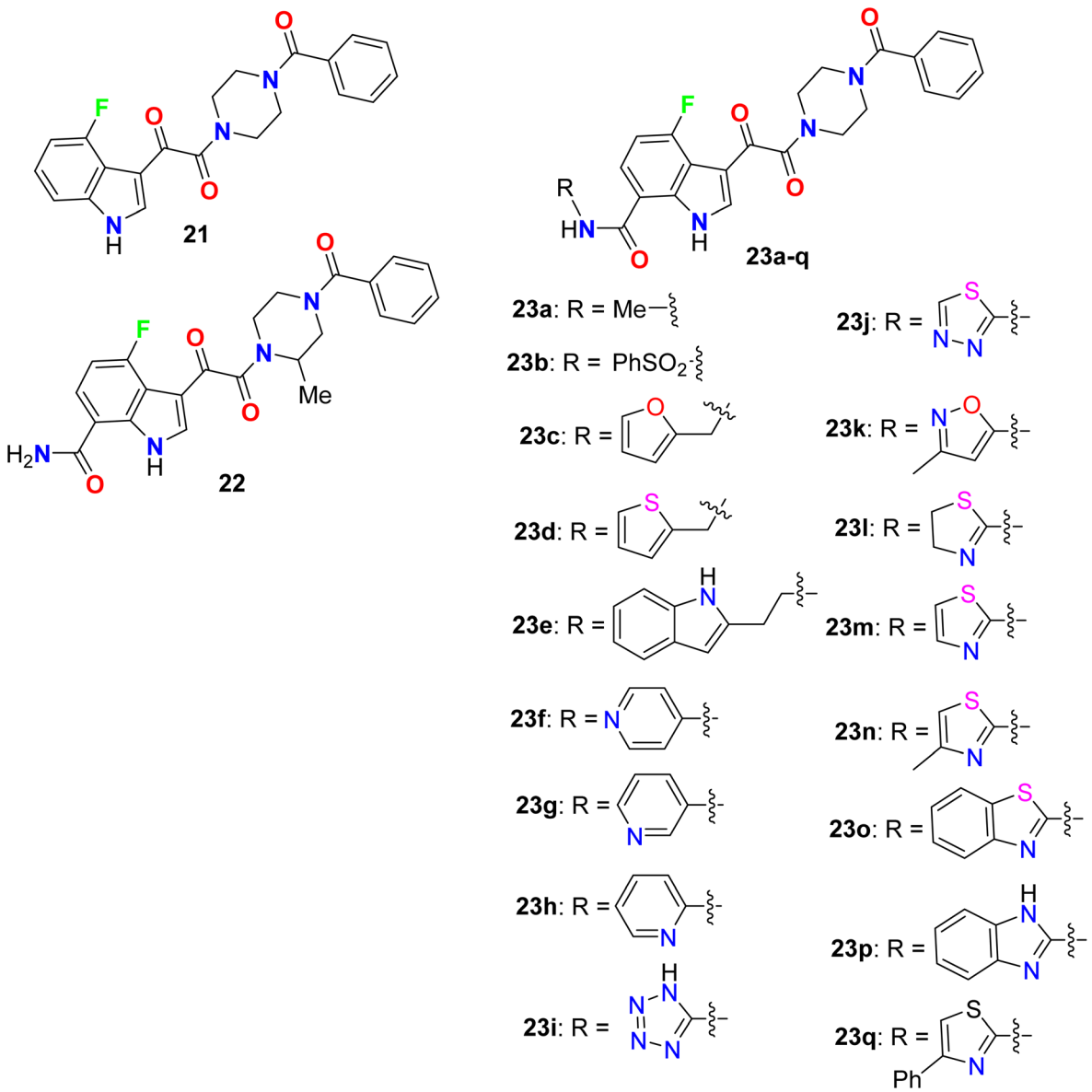

Fig. 16 Structure of 7-substituted carboxamides-4-fluoro indole derivatives 21–23.

000 nM. The 4-fluoroindole derivative **20h** was the most potent in MT-4 and C8166 cells with ED_{50} values of 0.5 nM and 0.8 nM, respectively. Compound **20i** proved to have the most potent antiviral activity against the HIV-1 WT, Y181C, and K103N-Y181C resistant strains in MT-4 Cells, with ED_{50} values of 0.5 nM, 4 nM, and 300 nM, compared with efavirenz reference with ED_{50} values 3 nM, 10 nM, and 200 nM, respectively. Therefore, compound **20i** was reported as a promising candidate for further development of NNRT inhibitors.[65]

Yeung *et al.* described the synthesis of a series of 7-substituted carboxamides-4-fluoro indole and screened out their inhibition of HIV-1 activity (Fig. 16). All compounds provided higher inhibition potency than the lead compound **21** *in vitro* for human liver microsomal (HLM) stability in the primary cell-based assay with EC_{50} in nanomolar scale, and the fluorinated derivatives **23a** (of alkylamide series) and **23b** (of sulfonamide series), presented promising inhibitions with EC_{50} values of 0.29 nM and 0.52 nM. Among the fluorinated indoles having a primary amide group at C-7, compound **22** showed the highest inhibition activity with $EC_{50} = 0.14$ nM. The fluorinated indole series having a heteroaryl-carboxamide group at C-7, particularly compounds **23l–n** and **23p** demonstrated extraordinary antiviral activity in picomolar scale with EC_{50} values of 0.02 nM, 0.057 nM, 0.0058 nM and 0.04 nM, respectively. The most active derivatives among each series were further investigated *in vivo* for oral exposure in rats and *in vitro* for Caco-2 permeability and human liver microsomal (HLM) stability. Phenylsulfonamide **23b** and tetrazolylamide **23i** provided greater HLM stability but showed poor permeability and poor oral exposure in rats. The thiazol-2-acrylamide derivative **23m** exhibited high permeability but was unstable in HLM, compound **23a**, however, displayed good metabolic stability and permeability with high oral exposure in rats. The SAR studies revealed that the presence of heteroatom(s) in an arylmethyl group away from the C-7 carboxamide nitrogen led to enhanced potency (*e.g.* compounds **23c–e**). In addition, the presence of hetaryl carboxamides such as pyridyl, tetrazolyl, thiadiazolyl, isoxazolyl, thiazolyl, benzothiazolyl, and benzimidazolyl (**23h–j** and **23k–q**), resulted in subnanomolar to picomolar potency of antiviral activity. The antiviral potency of heterocycles having N-atom closer to the amide nitrogen was more potent than those with far N-atom from the amide group (for example 2-pyridyl (**23h**) > 3- and 4-pyridyl (**23f**, **23g**)), and those having the thiazol-2-yl group **23m**, **23n** and exhibited half-maximal inhibition at picomolar concentrations.[66,67]

The antiviral activity of the tetrazole-based 4-fluoroindole hybrids **24a–d** as inhibitors of HIV-1 attachment was reported (Fig. 17). The antiviral activity of the synthesized compounds was conducted in the single-cycle infectivity assay against HIV-JRFL pseudotyped virus. The reported compounds **24a–d** showed potent inhibition with EC_{50} values ranging between 20–190 nM, and compound **24d** had the highest potency with EC_{50} 20 nM. Compounds **24b–d** were examined also *in vivo* as potential oral prodrugs in rats at 30 and 120 min post-dosing, where compound **24b** was found to have a great enhancement of the plasma concentration, but compound **24c** proved to be ineffective in improving the plasma concentration. Interestingly, oral dosing of compound **24d** provided an extraordinary increase in the plasma concentration in rats. Thus, these examples had the potentials to act as a prodrug for HIV-1 inhibition.[68]

A series of *N*-cyclobutyl 4-fluoro- and 5-fluoroindole-3-carbonitrile derivatives **25a–j** were designed, synthesized, and evaluated for their inhibition of HCV replicon activity (Fig. 18). All the 4-fluro- and 5-fluoroindole-3-carbonitrile series **25a–j** showed high potency (EC_{50} = 4–460 nM), particularly compound **25c** provided the highest activity ($EC_{50} = 4$ nM). SAR revealed that the 5-fluoroindoles had better activity when compared with their 4-fluoroindole analogues. For example, compound **25b** ($EC_{50} = 7$ nM) had 22-fold better activity than its isomer **25j** ($EC_{50} = 153$ nM), and compound **25a** ($EC_{50} = 7$ nM) had 2.6-fold better activity than its isomer **25i** ($EC_{50} = 18$ nM). Also, the more lipophilic groups greatly enhanced the inhibitory potency, for example; compound **25b** having a 6-Me group ($EC_{50} = 7$ nM) had 58.6-fold higher activity than **25f** having a 6-OH group ($EC_{50} = 410$ nM). Furthermore, another series of *N*-(heteroaryl) 5-fluoroindole-3-carbonitrile derivatives **26a-aa** were evaluated for their inhibition of HCV replicon activity targeting NS4B and to evaluate their drug metabolism and pharmacokinetics (DMPK) properties. Most of the fluorinated derivatives **26a-aa** exhibited high potency with EC_{50} = 2–32 nM. Interestingly, compound **26q** demonstrated excellent potency in the cell-based HCV 1b replicon with $EC_{50} = 2$ nM, with more than 5000-fold selectivity concerning cellular GAPDH. Compound **26q** proved to have acceptable pharmacokinetic properties with oral bioavailability values of 78%, 62%, and 18% in dogs, rats,

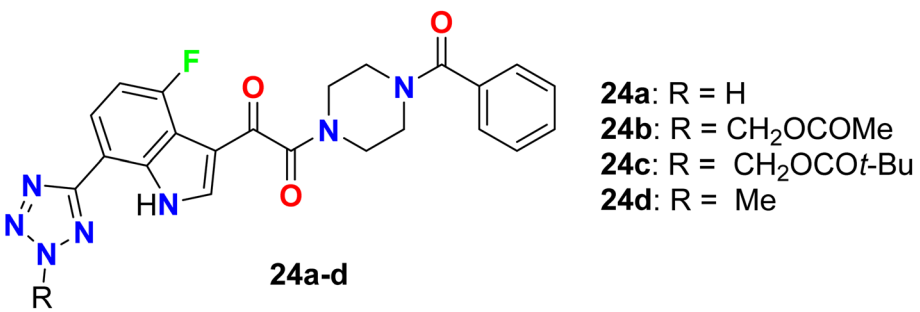

Fig. 17 Structure of tetrazole-based 4-fluoroindole hybrids **24a–d**.

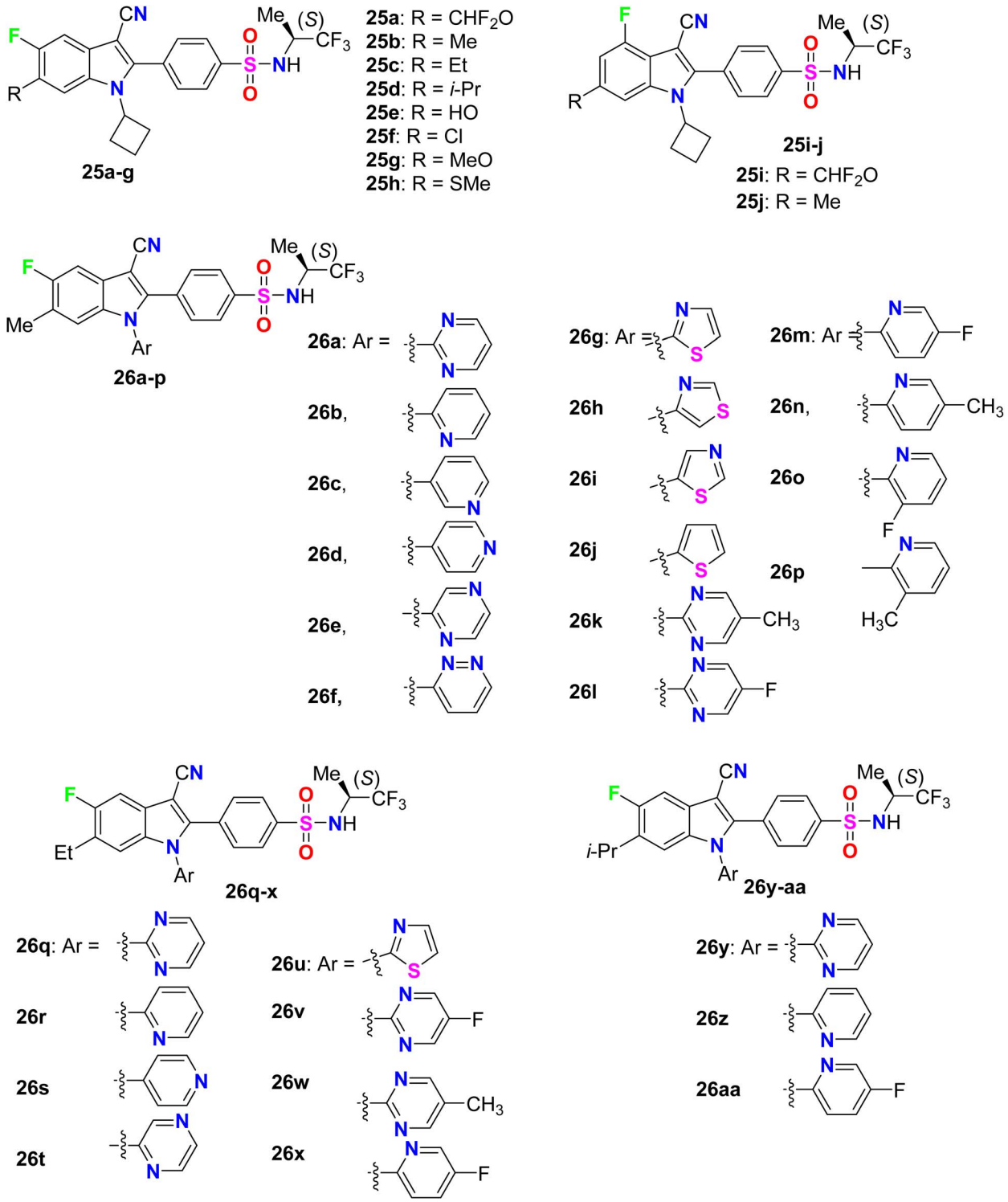

Fig. 18 Structure of 4-fluoro- and 5-fluoroindole-3-carbonitrile derivatives **25–26** derivatives.

and monkeys, respectively. Compound **26q** had also favorable tissue distribution properties with a liver-to-plasma exposure ratio of 25 in rats.[69]

It was reported by Cihan-Üstündağ *et al.* that the synthesized 5-fluoroindole-thiosemicarbazide derivatives **27a–d** provided significant antiviral activities against CVB4 (Coxsackie B4) various (Fig. 19). All the derivatives displayed interesting inhibition of CVB4 virus in Hela and Vero cell lines with EC_{50} values ranging between 0.4–2.1 μg mL^{-1}. The thiosemicarbazide derivative **27b** had the most potent activity with EC_{50} equal to 0.87 and 0.4 μg mL^{-1} in Hela and Vero cell lines, respectively. Furthermore, compounds **27b–d** could inhibit replication of

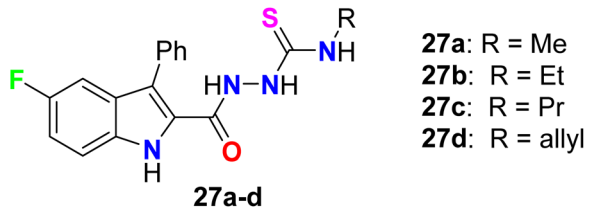

Fig. 19 Structure of 5-fluoroindole-thiosemicarbazide derivatives 27a–d.

two other RNA viruses but with higher values of EC_{50} in comparison with the CVB4 virus, particularly Sindbis virus (EC_{50} 2.3–4 μg mL^{-1}, in Vero cells) and respiratory syncytial virus (EC_{50} 3.2–6.5 μg mL^{-1}, in Hela cells). Thus, compound **27b** was considered as a promising scaffold for development of antiviral drugs.[70]

2.8. Antiviral activity fluorinated benzimidazoles

The bis-(fluorobenzimidazole) derivatives **28b–e** (Fig. 20) were assigned as potent, broad-genotype *in vitro* inhibitory activity HCV genotypes 1–6 replicons. The fluorinated benzimidazoles **28b–e** provided highly potent activity against most HCV genotypes (1a, 1b, 2b, 4a) with EC_{50} values ranging between 0.008–0.57 nM, much better than the non-fluorinated benzimidazole **28a**. In particular, compound **28d** was the most potent one against all HCV genotypes. The other series of bis-(fluorobenzimidazole) derivatives **29a–c** showed also excellent inhibitory results against all HCV replicon subtypes, especially compound **22** had fascinating activity in the picomolar scale against all wild-type replicons (1a, 1b, 2a, 2b, 3a, 4a and 6a) with EC_{50} values ranged between 0.007–0.015 nM. The inhibition potency of the fluorobenzimidazoles **29a–c** was also high against the genotype 1a NS5A variants M28T, Q30R, Y93C, and Y93H, particularly compound **29a** demonstrated the best activity EC_{50} values 0.004, 0.005, 0.005, and 0.059 nM, respectively.[71]

3. Anti-inflammatory activity of fluorinated heterocycles

3.1. Anti-inflammatory activity of fluorinated pyrazoles

Dressen *et al.* described the synthesis of the 4-fluorpyrazole molecular hybrid **30** and evaluated its potency as a human bradykinin (B1 and B2) receptor antagonist for the treatment of pain and inflammation. The bioassay was carried out using a fluorescent imaging plate reader (FLIPR) utilizing IL-1â stimulated IMR-90 human lung fibroblast cells. Compound **30**

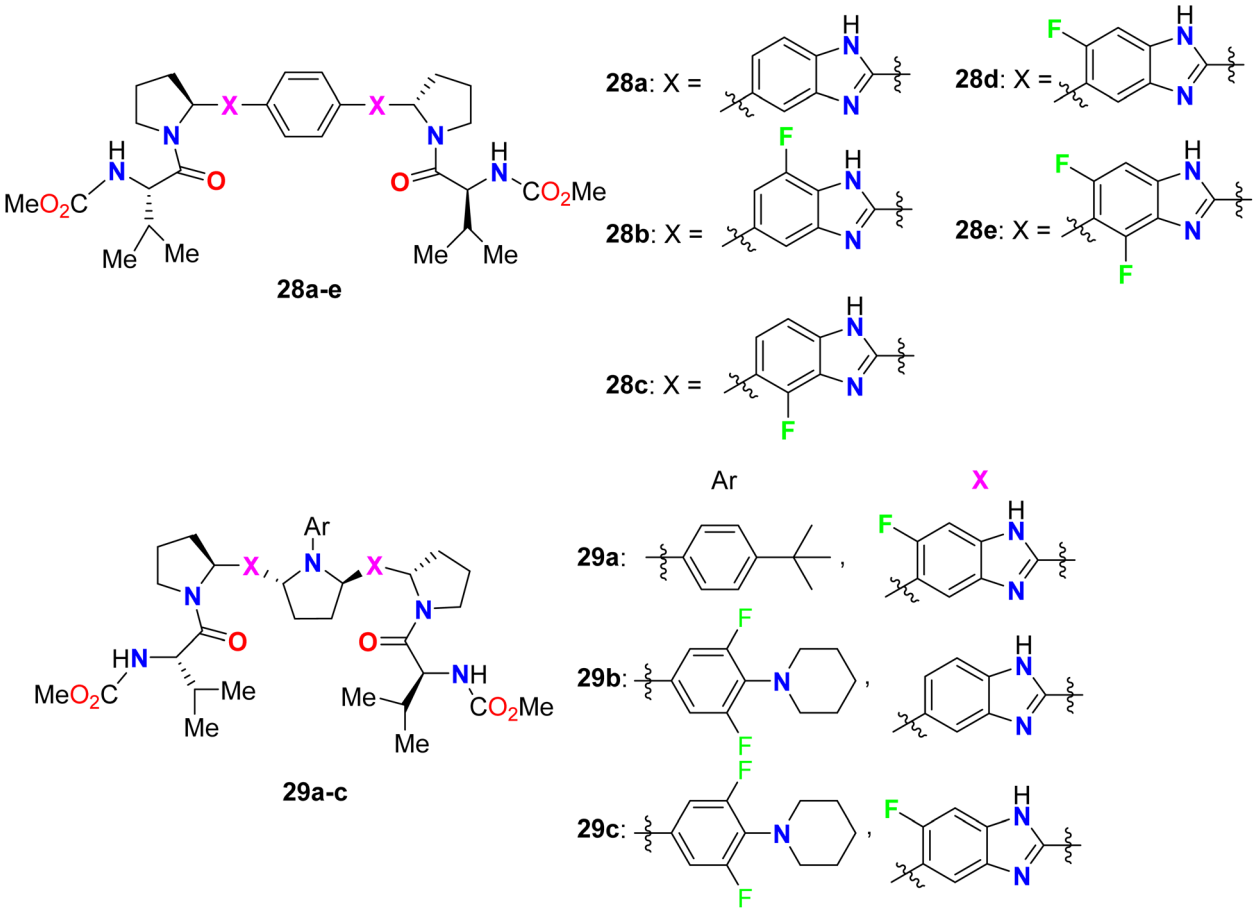

Fig. 20 Structure of bis-(fluorobenzimidazole) derivatives 28–29.

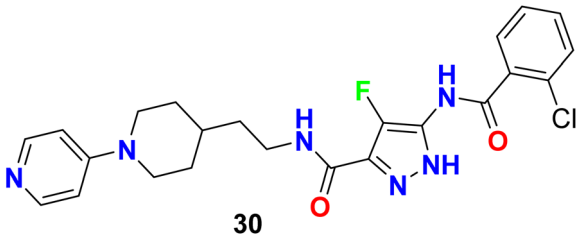

Fig. 21 Structure of 4-fluorpyrazole derivative **30**.

showed promising activity with an IC_{50} value of 23 nM against B1 with high selectivity over B2 (Fig. 21).[72]

Two series of fluorinated-pyrazole heterocyclic hybrids **31** and **32** were invented, patented, and screened as human bradykinin (BK B2) receptor antagonists (Fig. 22). Most of the reported derivatives were found to possess a wide range of properties such as high selectivity, low toxicity, low drug–drug interaction, good metabolic stability, good bioavailability, good stability in microsomal degradation assay as well as good solubility. Most of the assigned compounds demonstrated IC_{50} values of $\leq$50 nM.[73,74]

A series of 5-fluorothiazole **33** and 3-fluorpyrazole **34** heterocycles were invented, patented, and screened out as modulators of mGluR4 (metabotropic glutamate receptors-subtype 4) for the treatment of central nervous system disorders (Fig. 23). The activity of the invented compounds was tested on recombinant human mGluR4a receptors by detecting variations in intracellular Ca^{2+} concentration using Fluorometric Imaging Plate Reader (FLIPR). The assigned compounds showed positive allosteric modulator effect at mGluRA *via* enhancing the activity of the receptor with EC_{50} values were less than 100 nM.[75]

A series of 4-fluoropyrazole scaffolds **35a–c** and **36a–j** were patented by Sakagami and his co-workers as NPYY5 receptor antagonists (Fig. 24). All the invented compounds exhibited NPYY5 receptor antagonistic activity to be useful in the medication of obesity, depression, and sexual disorders. The reported compounds had little inhibition on drug-metabolizing enzymes, had good metabolic stability and water solubility as well as low toxicity, and were sufficiently safe for use in medication. The invented fluorinated pyrazoles showed a good binding affinity for the mouse NPYY5 receptor with IC_{50} values varying between 0.22 nM to 2.2 nM.[76]

The guanidine-based 4-fluoropyrazole derivatives **37a**, **37b** were reported to have good inhibitory activity of F_1F_0-ATPase synthase enzyme for treatment of the inflammatory disease (Fig. 25). The bioactivity experiment measured the ability of compounds **37a**, **37b** to inhibit the ATP synthesis, as well as the cytotoxicity in Ramos cells. The biological activity results

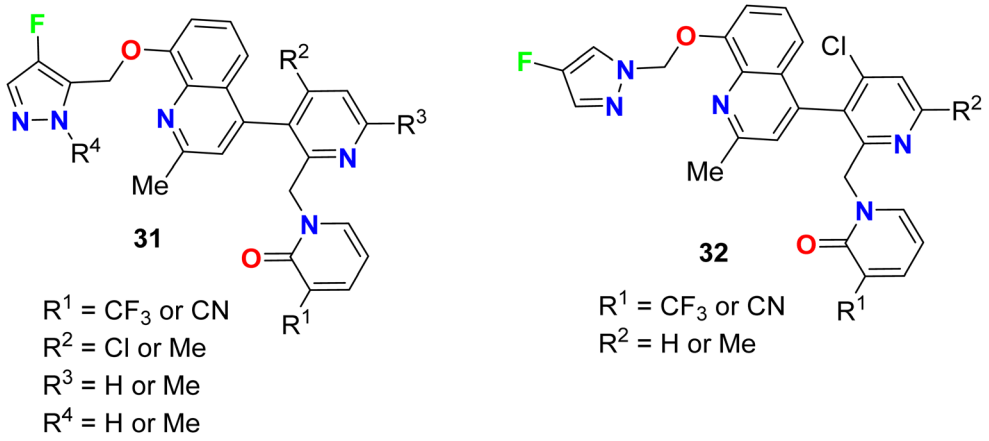

Fig. 22 Structure of fluorinated-pyrazole heterocyclic derivatives **31** and **32**.

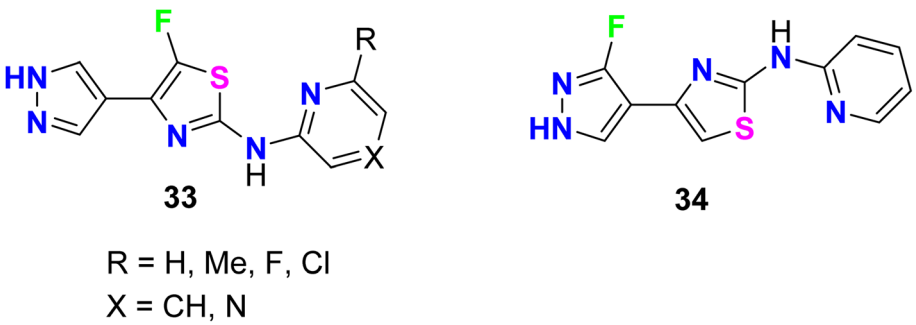

Fig. 23 Structure of 5-fluorothiazole **33** and 3-fluorpyrazole **34** heterocycles.

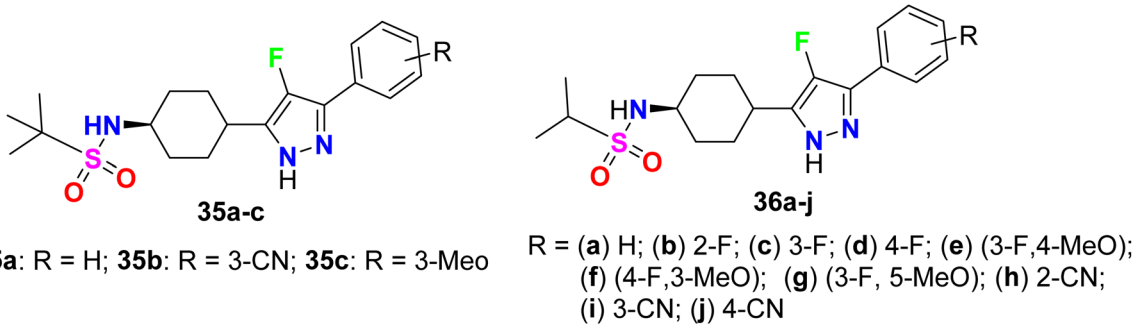

Fig. 24 Structure of 4-fluoropyrazole scaffolds 35a–c and 36a–j.

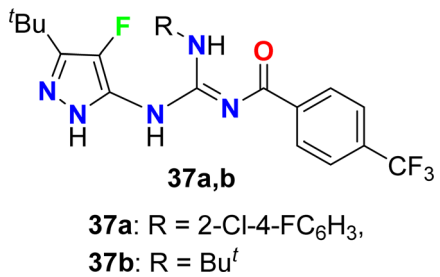

Fig. 25 Structure of 4-fluoropyrazole derivatives 37a, 37b.

disclosed that both compounds **37a, 37b** inhibited F_1F_0-ATPase activity in synthesizing ATP with IC_{50} values <10 μM. In addition, cytotoxicity in Ramos cells was also measured and both compounds presented EC_{50} < 10 μM.[77]

Synthesis and anti-inflammatory activity of a series of 5-fluoropyrazole molecular hybrids **38a–d** and **39a–e** (Fig. 26) were invented and patented by Mingchun *et al.* The bioassay study employed RAW 264.7 cells that were cultured in a high-sugar DMEM complete medium containing 10% FBS (fetal bovine serum). The COX-2 protein expression level was up-regulated, confirming the success of the cell inflammation (P < 0.001). After mixing celecoxib, as positive medicine, with the synthesized compounds in equal concentration, the COX-2 protein expression was significantly decreased compared with the neat celecoxib. Compounds **38a–d** and **39a–e** showed more remarkable COX-2 protein inhibitory activity (Δ P < 0.05) than the positive drug celecoxib. Thus, the patented fluoropyrazoles **38a–d** and **39a–e** showed anti-inflammatory activity through a potent inhibition effect on the key protein COX2 in a rheumatoid arthritis model and had good potential for further drug development.[78]

3.2. Anti-inflammatory activity of fluorinated indazoles

The 6-fluoroindazole scaffold **40** was developed as a selective antagonist of the TRPA1 (transient receptor potential A1) cation channel (Fig. 27). The *in vitro* study using an antagonist mode

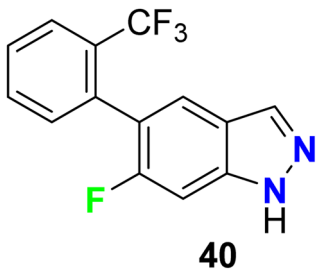

Fig. 27 Structure of 6-fluoroindazole scaffold 40.

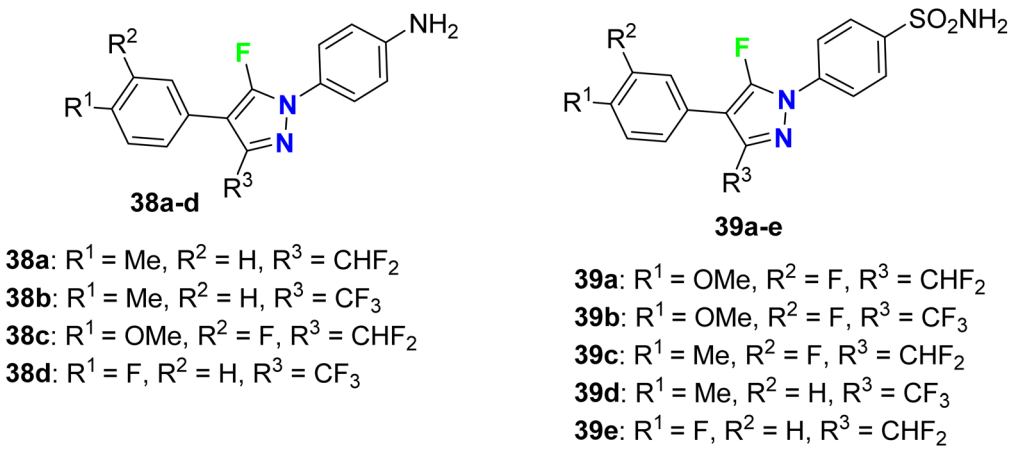

Fig. 26 Structure of 5-fluoropyrazole derivatives 38a–d and 39a–e.

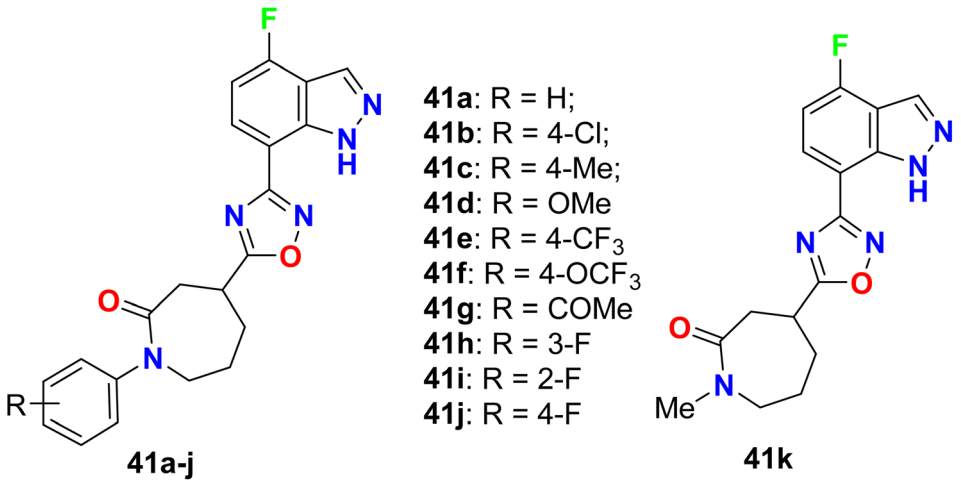

Fig. 28 Structure of 4-fluoroindazole derivatives **41a–k**.

FLIPR calcium cation imaging assay in 1536-well format, revealed that compound **40** possessed a potent and selective antagonist of hTRPA1 with IC_{50} 0.043 μM and 98% inhibition. Thus, compound **40** had moderate oral bioavailability in rodents and exhibited *in vivo* anti-inflammatory activity.[79]

The 4-fluoroindazole derivatives **41a–k** were reported as selective cannabinoid receptor (CB2) agonists for inflammation treatment without psychiatric side effects (Fig. 28). All compounds showed good to high potency as selective CB2 agonists. SAR investigations confirmed compound **41j** as the most potent one showing high selectivity for CB2 *versus* CB1 (CB2: EC_{50} = 21.0 nM, E_{max} = 87%, compared with CB1 EC_{50} > 30 μM, and CB1/CB2 ratio >1428) with promising *in vivo* pharmacokinetic (PK) properties. In addition, compound **41j** displayed significant efficacy in the analgesic model of rodent inflammatory pain. Therefore, compound **41j** could be useful as a lead structure for treating inflammatory pain after further studies.[80]

The 5-fluoroindazole derivative **42** (Fig. 29) was synthesized and evaluated for its inhibitory activity against human neutrophil elastase (HNE), for treatment of pulmonary diseases. Compound **42** showed good inhibitory potency, good stability, and selectivity for HNE over other serine proteases, with an IC_{50} value of 0.1 μM.[81]

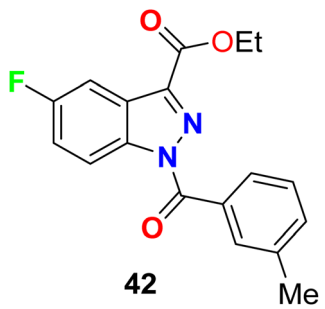

Fig. 29 Structure of 5-fluoroindazole derivative **42**.

Some 7-fluoroindazole derivatives **43a–m** were patented and their biological activity as inhibitors of human spleen tyrosine kinase (Syk) were screened, for possible treatment of inflammatory disorders (Fig. 30). All the tested compounds showed excellent human Syk kinase inhibitory potency with IC_{50} ranging between 10 nM and 50 nM. Evaluating the inhibitory activity of TNFα production was also reported, and most of the patented compounds **43a–g**, **43k**, **43m** provided IC_{50} values about 65 nM.[82]

Synthesis of the 6-fluoroindazole molecular hybrids **44a–h** was described by Padilla *et al.* and screened their inhibitory activity of Syk enzyme in addition to the selectivity of Syk/JAK and human whole blood (HWB) assay was studied (Fig. 31). The synthesized compounds were found to be potent and selective Syk inhibitors with IC_{50} values ranging between 4 nM to 64 nM, where structure **44g** was the most potent one with IC_{50} = 4 nM, with high selectivity for Syk kinase (3/386) over the JAK (Janus kinase) family. The fluorinated compounds **44a–h** showed also very good potency in Ramos B cell and HWB potency assays with IC_{50} values 0.151–3.70 μM and IC_{50} values 0.376–1.43 μM respectively.[83]

Hurd *et al.* described the synthetic routes to the monofluorinated 3-guanidyl-indazole structures **45–47** as shown in Fig. 32. All the reported compounds were tested for their activity against F_iF_0-ATPase by measuring their capability to inhibit ATP synthesis. In addition, the cytotoxicities of the indazole derivatives in Ramos cells (B lymphocyte cell line) were also assessed. The bioactivity results showed that most of the constructed fluorinated indazole scaffolds demonstrated potent inhibition of F_1F_0-ATPase activity with IC_{50} values <5 μM as well as cytotoxicity in Ramos cells with EC_{50} <5 μM.[84]

The 5-fluroindazole derivatives **48a–j** were invented and characterized as inhibitors of RIP2 kinase (receptor-interacting protein 2) that were useful for the treatment of inflammatory diseases (Fig. 33). Most of the designed compounds showed promising inhibitory action against RIP2 kinase with pIC_{50} values < 8. 5-Fluoroindazole **48a** (R^1 = H, R^2 = Me, R^3 = 3,4,5-

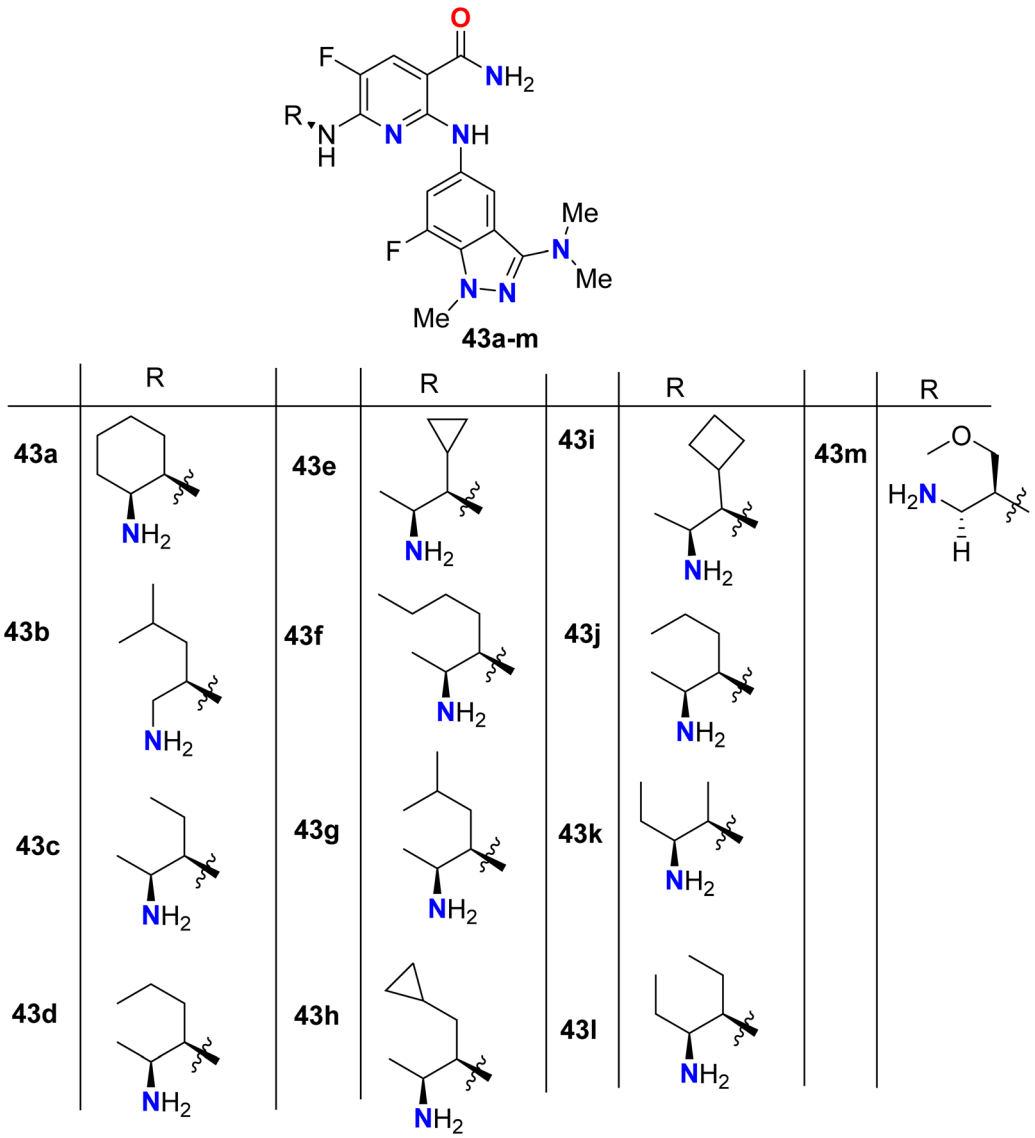

Fig. 30 Structure of 7-fluoroindazole derivatives **43a–m**.

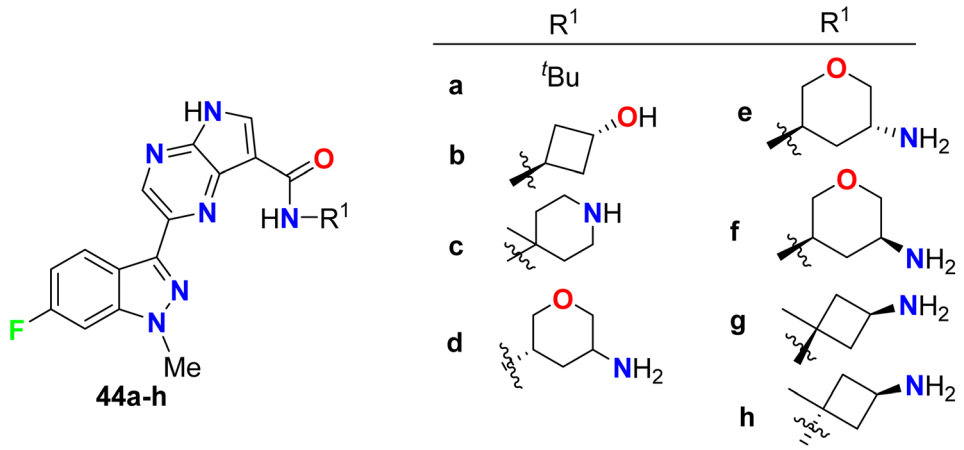

Fig. 31 Structure of 6-fluoroindazole molecular hybrids **44a–h**.

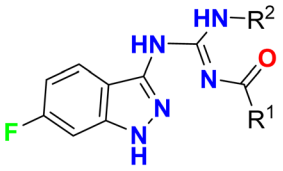

45a-l

	R^1	R^2		R^1	R^2
45a	3-ClC_6H_4	iBu	**45g**	4-$CF_3C_6H_4$	CH(Me)CH_2OMe
45b	4-ClC_6H_4	sBu	**45h**	3-ClC_6H_4	CH_2CH_2OMe
45c	3-FC_6H_4	tBu	**45i**	4-ClC_6H_4	CH_2CH_2OEt
45d	4-FC_6H_4	Et	**45j**	3-FC_6H_4	cPr
45e	3,4-$Cl_2C_6H_3$	Pr	**45k**	4-FC_6H_4	cPr
45f	3,4-$F_2C_6H_3$	iPr	**45l**	3,4-$Cl_2C_6H_3$	cPr

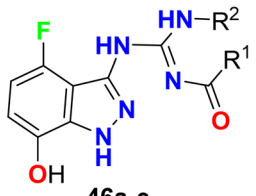

46a-e

	R^1	R^2
46a	3,4-$(F)_2C_6H_3$	sBu
46b	4-$CF_3C_6H_4$	iPr
46c	3-ClC_6H_4	CH(Me)CH_2OMe
46d	4-ClC_6H_4	-CH_2CH_2OMe
46e	3-FC_6H_4	-CH_2CH_2OEt

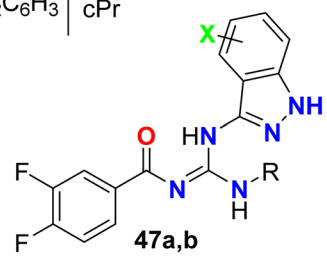

47a,b

X = 4-F, 5-F
R = *i*Bu, t-Bu

Fig. 32 Structure of monofluorinated 3-guanidyl-indazole structures **45–47**.

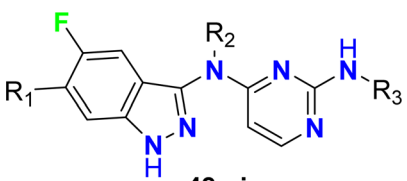

48a-j

	R_1	R_2	R_3		R_1	R_2	R_3		R_1	R_2	R_3
48a	H	Me	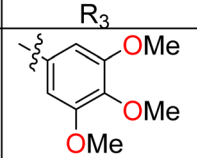	**48e**	H	Me	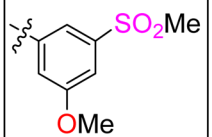	**48h**	Me	Me	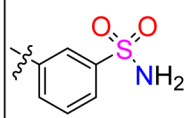
48b	H	H		**48f**	H	H	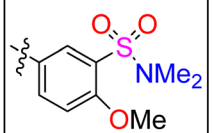	**48i**	Me	Me	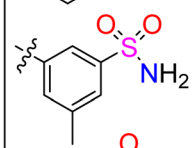
48c	H	H	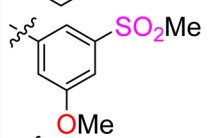	**48g**	H	H	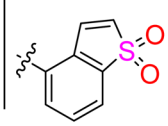	**48j**	H	H	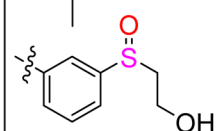
48d	Me	Me									

Fig. 33 Structure of 5-fluroindazole derivatives **48a–j**.

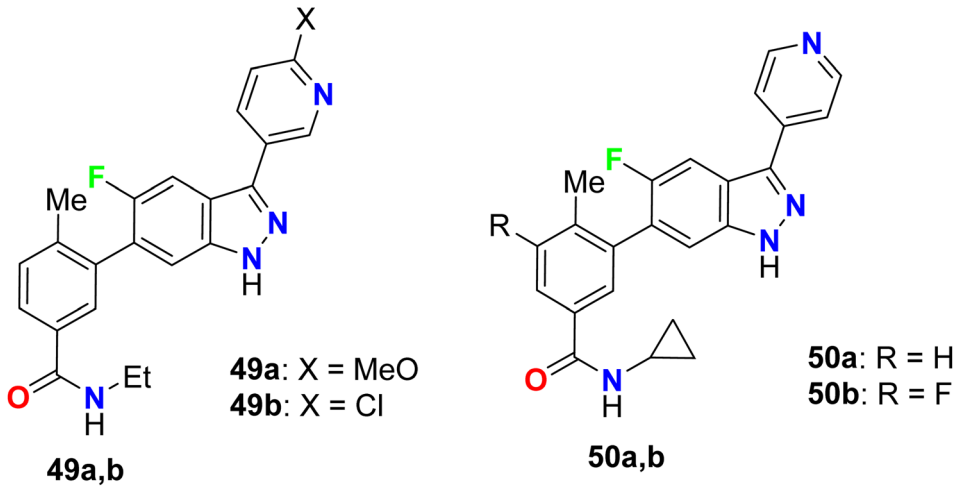

Fig. 34 Structure of 5-indazole derivatives **49** and **50**.

triMeOC_6H_2) interestingly displayed the best inhibition of the RIP2 kinase with pIC_{50} value of 6.0.[85]

The 5-indazole derivatives **49a**, **49b**, and **50a**, **50b** were patented as inhibitors of the p38 kinase and were useful for the treatment of inflammatory diseases (Fig. 34). The inhibitory activity of the invented fluorinated compounds against p38 kinase was determined by *in vitro* fluorescence anisotropy kinase binding assay 1 and all compounds had IC_{50} values of <10 μM.[86]

Two examples of the fluorinated indazoles **51** and **52** were synthesized and evaluated as inhibitors of Rho kinase (ROCK1) activity (Fig. 35). The *in vitro* bioassay results showed that the presence of fluorine at C4 (compound **51**) displayed low potency with IC_{50} of 2500 nM. However, the presence of fluorine at C6 (compound **52**) significantly enhanced the ROCK1 inhibitory potency with an IC_{50} value of 14 nM as well as a dramatic increase of oral bioavailability (61%) was reported for 6-fluoroindazole **52**. The experiments showed also good *in vivo* results, where compound **52** dramatically reduced mean arterial pressure in spontaneously hypertensive rats after oral administration.[87,88]

Two further examples of 6-fluoroindazoles **53a**, **53b** were found to have promising inhibitory activity of ROCK1 with IC_{50} values of 7 and 6 nM, respectively (Fig. 36). These compounds were also examined for P450 properties and rat PK (pharmacokinetics) studies. Both compounds **53a** and **53b** showed good oral bioavailability 49% and 53%, respectively, and both compounds showed improved P450 profile (2.1–5.3 μM at all isozymes tested; CYP2C9, CYP2D6, and CYP3A4). Compound **53a** was tested for *in vivo* efficacy studies in a spontaneously hypertensive rat (SHR) model of hypertension, where at 30 mg

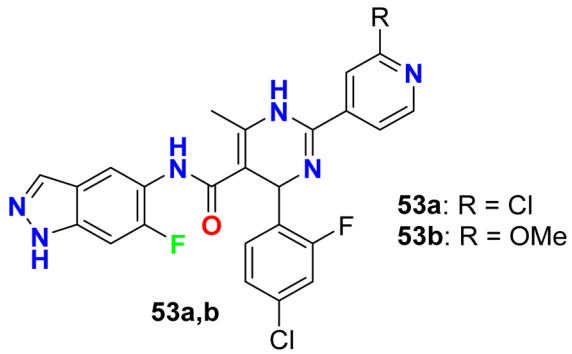

Fig. 36 Structure of 6-fluoroindazoles **53a**, **53b**.

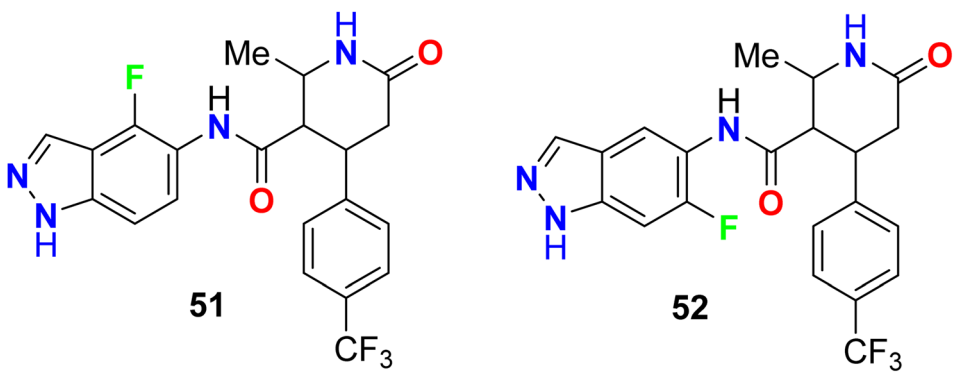

Fig. 35 Structure of fluorinated indazoles **51** and **52**.

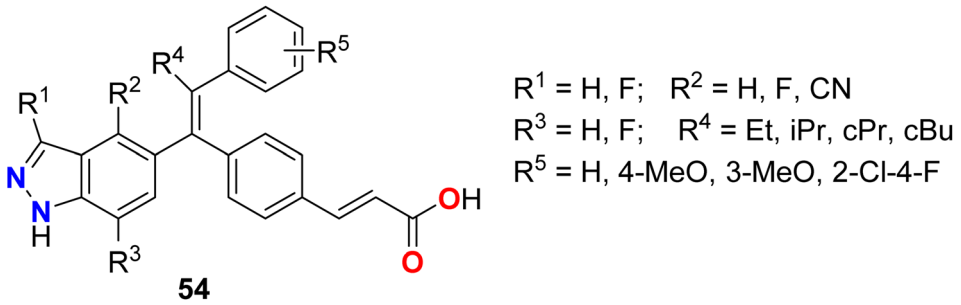

Fig. 37 Structure of fluorinated indazole derivatives **54**.

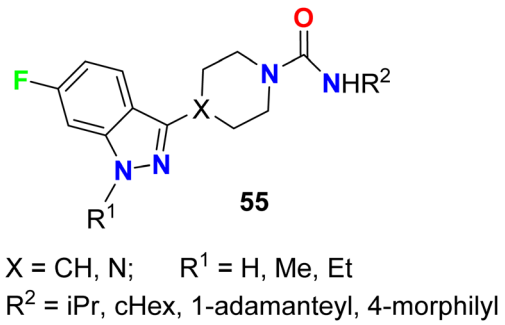

Fig. 38 Structure of 6-fluoroindazole scaffolds **55**.

kg^{-1} (po) compound **53a** induced a 25 mmHg ($t = 3$ h) drop in arterial blood pressure. Thus Compound **53a** demonstrated a good potency *in vivo* experiments.[89]

Some fluorinated indazole derivatives **54** (Fig. 37) were patented as estrogen receptors (ER) modulators to be useful for the treatment for treating diseases that are dependent upon estrogen receptors. The bioassay results of all the invented derivatives for ER-α in cell western assay (SPI) showed inhibitory activity with IC_{50} values < 100 nM.[90]

6-Fluoroindazole scaffolds **55** (Fig. 38) were invented and evaluated for their positive allosteric modulators (PAM) activity using human α7nAChR stable expressing cells. The invented compounds exhibited promising α7 nAChR PAM activity at 10 μM with α7PAM% varied between 189–4639, particularly compound **55** (R^1 = H, R^2 = cHex, X = CH) had the highest PAM activity active with 4639%. These compounds might be used as therapeutic agents to cure diseases involving the cholinergic properties of CNS.[91]

3.3. Anti-inflammatory activity of fluorinated benzimidazoles

Calderini *et al.* invented some fluorinated pyrazole-based heterocycles **56–57** and evaluated their biological activities as inhibitors of PDK1 (pyruvate dehydrogenase kinase 1) for treating inflammatory diseases (Fig. 39). Thus, the fluoropyrazole derivatives **56** and fluorobenzimidazole derivatives **57** were tested for inhibition of PDK1 using a flash-plate system with 384 wells/micro-titration assay. Interestingly all the fluorinated derivatives exhibited high potency with IC_{50} values varying between 1 nM to 0.1 μM.[92]

3.4. Anti-inflammatory activity of fluorinated benzothiazoles

The 6-fluorobenzothiazole derivatives **58a–i** (Fig. 40) were assembled by Sathe *et al.* and then screened for their *in vitro* anti-inflammatory activity using the technique of inhibition of albumin denaturation. The tested compounds showed in moderate to high range of activity from 20.40–79.93% of inhibition compared with the anti-inflammatory drug ibuprofen (93.87%). Compound **58h**, specifically, had the best inflammation inhibition with 79.93%.[93]

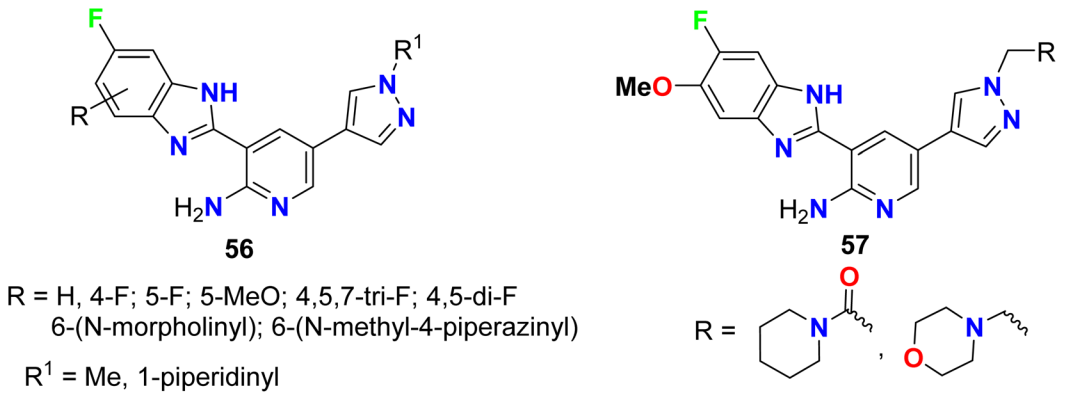

Fig. 39 Structure of pyrazole-based heterocycles **56–57**.

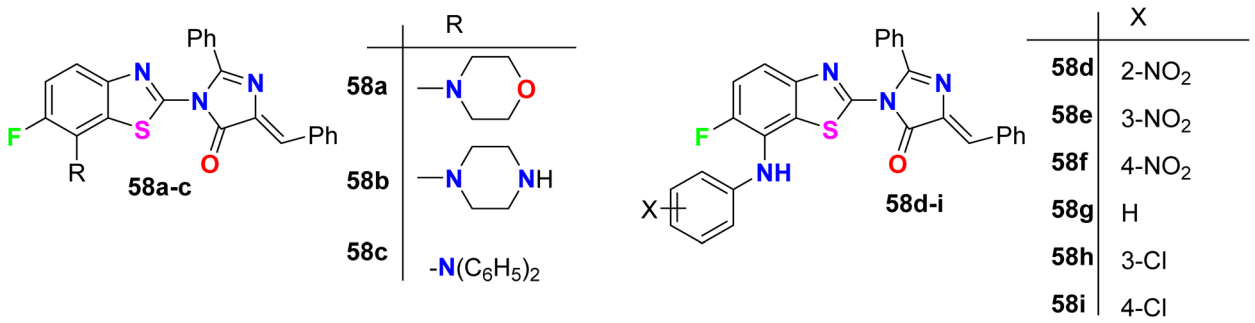

Fig. 40 Structure of 6-fluorobenzothiazole derivatives **58a–i**.

3.5. Anti-inflammatory activity of fluorinated indoles

Varpe *et al.* reported the synthesis of 5-fluoroisatin derivatives **59a–g** and evaluated their anti-inflammatory activity (Fig. 41). The anti-inflammatory activity was examined *in vitro* by measuring the inhibition % of denaturation of Bovine Serum Albumin (BSA). All compounds showed good inhibition %, especially the piperazine-based 5-fluoroisatin **59d** at 100 μg mL^{-1}. Compound **59d** showed the highest anti-inflammatory activity with 80.08% inhibition compared with the standard drug diclofenac sodium with 89.38% inhibition, and compounds **59c** and **59g** showed 72.56 and 62.38% inhibition. Docking analysis disclosed that the compounds exhibited good interactions with the COX-2 enzyme binding site.[94]

3.6. Anti-inflammatory activity of fluorinated benzofurans

The anti-inflammatory effects of the fluorinated benzofuran derivatives **60–63** in macrophages and in the air pouch model of inflammation, were investigated (Fig. 42). Most compounds suppressed the lipopolysaccharide-stimulated inflammation by inhibiting the expression of cyclooxygenase-2 and nitric oxide synthase-2 and decreased the secretion of the tested inflammatory mediators. Their IC_{50} values ranged between 1.2–9.04 μM for interleukin-6; between 1.5–19.3 μM for Chemokine (C–C) ligand 2; between 2.4–5.2 μM for nitric oxide; and between 1.1–20.5 μM for prostaglandin E2. Three fluorinated benzofuran compounds significantly inhibited cyclooxygenase activity. Most of these compounds showed anti-inflammatory effects in the zymosan-induced air pouch model.[95]

4. Enzymatic inhibitory activity of fluorinated heterocycles

4.1. Enzymatic inhibitory activity of fluorinated thiophenes

Fuchigami designed and synthesized the monofluorinated 3-thiolanones (*cis*/*trans* isomers) **64a**, **64b** and evaluated their *in vitro* human type II phospholipase A2 ($hPLA_2$) inhibitory activity for possible treatment of inflammatory diseases (Fig. 43). Interestingly, the *cis*/*trans* mixture of **64a**, **64b** showed substantial inhibitory action against PLA_2 with IC_{50} = 0.2 μM much better than the manoalide reference drug with IC_{50} = 0.34 μM. The pure *cis* isomer of **64b** (IC_{50} = 0.21 μM) was found to present higher activity than its *trans* isomer **64a** (IC_{50} = 1.27 μM).[96]

4.2. Enzymatic inhibitory activity of fluorinated pyrroles

Some chiral fluorinated pyrrolidine hybrids **65a–j** (Fig. 44) were synthesized and *in vitro* evaluated as MAO-B/MAO-A (monoamine oxidase B/A) inhibitors that were useful for Parkinson's disease (PD) in clinics. The biological experiments disclosed that compound **65a** was the most potent, selective MAO-B inhibitor with 10-fold activity more than that of the safinamide drug, where compound **65a** had IC_{50} = 0.019 μM, with

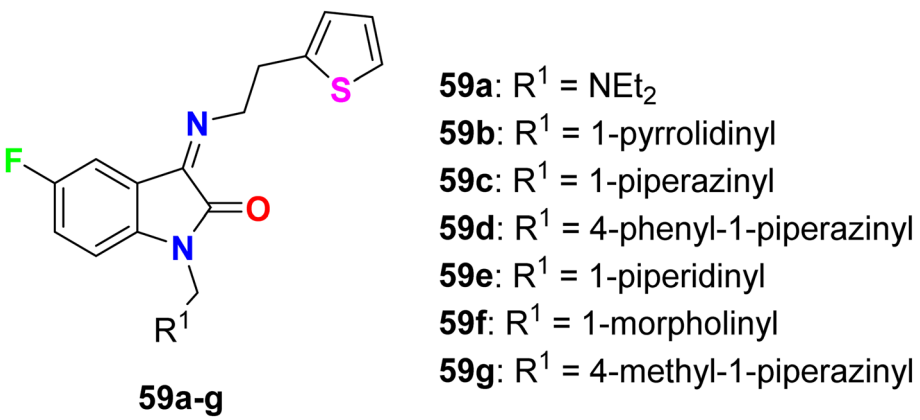

Fig. 41 Structure of 5-fluoroisatin derivatives **59a–g**.

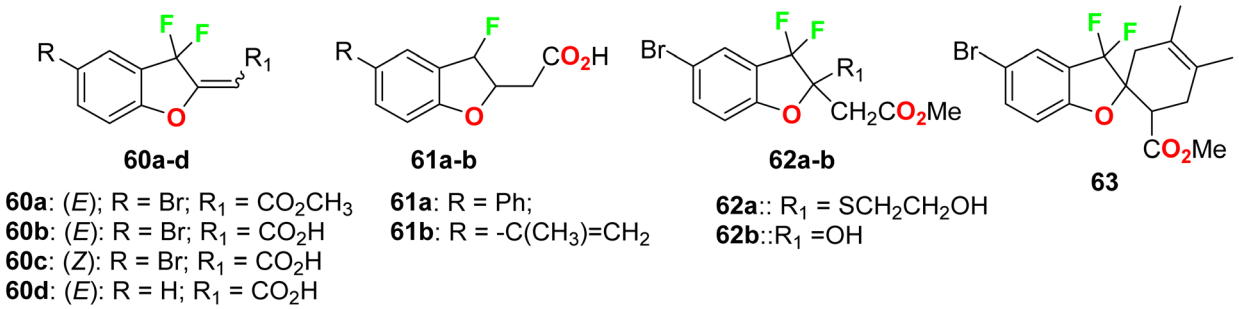

Fig. 42 Structure of fluorinated benzofuran derivatives **60–63**.

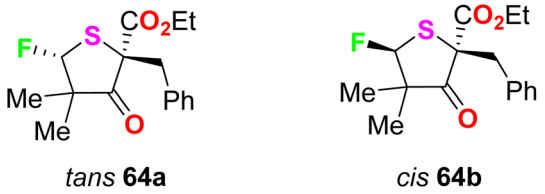

Fig. 43 Structure of monofluorinated 3-thiolanones (*cis*/*trans* isomers) **64a**, **64b**.

selectivity index (SI) = 2440 of MAO-A/MAO-B, compared with safinamide (IC_{50} = 0.163 μM, with SI = 172 for MAO-A/MAO-B). SAR study revealed also that 4*S* chiral F-substituent on the pyrrolidine ring were more potent MAO-B inhibitors than those with 4*R* ones, but replacing 2*S*-carboxamide with 2*R*-carboxamide on the pyrrolidine ring led to a lowering of MAO-B inhibitory activity. Molecular docking results confirmed that the enhanced hydrophobic interaction of **65a** increased the activity against MAO-B. Thus, **65a** was a promising drug candidate for the treatment of PD.[97]

Some fluorinated pyrrolidine-based isatin compounds **66a**, **66b**, **67a**, **67b**, and **68a**, **68b** were reported by Limpachayaporn *et al.* and their *in vitro* inhibitory actions against caspases-3 and -7 were recorded (Fig. 45). The bioassay study showed that all compounds disclosed high inhibitory activity with IC_{50} values ranging between 0.362–2.57 μM (for caspase-3) and 0.178–14.9 μM (for caspase-7). The 4,4-difluorinated compound **68b** presented the best enzyme inhibition results with IC_{50} values of 0.362 μM and 0.178 μM for caspases-3 and -7, respectively.[98]

Wang *et al.* reported a series of directly fluorinated pyrroloindole structures **69a–z** (Fig. 46) as potent acetylcholinesterase (AChE) inhibitors for possible treatment of Alzheimer's disease (AD). The bioassay experiments disclosed that most of the fluorinated heterocycles had potent AChE inhibitory activity, particularly compound **69a** (R = H, R^1 = Me, X =

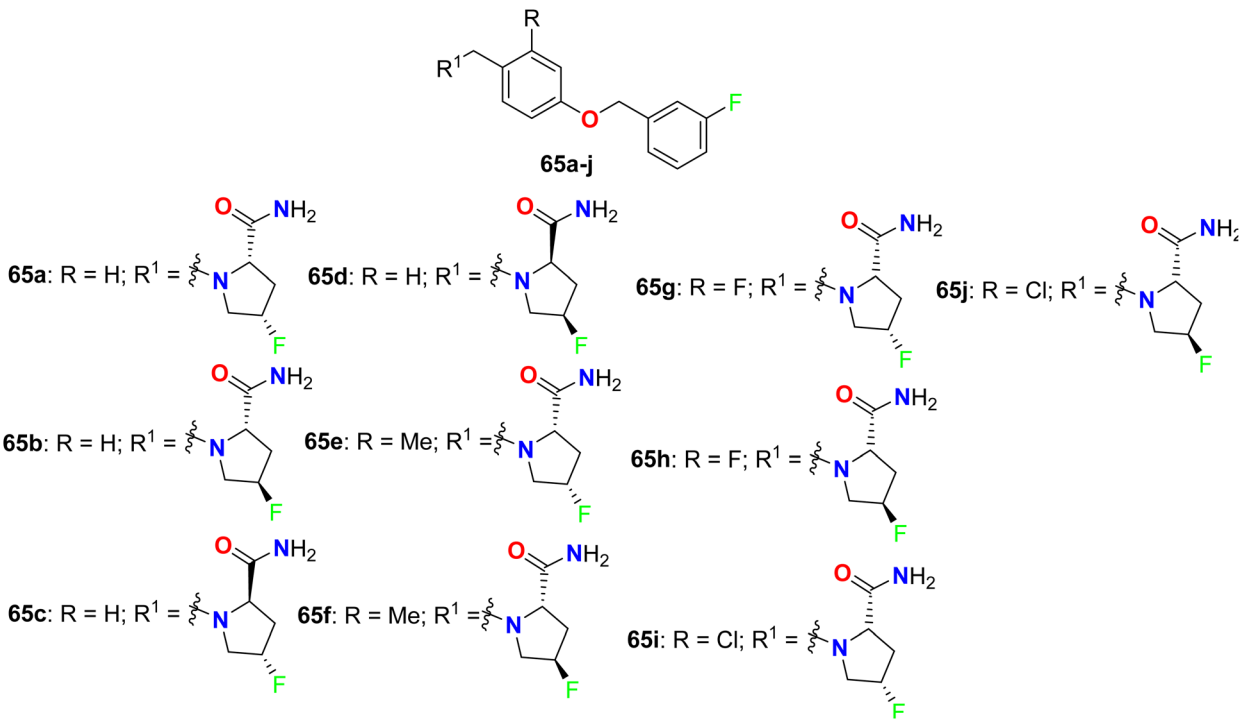

Fig. 44 Structure of chiral fluorinated pyrrolidine hybrids **65a–j**.

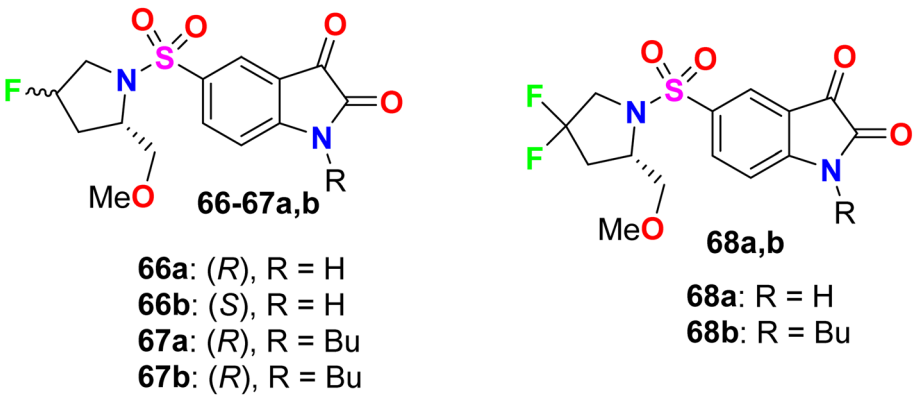

Fig. 45 Structure of fluorinated pyrrolidine-based isatin derivatives **66–68**.

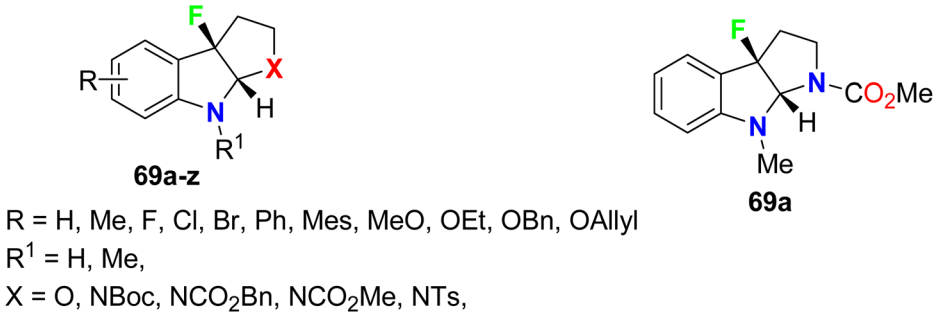

Fig. 46 Structure of fluorinated pyrroloindole derivatives **69a–z**.

NCO_2Me) displayed promising inhibitory activity against AChE with IC_{50} value 16.0 μM. The presence of bulky groups (such as Boc or Ts) of *N*-nucleophiles was essential for interaction with AChE. Therefore, compound **69a** was a potential candidate for the treatment of AD.[99]

4.3. Enzymatic inhibitory activity of fluorinated indoles

Crosignani *et al.* described a series of 6-fluoroindole derivatives **70–73** and were screened as tryptophan 2,3-dioxygenase enzymatic (TDO2) inhibitors to be useful in the treatment of cancers (Fig. 47). Most of the invented compounds greatly inhibited the enzymatic activity of human TDO2 with IC_{50} values ranging between 1 μM and 10 μM, and some compounds such as **71a**, **72**, and **73a** had significant inhibitory activity with IC_{50} < 1 μM.[100]

The 6-fluorotryptophan derivatives **74a**, **74b** (Fig. 48) were synthesized and screened for their *in vitro* tyrosinase inhibitory activity. The *in vitro* inhibitory activity assay was evaluated on

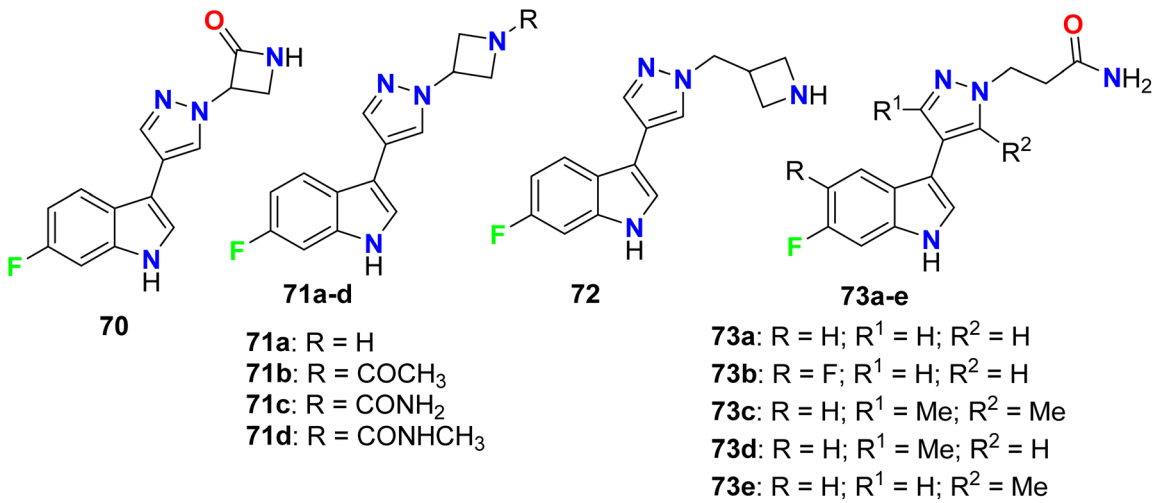

Fig. 47 Structure of 6-fluoroindole derivatives **70–73**.

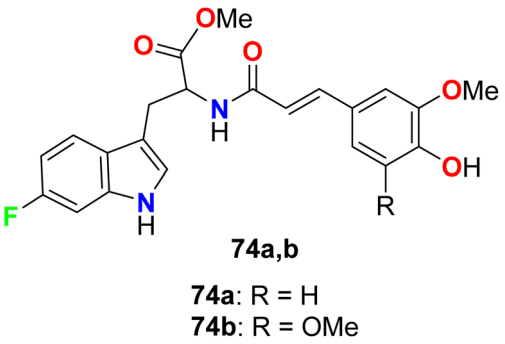

Fig. 48 Structure of 6-fluorotryptophan derivatives 74a, 74b.

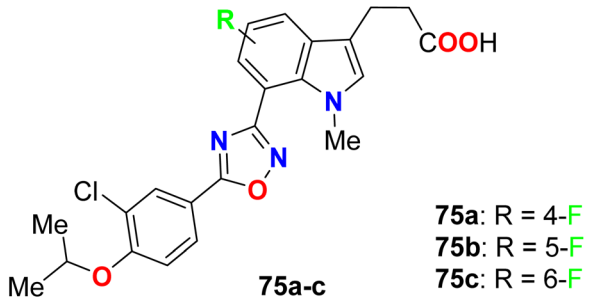

Fig. 49 Structure of fluorinated indole derivatives 75a–c.

mushroom tyrosinase using L-tyrosine as a substrate. The bioassay results disclosed that compounds **74a**, **74b** were highly effective as tyrosinase inhibitors much better than the hydroquinone reference standard.[101]

Three fluorinated indole hybrids **75a–c** (Fig. 49) were synthesized and screened as S1P (sphingosine-1-phosphate) receptor agonists by an *in vivo* peripheral lymphocyte reduction assay. The reported derivatives **75a–c** proved to be promising selective $S1P_1$ agonists, where compounds **75a** and **75b** both showed pEC_{50} value > 11 (for $S1P_1$) compared with pEC_{50} < 5 (for $S1P_3$). Compound **75a** showed similar activity as the fingolimod reference standard. On the other hand, 6-fluoroindole molecule **75c** provided less S1P1 agonist potency when compared with 4- and 5-fluoroindole derivatives **75a** and **75b**.[102]

Some fluorinated indole hybrids **76a–d**, and 77 were synthesized and evaluated for their potency as GPR119 agonist activity. GPR119 (G-protein-coupled receptor) is a target for antidiabetic agents (Fig. 50). The bioassay study was carried out utilizing a cAMP reporter assay in CHO (Chinese hamster ovary) cells stably expressing human GPR119. All compounds displayed a nanoscale activity and the most active compounds were **76d** and 77 with EC_{50} values of 6.8 and 3.9 nM, respectively. The marked increase in agonist potency of compound 77 might be due to the participation of carbonyl function in the carbamate spacer in interactions with GPR119 as a hydrogen bond acceptor.[103]

Nomura *et al.* constructed some fluorinated-indole-*N*-glucosides **78a–e** (Fig. 51) and evaluated their inhibition effects on hSGLT activity (human sodium-glucose co-transporter) as antihyperglycemic agents. The selectivity of the highly active

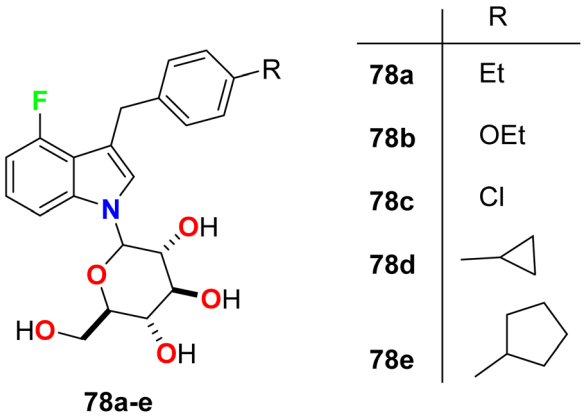

Fig. 51 Structure of fluorinated-indole-*N*-glucosides 78a–e.

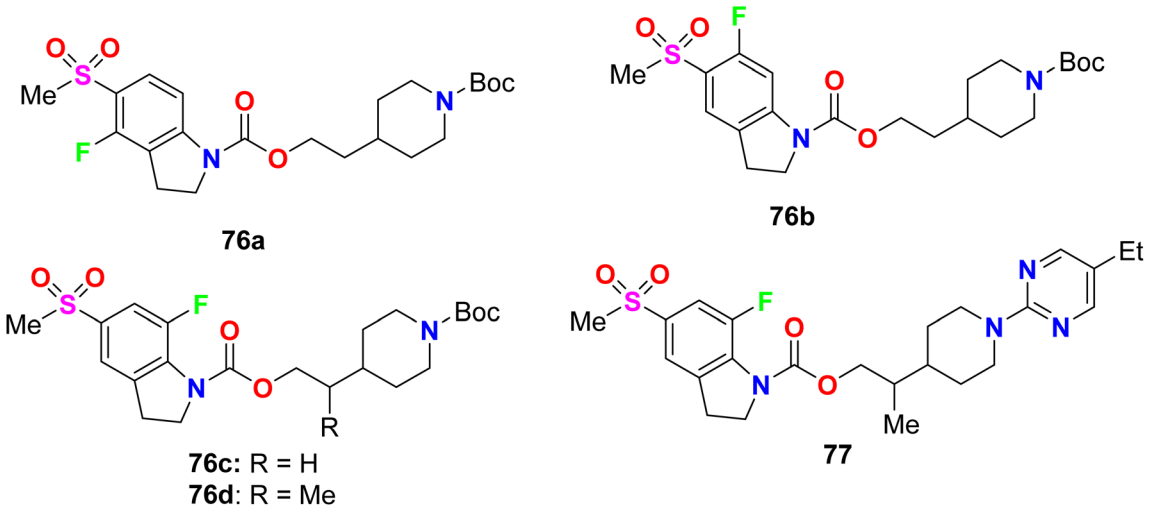

Fig. 50 Structure of fluorinated indole derivatives 76–77.

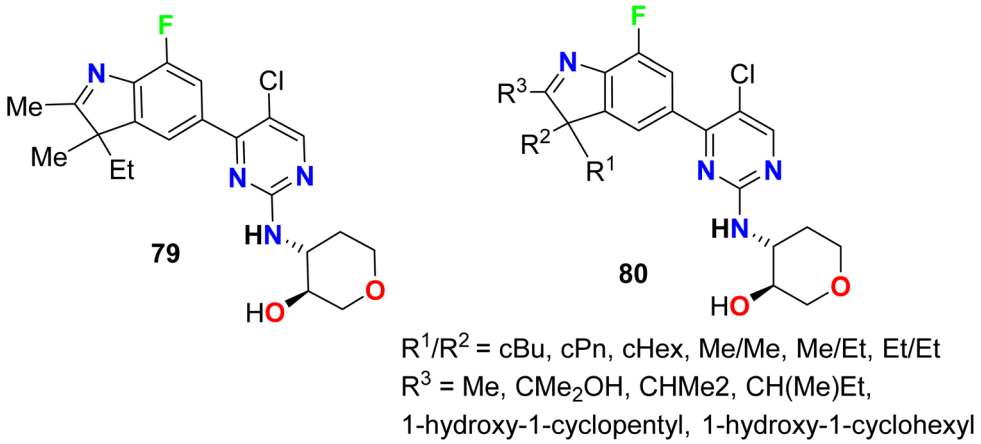

Fig. 52 Structure of fluorinated indoline hybrids **79–80**.

transporters of hSGLT1 or hSGLT2 was also determined. The synthesized 4-fluoroindole hybrids **78a–e** were found to have substantial potency and selective hSGLT2 inhibitor with IC_{50} values ranged between 1.4 to 24 nM with high anti-hyperglycemic activity in high-fat diet-fed KK mice. Compound **78d** was the most potent and most selective inhibitor of hSGLT2 both *in vitro* and *in vivo* with $IC_{50} = 1.4$ nM, and could be considered as lead compound for further developments.[104]

A series of patented fluorinated indoline hybrids **79–80** were synthesized and evaluated as CDK4/CDK6 (cyclin-dependent kinases 4 and 6) inhibitors (Fig. 52). The inhibitory effect of the invented compounds **79–80** on CDK4/CDK6 enzymes was measured using the EnVision multi-mode detection platform to detect the fluorescence values at 665 nm and 620 nm excited at 337 nm in HTRF mode. The IC_{50} values of the tested compounds on the inhibition of CDK4 enzyme activity was found to range between 0.9 nM–9.6 nM, however, the IC_{50} values for inhibition of CDK6 enzyme activity ranged between 7.3 nM and 1038 nM. Particularly, compound **79** showed the best inhibition against both CDK4 and CDK6 enzymes with IC_{50} values of 0.9 nM and 7.3 nM, respectively.[105]

4.4. Enzymatic inhibitory activity of fluorinated benzofurans

A series of fluorinated dihydrobenzofuran scaffolds **81–83** were patented and evaluated for their enzymatic inhibitory activity against G protein-coupled receptor kinase (GRK) (Fig. 53). The *in vitro* and *in vivo* inhibition of GRK2 and/or GRK3 activity was examined to reduce the tumor growth. Most of the compounds were selective inhibitors for GRK2, and showed excellent GRK2 enzymatic inhibition potency with IC_{50} values in nanomolar scale varied between 0.53 nM to 9.17 nM and the most active compound was **83** ($IC_{50} = 0.53$ nM).[106]

4.5. Enzymatic inhibitory activity of fluorinated pyrazoles

The fluorinated pyrazol-3-caarboxylic acid derivatives **84** were reported as antilipolytic agents and against the human receptor RUP25 for the treatment of dyslipidemia (Fig. 54). The *in vitro* biological activity was evaluated using the cAMP Whole Cell

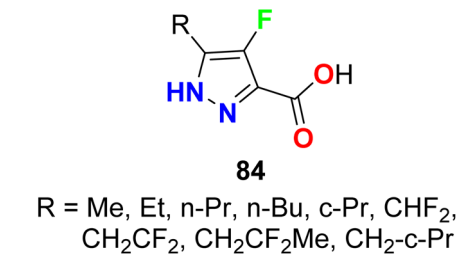

Fig. 54 Structure of fluorinated pyrazol-3-caarboxylic acid derivatives **84**.

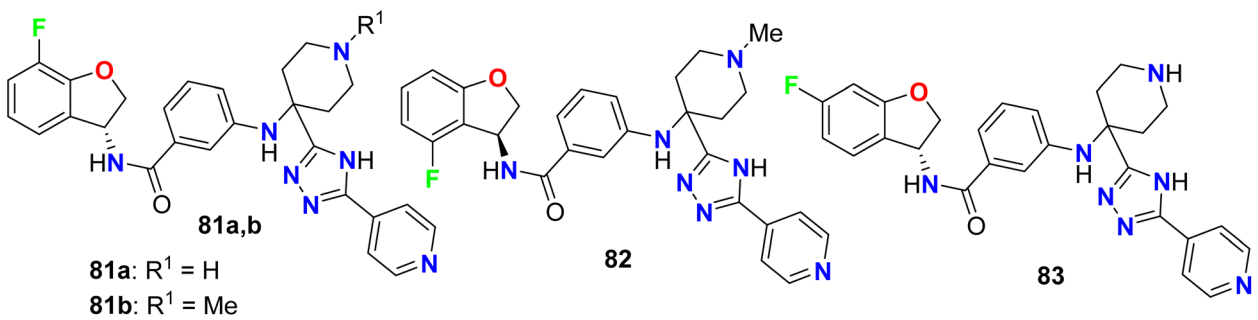

Fig. 53 Structure of fluorinated dihydrobenzofuran scaffolds **81–83**.

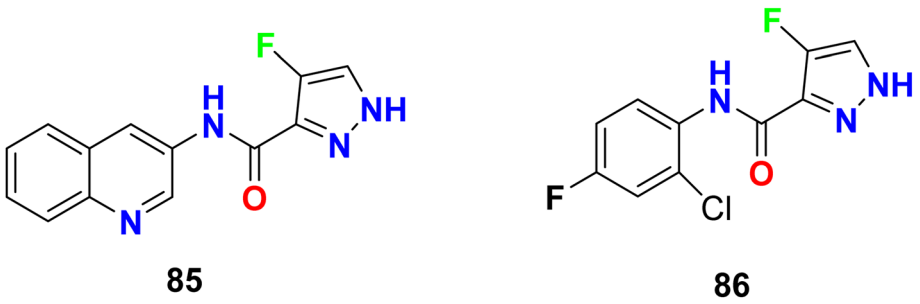

Fig. 55 Structure of fluoropyrazole-carboxamides derivatives **85–86**.

method and most of the compounds showed good activity against hRUP25, particularly compound **84** (R = Bu) had an IC_{50} value of 0.9 μM.[107]

In addition, Pelcman *et al.* patented the fluoropyrazole-carboxamides **85–86** (Fig. 55) as inhibitors of 15-lipoxygenase activity, that catalyzes arachidonic acid oxygenation at position 15, that were useful in the treatment of inflammatory diseases. The tested compounds exhibited inhibition of 15-lipoxygenase activity with an IC_{50} value of 10 μM.[108,109]

The fluoropyrazole-carboxamides **87a–d–90a–d** (Fig. 56) were reported to display a high inhibitory activity of a7 nicotinic acetylcholine receptor (a7nAChR), ligand-dependent ionic channel in muscle fiber membrane. The bioassay was conducted using a FLIPR (Fluorescent Imaging Plate Reader) screening protocol employing the stable recombinant GH4C1 cell line expressing a7nAChR. Most of the fluoropyrazoles exhibited high inhibitory potency with EC_{50} values ranging between 10 nM and 10 μM.[110]

Trabanco-Suarez *et al.* patented the synthesis of many fluorinated pyrazole-based heterocyclic hybrids **91a–f** and **92a–f** and examined their activities as inhibitors of BACE1 (β-site APP-cleaving enzyme 1), for the treatment of Alzheimer's Disease (AD) (Fig. 57). The biological results were based on the FRET (Fluorescence Resonance Energy Transfer) assay, where the candidate for this assay was an APP (amyloid precursor protein). The examined compounds showed inhibition of FRET with pIC_{50} values 6.90–7.23.[111]

Gege *et al.* invented and patented some fluorinated pyrazole molecular hybrids **93–95** (Fig. 58) as modulators of the activity of human RAR-related orphan receptors gamma (RORγ) that are expressed in immune cells (Th17 cells) and useful in the regulation of circadian rhythms, for the treatment of the RORγ mediated chronic inflammatory. Applying the Gal4 reporter gene assay, the invented compounds displayed promising inhibitory action against RORγ with IC_{50} values < 10 nM. The pIC_{50}-values of the tested compounds were 6.2–8.3 for fluorescence resonance energy transfer (FRET), firefly (FF) and renilla normalized (REN-norm).[112]

The fluorinated pyrazole-based heterocyclic hybrids **96–97** were patented by Ahn *et al.* as good inhibitors of the activity of the diacylglycerol-acyltransferase-2 (DGAT2). The *in vitro* inhibition activity against DGAT2 was recorded in a nanomolar scale with IC_{50} values ranging within 90–128 nM (Fig. 59).[113]

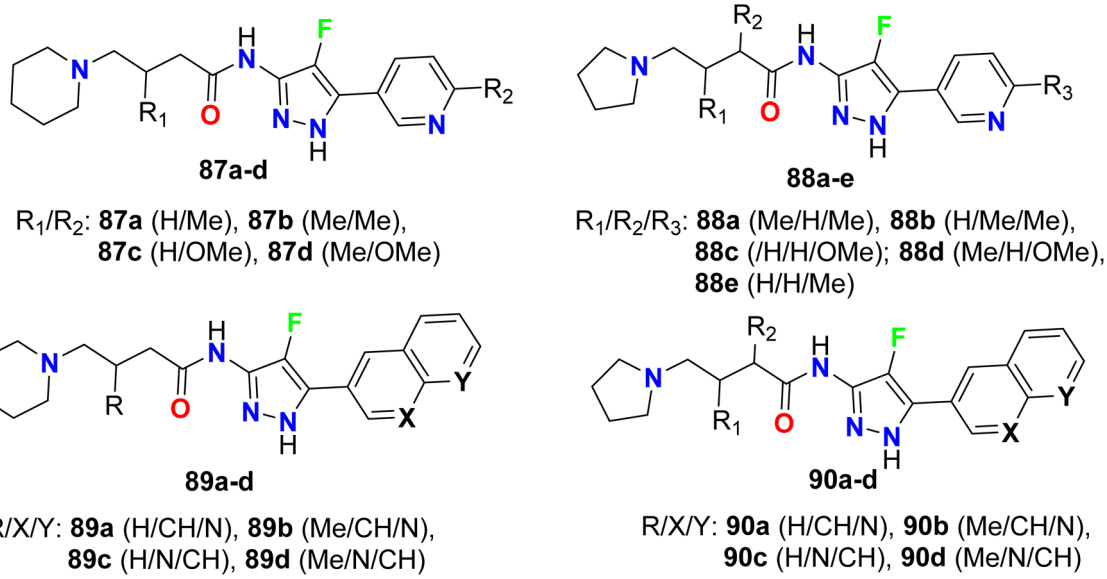

Fig. 56 Structure of fluoropyrazole-carboxamides derivatives **87–90**.

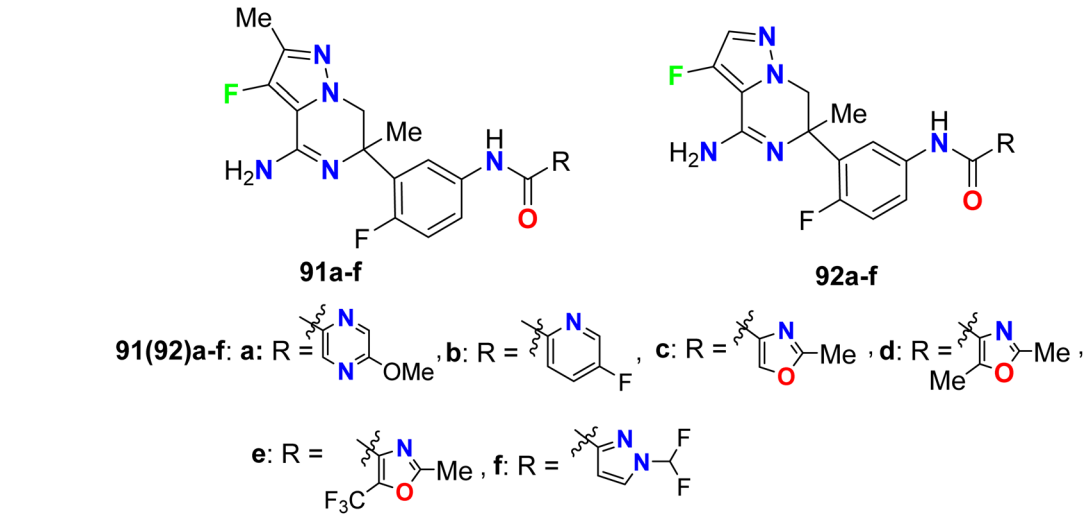

Fig. 57 Structure of fluorinated pyrazole-based heterocyclic hybrids **91–92**.

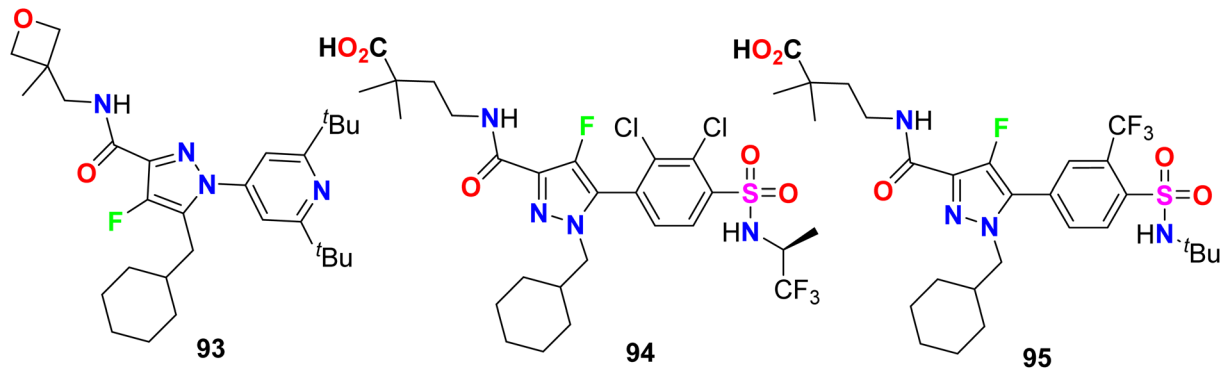

Fig. 58 Structure of fluorinated pyrazole derivatives **93–95**.

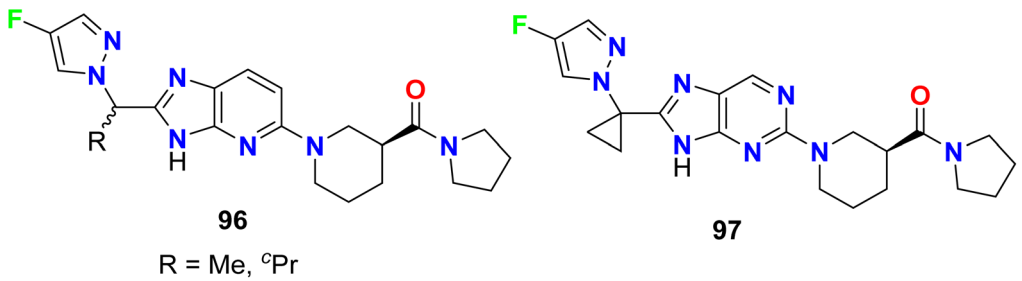

Fig. 59 Structure of fluorinated pyrazole derivatives **96–97**.

Zhou *et al.* reported two fluorinated pyrazole-based molecular hybrids **98** and **99** to be useful as inhibitors of hypoxia induced factor (HIF) prolyl hydroxylase (PHD2) for treatment of anemia. The reported invented compounds **98** and **99** displayed significant inhibition activities against HIF PHD2 with IC_{50} values of 0.5 nM and 20 nM, respectively (Fig. 60).[114,115]

Dodd *et al.* patented several fluoropyrazole hybrids **100** and **101** (Fig. 61) and evaluated their inhibition of the tyrosine kinase enzymatic activity of ABL1 (Abelson protein). The experimental bioassay measured the ABL kinase activity in a radiometric filter binding (Radio) and microfluidic mobility shift (Caliper) assays. The invented hybrids revealed high potency in the nanomolar scale with IC_{50} values ranging between 1 to 7 nM (Radio-ABL1) and 0.2–1.2 nM for (Caliper ABL1) inhibition, respectively.[116,117]

4.6. Enzymatic inhibitory activity of fluorinated indazoles

Claramunt *et al.* designed several fluorinated indazoles **102** and examined their activity as selective inhibitors of two nitric oxide synthase enzymes; inducible nitric oxide synthase (iNOS) and

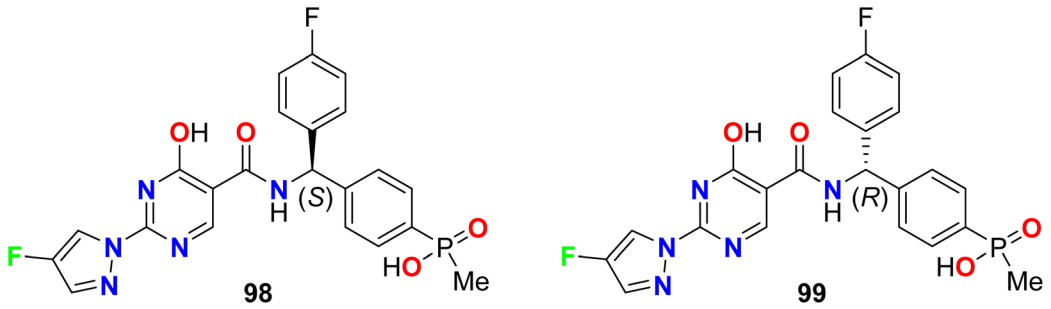

Fig. 60 Structure of fluorinated pyrazole derivatives **98–99**.

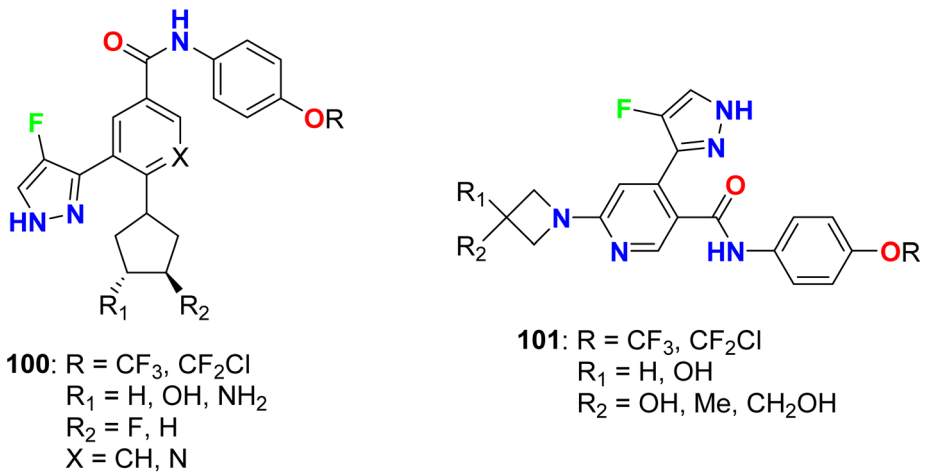

Fig. 61 Structure of fluoropyrazole derivatives **100–101**.

neuronal nitric oxide synthase (nNOS), that were useful for the regulation of blood pressure, neurotransmission, and the immune response. SAR study confirmed that R-substituents and the number and location of fluorine atoms greatly influenced the NOS inhibition process. The increasing number of fluorine atoms increased the inhibitory potency and nNOS selectivity, where fluorine atoms might form hydrogen bonds with the active center. The tetrafluoro-indazole derivative **102a** (R = Me) displayed the best inhibitory activity among the tested compounds, where it inhibited iNOS by 63% and nNOS by 83%. Surprisingly, compound **102d** (R = perfluorophenyl) showed the highest selective inhibition of nNOS activity by 80% but did not affect iNOS activity. The other derivatives exhibited partial selectivity for inhibition of iNOS and nNOS. Selective inhibition of nNOS was reported to be of great therapeutic importance for treating diabetes, neurodegenerative disorders, sepsis, and arthritis (Fig. 62).[118]

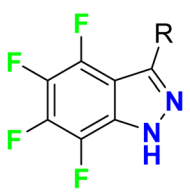

102a-e

102a: R = Me, **102b**: R = CF_3, **102c**: R = Ph,
102d: R = F_5C_6, **102e**: R = OH

Fig. 62 Structure of f fluorinated indazoles derivatives **102**.

Ballard and his research group designed a series of fluorinated indazole derivatives **103–104** (Fig. 63) that were assigned as M1-PAM (muscarinic receptor positive allosteric modulators) for the treatment or prophylaxis of Alzheimer's disease. The assay disclosed that those derivatives had potent modulator activity at the acetylcholine muscarinic receptor expressed in CHO (Chinese hamster ovary) cells by measuring the intracellular calcium with a Fluorometric Imaging Plate Reader System (FLIPR). The EC_{50} (concentration effective in producing 50% of the maximal response) of hM1 of the fluorinated pyrazoles ranged between 0.025–0.266 μM, particularly compound **104** was the most efficient with EC_{50} = 0.025 μM. Thus, these compounds were assigned as possible neurogenic agents.[119]

Hoyt *et al.* designed several fluorinated indazole hybrids **105–110** (Fig. 64) and reported them as selective inhibitors of aldosterone synthase enzyme (CYP 11B2) with little effect on steroid-11-β-hydroxylase (CYP1 1B1). The study employed V79-human cell assay and the studied compounds demonstrated potent inhibition activity of CYP 11B2 with IC_{50} values ranging between 2 nM and 250 nM, some compounds reached 60-fold

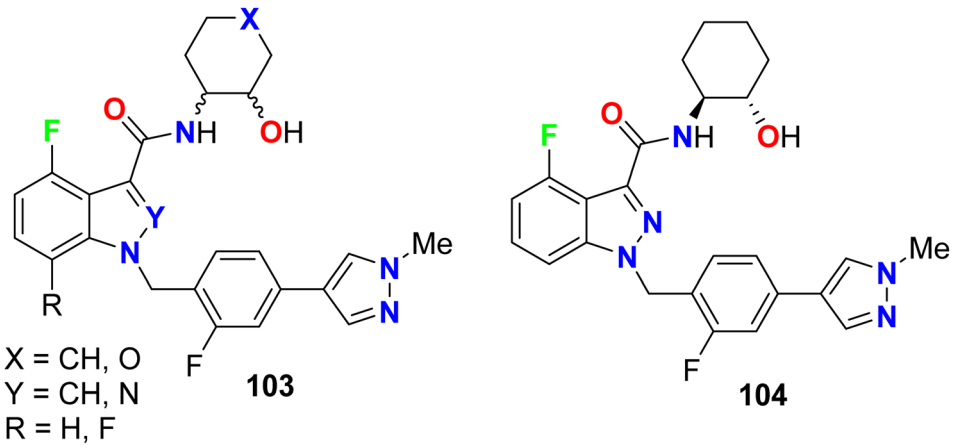

Fig. 63 Structure of f fluorinated indazoles derivatives **103–104**.

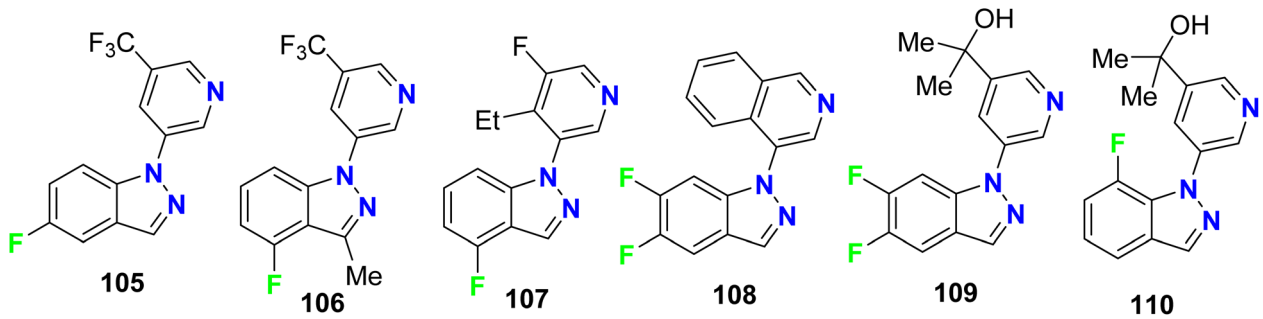

Fig. 64 Structure of fluorinated indazoles derivatives **105–110**.

selectivity for inhibition of CYP 11B2 better than CYP 11B1. For example, compounds **105**, **106**, **108–110** demonstrated inhibitions of CYP 11B2 with IC_{50} values of 83, 17, 1.9, 23, and 1.2 nM compared with 1911, 275, 107, 305 and 36.4 nM for of CYP 11B1 with selectivities of 23-, 16-, 56-, 13-, and 30-folds for CYP 11B2CYP 11B1.[120]

Some 5-fluoro- and 7-fluoroindazole derivatives **111a–h** and **112a–h** (Fig. 65) were patented as potent inhibitors of human cannabinoid receptor-1 (hCB1) receptors and their binding affinity K_i varied from 0.08–51 nM. K_i value (inhibitor constant) measure the potency of an inhibitor and it is the concentration necessary to produce half maximum inhibition. It was reported that compounds having *N*-cyclohexylmethylene moiety in general were more potent than those having *N*-pyranylmethylene moiety. In addition, the 7-fluoroindazole derivatives had better binding affinity than those of 5-fluoro isomers. The best binding affinity was recorded for compound **112f** (K_i 0.087 nM).[121]

Some 7-fluoroindazole derivatives **113a–q** (Fig. 66) were found to possess glucagon receptor antagonist activity to be useful for the treatment of type-2 diabetes mellitus *via in vitro* bioassay study. The results revealed that most of the invented fluorinated compounds had good to excellent inhibitory activity with IC_{50} values ranging between 1 nM and 500 nM. The most active compounds were **113a**, **113d**, and **113q** with IC_{50} = 0.8–2.6 nM and these fluorinated derivatives were useful as glucagon antagonists.[122]

The fluoroindazole compounds **114–116** (Fig. 67) were designed and evaluated as inhibitors of glycogen synthase kinase-3 (GSK-3) using a standard coupled enzyme system. The designed compounds were screened for their ability to inhibit the phosphorylation of tyrosine (TYR) residues through the use of western blotting of Jurkat cells dosed with the reported compounds. The phosphorylation of the specific TYR residues tested were GSK3α (TYR 279) and GSK3β (TYR 216). The synthesized compounds exhibited moderate to high inhibitory activities of both GSK3α and GSK3β.[123]

Claramunt *et al.* also reported the inhibitory action of the fluorinated indazoles **102**, **117–127** against both iNOS and nNOS. The bioassay results declared that the most potent iNOS inhibitors were arranged in descending order as follows: **102f** (98.7%) > **120** (95.6%) > **119a** (92%) > **119b** (91%)> **118b** (89.1%) > **102a** (83%), however, the most potent inhibitors of nNOS were **119a** (90.0%) and **120** (85.4%). Most of the evaluated indazoles had better selective iNOS inhibitors than nNOS, for example, at a concentration of 1 mM, compounds, **117** (10-fold), **119b** (6-fold), and **102f** (2-fold) showed the highest iNOS selective inhibitors. The indazoles having a CO_2H or CO_2R groups, **122a–c**, **123a–c** and **124a–c**, were moderate iNOS inhibitors and very weak nNOS ones. Among all fluorinated indazole derivatives

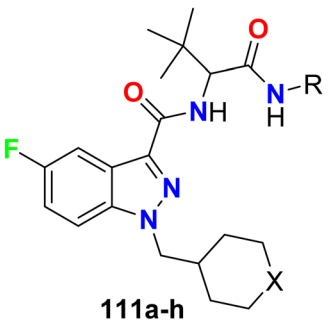

111a-h

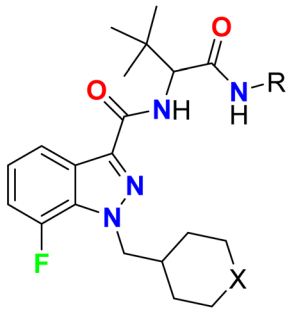

112a-h

111a: X = O; R = OH
111b: X = O; R = CH_2CONH_2
111c: X = O; R = CH_2CH_2OH
111d: X = CH_2; R = CH_2CH_2OH
111e: X = CH_2; R = CH_2CONH_2
111f: X = CH_2; R = H
111g: X = CH_2; R = $CH_2CH_2CH_2OH$
111h: X = O; R = $CH_2CH_2CH_2OH$

112a: X = O; R = cPr
112b: X = O; R = CH_2CH_2OH
112c: X = O; R = $CH_2CH_2CH_2OH$
112d: X = O; R = H
112e: X = O; R = CH_2CONH_2
112f: X = CH_2; R = CH_2CH_2OH
112g: X = CH_2; R = H
112h: X = CH_2; R = CH_2CONH_2

Fig. 65 Structure of 5-fluoro- and 7-fluoroindazole derivatives **111** and **112**.

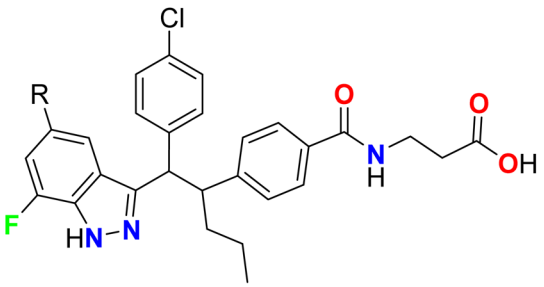

113a-q

113a: R = 4-MeC_6H_4
113b: R = Br
113c: R = H
1c3d: R = R = 3-FC_6H_4
113e: R = Ph
113f: R = 4-FC_6H_4
113g: R = 4-ClC_6H_4
113h: R = 4-MOC_6H_4
113i: R = pyridin-4-yl
113j: R = $CH_3SO_2C_6H_4$
113k: R = $CF_3C_6H_4$
113l: R = $CF_3OC_6H_4$
113m: R = 3-F-4-$MeOC_6H_3$
113n: R = 3-Cl-4-$MeOC_6H_3$
113o: R = 3,4-$F_2C_6H_3$
113p: R = CN
113q: R = Me

Fig. 66 Structure of 7-fluoroindazole derivatives **113**.

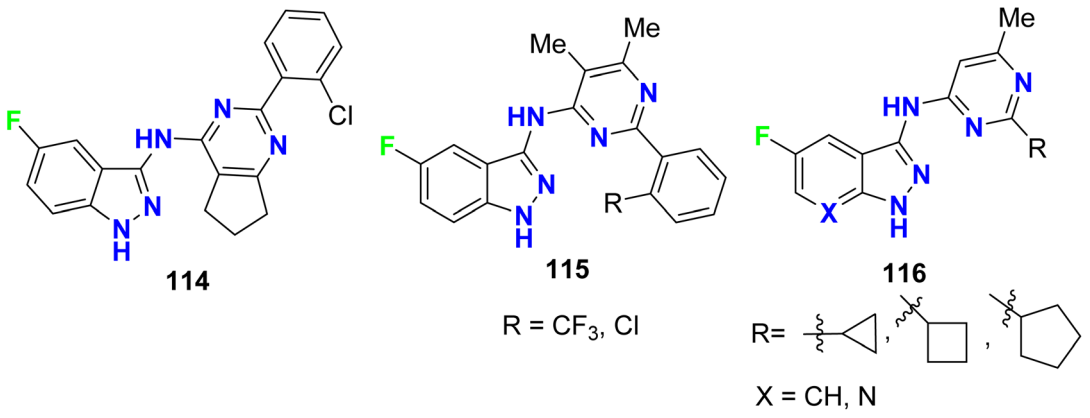

114

115

R = CF_3, Cl

116

R=

X = CH, N

Fig. 67 Structure of fluoroindazole derivatives **114–116**.

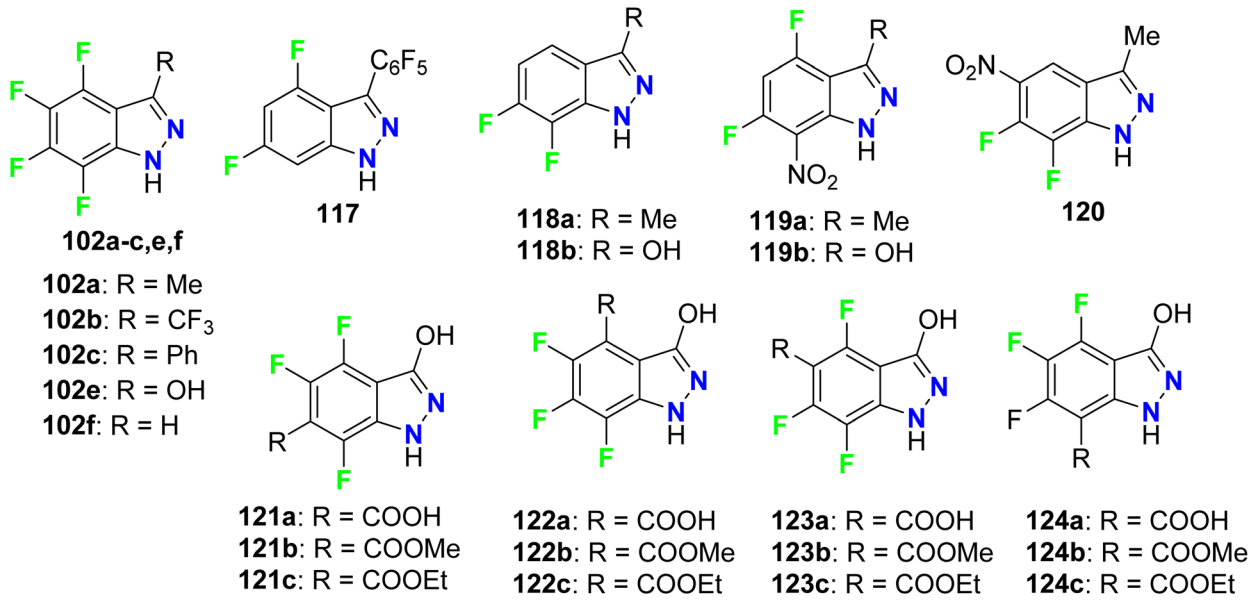

Fig. 68 Structure of fluorinated indazoles derivatives 102, 117–124.

compound **102f**, had an outstanding iNOS inhibitory action, and was a promising candidate for further drug development (Fig. 68).[124]

4.7. Enzymatic inhibitory activity of fluorinated benzothiazoles

Diabetes mellitus type II is a metabolic disease characterized by insulin resistance and high blood glucose levels. The polyol pathway was significantly activated under hyperglycemic conditions, resulting in a series of stress conditions and, eventually, cellular damage. The first enzyme of the polyol pathway implicated in the onset of long-term diabetic complications was aldose reductase.

The fluorinated benzothiazole hybrid **125** was synthesized and evaluated for its inhibitory activity against aldose reductase (ALR2/ALR1) and human protein tyrosine phosphatase-1B (PTP1B) enzymes (Fig. 69). The fluorinated benzothiazole hybrid **125** exhibited aldose reductase inhibitory activity with IC_{50} values of 46 nM (for ALR2) and 6021 nM (for ALR1), compared with Epalrestat reference (IC_{50} = 227 nM) using rat lens ALR2. Interestingly, compound **125** displayed a potent selective inhibition of ALR2 with optimal selectivity index 131. Moreover, compound **125** was found to have potent protein tyrosine phosphatase 1B (PTP1B) inhibitory activity with IC_{50} = 58.79 μM. Thus, compound **125** was a dual ALR2/PTP1B inhibitor and had promising capability for treating diabetes mellitus. Docking study proved that compound **125** adopts two hydrogen bond (HB) interactions with OH– and SH– groups of Tyr48 and Cys298, in addition to a salt bridge interaction between the carboxylate moiety and the positively charged nicotinamide ring of $NADP^+$.[125]

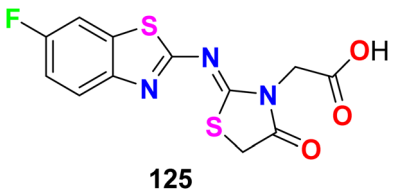

Fig. 69 Structure of fluorinated benzothiazole derivatives 125.

5. Miscellaneous bioactivity of fluorinated heterocycles

5.1. Antimalarial activity of fluorinated pyrazoles

Some fluorinated pyrazole sulfonamides were synthesized **126–128** (Fig. 70) to determine their potential ligands with selective affinities for human and *plasmodium* dihydrofolate reductase (DHFR). With AutoDock Vina and the Molecular Operating Environment (MOE), binding affinities and interactions of the fluorinated sulfonamides were benchmarked with antimalarial drugs. The binding affinity scores from both programs identified three sulfonamides with strong interactions that were comparable to or greater than the current antimalarial drugs. Compound **128** displayed strong hydrogen bonding interactions with quadruple mutated *P. falciparum* DHFR active site residues and an estimated binding energy of −7.6 kcal mol^{-1}. The presented fluorinated heterocyclic sulfonamides were promising pharmacophores and competitors to current folate pathway inhibitors. The molecular docking simulations supported the fluorinated sulfonamide ligands as promising molecules that could be used to target critical enzymes like DHFR in the *Plasmodium* folate pathway. The estimated binding affinity of fluorinated sulfonamides docked with human and *P. falciparum* DHFR isoforms were comparable to the benchmark antimalarial drugs like artesunate and stronger than sulfadoxine and pyrimethamine. The fluorinated pyrazolesulfonamide

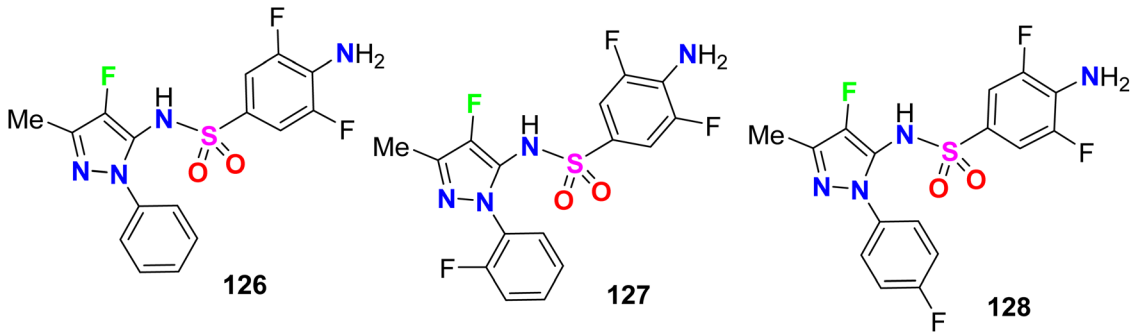

Fig. 70 Structure of fluorinated pyrazole sulfonamides derivatives **126–128**.

derivatives **126–128** matched the binding affinity of artesunate to within 0.25 kcal mol^{-1}. The fluorinated sulfonamide framework for drug design had the potential to mitigate the impacts caused by DHFR mutations. The fluorinated sulfonamides modeled also had good drug-like characteristics based on the Lipinski rule of 5, and thence became important pharmacophores for the development of potent antimalarial drugs.[126]

5.2. Anticoagulant activity of fluorinated pyrazoles

Recently, a series of *N*-acylpyrazole derivatives **129** (Fig. 71) was prepared with fluorine substitution at position-4 of the pyrazole ring and investigated their inhibition against thrombin *in vitro* to be useful as effective anticoagulants. It was reported that the efficacy in the thrombin generation assay (TGA) increases with increasing the potency in the thrombin enzyme assay, however, the fluorinated pyrazoles **129** consistently imparted decreased stability against all plasma species studied. All the fluorinated pyrazole derivatives **129** showed promising thrombin inhibition with IC_{50} values ranging from 0.004 μM to 0.06 μM with ETP (TGA) varied between 2.3 μM and 46 μM. Thus, the 4-fluoropyrazoles **129** were recommended as ideally safe and effective anticoagulants.[127]

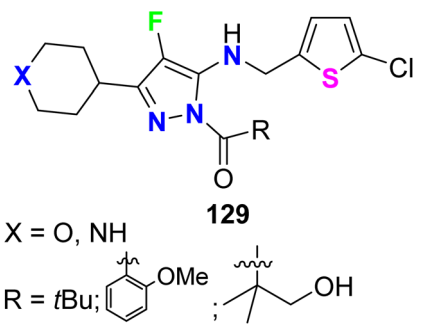

Fig. 71 Structure of *N*-acylpyrazole derivatives **129**.

5.3. Antipsychotic activity of fluorinated indoles

Four fluoroindole derivatives **130a–c** and **131** (Fig. 72) were synthesized and investigated as potent and selective dopamine receptor 4 (D_4R) antagonists for the treatment of the diseases of central nervous system. All compounds displayed high activities in the nanomolar scale, and the 6-fluoroindole derivatives **130a** and **130c** were the most active against D_4 with K_i values of 5.2 nM and 3.3 nM, also had IC_{50} values of 18.9 and 11.9 nM, respectively. On the other hand, the 6-fluoroindole derivatives **130a** were also active and selective against the dopamine receptors D_{2L} and D_{2S} with 78% and 76% inhibitions, respectively.[128]

Five fluorinated indol-2-carboxamide derivatives **132a–e** (Fig. 73) were assigned as NAM (negative allosteric modulators) of D_2R (dopamine D_2 receptor). Specifically, the 5-fluoroindole derivative **132c** (K_B = 91 μM) exhibited reduced affinity. In comparison, the 4-fluoro analogue **132b** (K_B = 18 μM, α = 0.07)

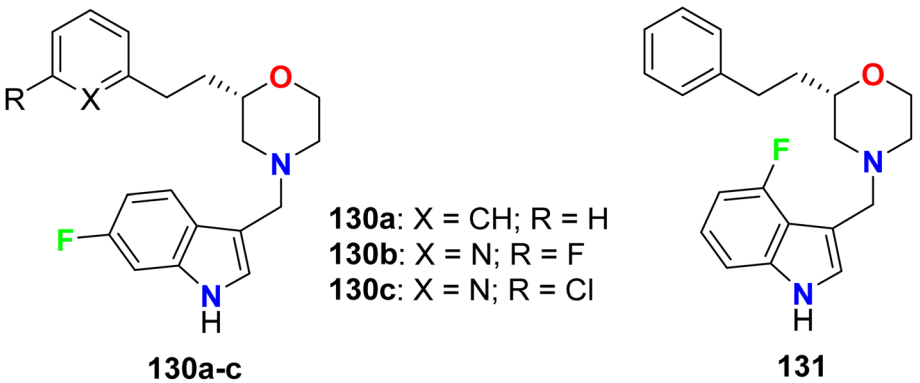

Fig. 72 Structure of fluoroindole derivatives **130a–c** and **131**.

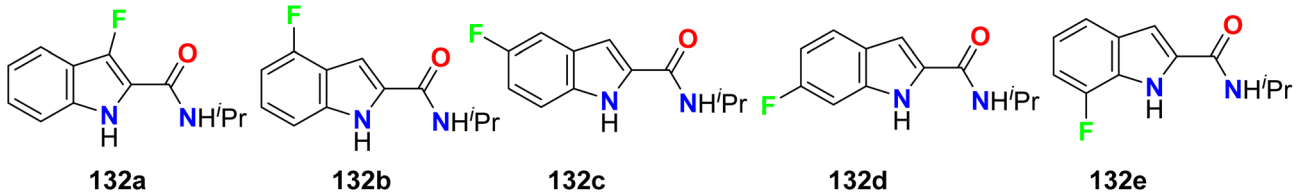

Fig. 73 Structure of fluorinated indol-2-carboxamide derivatives **132a–e**.

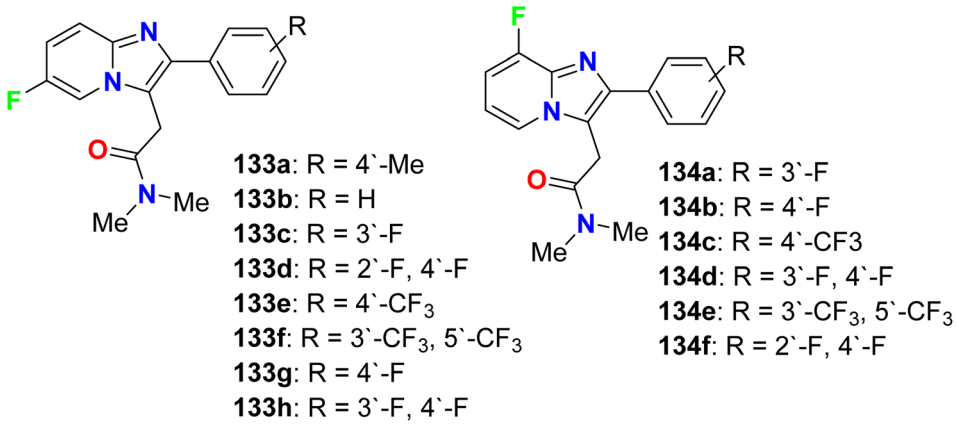

Fig. 74 Structure of 6-fluoro- and 8-fluoro-imidazo[1,2-*a*]pyridine derivatives **133** and **134**.

and 7-fluoro analogue **132e** ($K_B = 18$ μM, $\alpha = 0.11$) (where K_B is the equilibrium dissociation constant of the allosteric ligand and α is the binding cooperativity parameter between the orthosteric and allosteric ligand), both displayed enhanced binding affinity and displayed high negative cooperativity with the dopamine D_2R.[129]

Two series of (6-fluoro- and 8-fluoro-) imidazo[1,2-*a*]pyridine derivatives **133-h** and **134a–f** (Fig. 74) were reported as

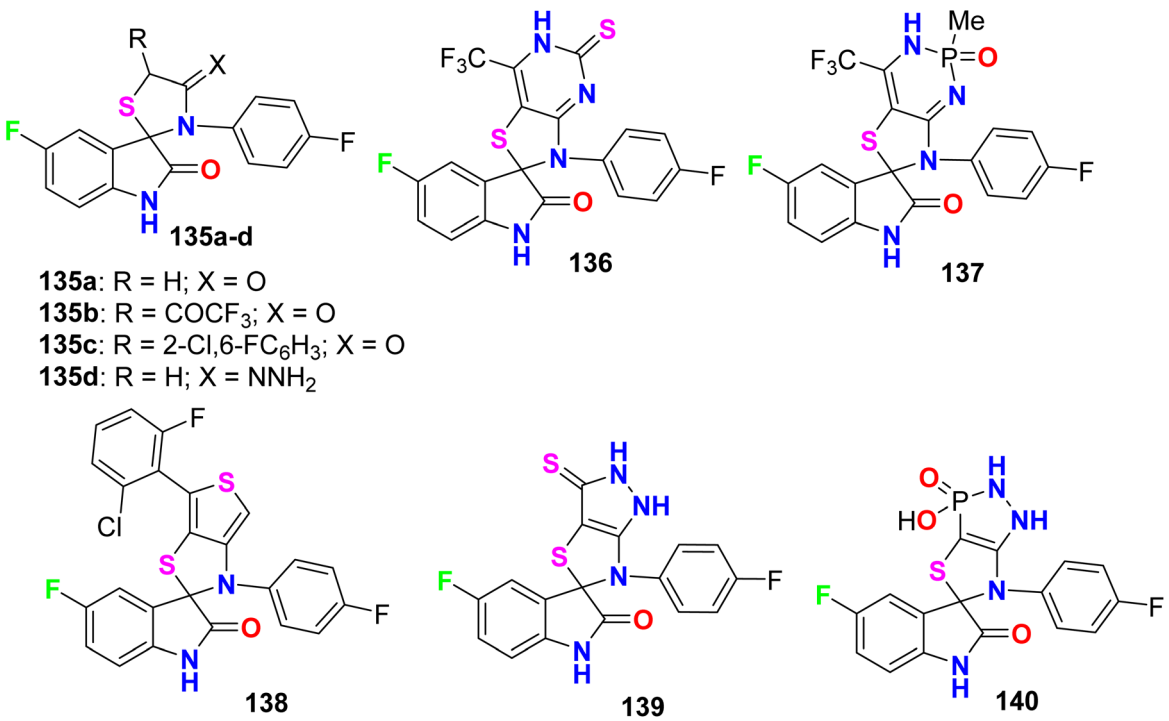

Fig. 75 Structure of fluorinated spiro[istin-thiazolidine] derivatives **135–140**.

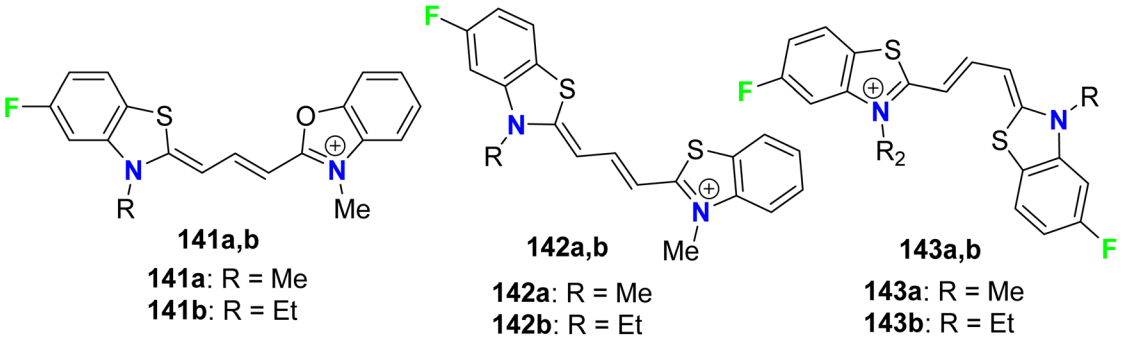

Fig. 76 Structure of fluorinated cyanine dyes benzoxazolyl or benzothiazolyl **141a**, **141b**–**143a**, **143b**.

a gamma-aminobutyric acid antagonist (GABA-A) receptors, to be useful as potential antipsychotic agents. These fluorinated derivatives showed high affinity and positive allosteric modulator properties at the GABA-A receptor and lack of hepatotoxicity when compared with zolpidem as a reference drug. Using rat brain tissue, the fluorinated compounds (**133a–h** and **134a–f**) were tested for affinity for the benzodiazepine site of the GABA-A receptor by measuring the competitive displacement of [3*H*]-flunitrazepam. SAR study revealed that 6-fluorinated derivatives were much more effective than their 8-fluorinated

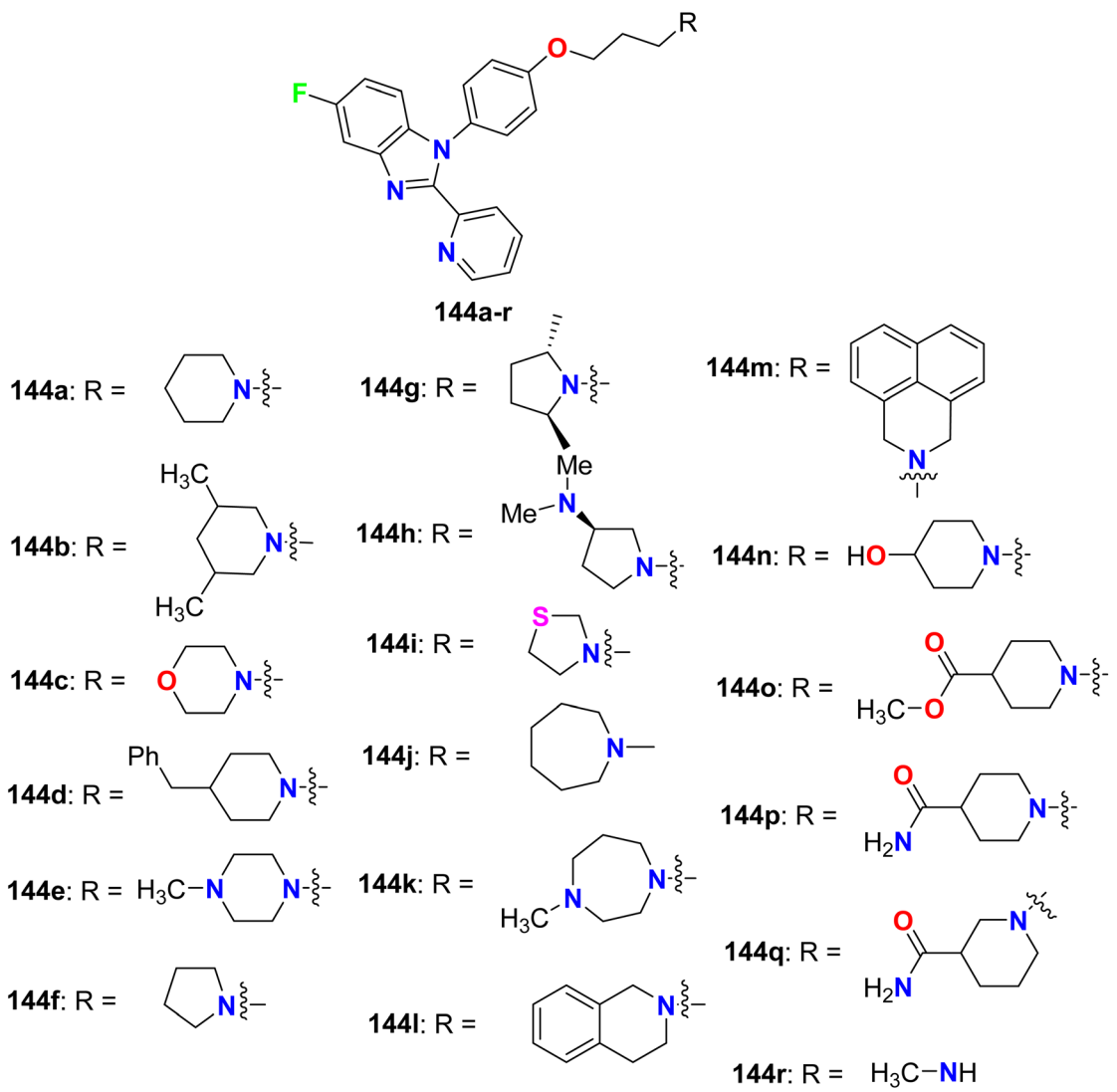

Fig. 77 Structure of 1,2-disubstituted-5-fluorobenzimidazole derivatives **144a–r**.

analogues. It was also found that compound **133a** had the highest affinity with (K_i = 25 nM), with 1.8-fold higher affinity compared with the reference drug zolpidem (K_i = 44 nM). Other 6-fluorinated derivatives **133g** (K_i = 55.6 nM), **133h** (K_i = 57.5 nM), and **133e** (K_i = 68.0 nM) showed acceptable affinities. A notable decrease in the affinity was observed after the introduction of another fluorine atom at *ortho*-position (**133d**), or its replacement into *meta*-position (**133c**). The presence of two sterically trifluoromethyl groups (**133f**) caused a complete loss of activity. In addition, compound **133g** demonstrated good antipsychotic-like activity in rats with EC_{50} = 408 nM compared with zolpidem drug (EC_{50} = 240 nM).[130]

5.4. Antioxidant activity of fluorinated indolinones

Some fluorinated spiro[istin-thiazolidine] derivatives **135–140** (Fig. 75) were synthesized and evaluated for their antioxidant activity by the 1,1-diphenyl-2-picrylhydrazyl (DPPH) protocol. The results of scavenging the stable DPPH radical were calculated at 150, 300, and 450 μM concentrations, where the fluorinated compounds scavenged 49–78% of the DPPH radicals. Compounds **136** and **137** proved to have potent antioxidant activities of 77.45% and 77.78% compared with ascorbic acid (55.2%), at 450 μM concentration, respectively.[131]

5.5. Antiprotozoal activity of fluorinated benzothiazoles

Some fluorinated cyanine dyes having benzoxazolyl or benzothiazolyl moieties **141a**, **141b**–**143a**, **143b** were synthesized and screened for their *in vitro* antiprotozoal activities (Fig. 76). The *in vitro* bioassay was conducted using *P. falciparum* (K1), *Trypanosoma cruzi*, *T. brucei rhodesiense*, and *L. donovani*. The antimalarial activities of the fluorinated cyanines incorporating benzoxazolyl and benzothiazolyl groups **141a**, **141b**, and **142a**, **142b** against *P. falciparum* (K1) demonstrated high antimalarial activity with IC_{50} values ranged between 2–7 nM with selectivity index (SI) varied between 32–586, where both compounds **143a**, **143b** both had the most antiprotozoal activity with IC_{50} = 2 nM.[132]

5.6. Histamine-H_3 receptor activity of fluorinated benzimidazoles

1,2-Disubstituted-5-fluorobenzimidazole derivatives **144a–r** (Fig. 77) were reported by Aslanian *et al.* and were evaluated for histamine H_3 receptor antagonists. The results showed that most of the derivatives had good to excellent H_3 binding affinity, particularly compounds **144a** (having piperidinyl group) and **144f** (having pyrrolidinyl group) were identified as the most potent H_3 antagonists with K_i value of 1.2 nM for both. Due to the excellent activity of compound **144a** at the human H_3 receptor, it was further profiled and tested against the mouse H_3 receptor with K_i of 1.8 nM. In addition, the *in vitro* human cAMP assay with an AlphaScreen cAMP assay kit, and showed functional activity with 0.1 nM. Furthermore, compound **144a** presented a reasonable oral pharmacokinetic profile in a high throughput rat pharmacokinetic assay.[133]

5.7. Serotonin receptor affinity of fluorinated indoles and indazoles

A series of 5-fluoroindole derivatives **145–150** (Fig. 78). were synthesized by Ojeda-Gómez *et al.* and investigated their *in vitro* affinities for the serotonin transporter (SERT). Among the synthesized compounds, the derivatives **145a–c** presented good

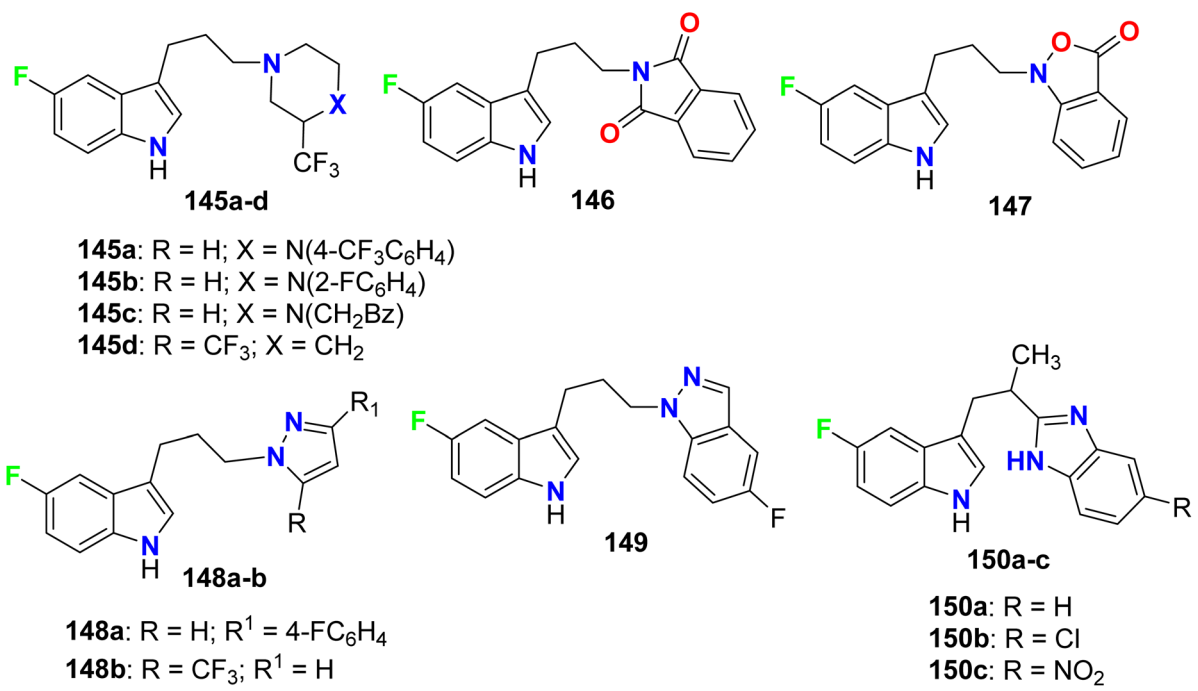

Fig. 78 Structure of 5-fluoroindole derivatives **145–150**.

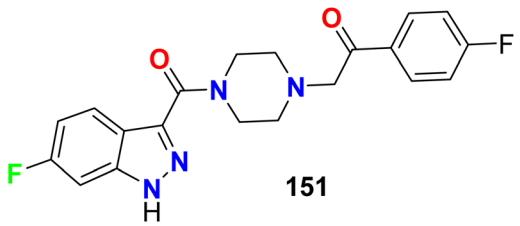

Fig. 79 Structure of 6-fluoroindazole derivative **151**.

binding affinities (K_i = 33.0, 48.0, and 17 nM, respectively). The rest compounds showed moderate or no binding affinities.[134]

The 5-HT receptors were divided into seven main groups (5-HT_{1-7}). The 6-fluoroindazole derivative **151** was reported as a modulator of the human serotonin (5-HT_{2A}) receptor, radioligand binding assay of compound **151** for human 5-HT_{2A} serotonin receptor was conducted using the 5-HT_2 agonist [^{125}I] DOI (2,5-dimethoxy-4-iodo-phenylisopropylamine) as radioligand. Compound **151** showed DOI binding affinity with an IC_{50} value of 2.3 nM (Fig. 79).[135]

A series of fluorinated indazole derivatives **152–154** (Fig. 80) having naphthylsulfonyl group were designed and their binding affinity for 5-HT_6 (5-hydroxytryptamine-6) receptor, for the treatment of central nervous system disorders, was patented. Compounds **152–154** demonstrated significant 5-HT_6 affinity and selectivity. Interestingly, all compounds showed promising binding affinity (K_i) in a nanomolar scale ranging between 0.01 nM ~45 nM, particularly compounds **153a**, **153b**, **153e**, and **153f** presented the highest binding affinity for 5-HT_6 receptor with K_i values of 0.01–10 nM.[136]

Several derivatives of fluorinated indazole **155–158** were invented and their agonist activity for the 5-HT_4 (5-hydroxytryptamine-4) receptor was screened out (Fig. 81). All compounds **155–158** possessed excellent 5-HT_4 receptor agonist activity in the nanomolar scale with IC_{50} values <40 nM and

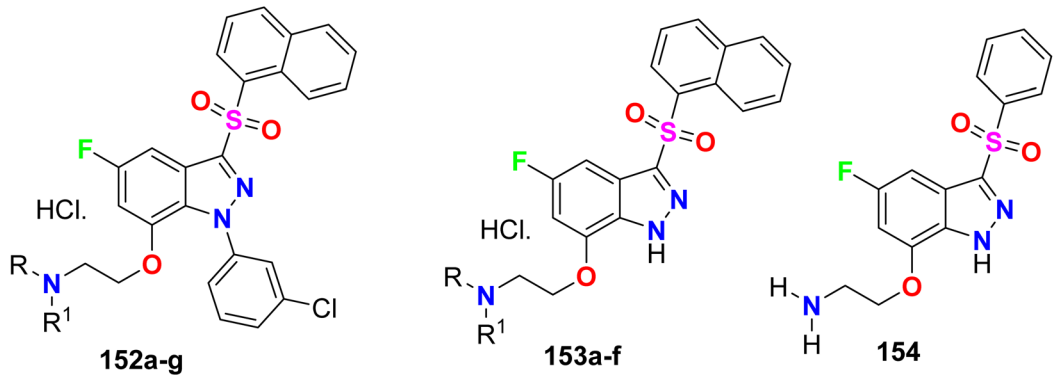

152a: R = H; R^1 = H
152b: R = Me; R^1 = H
152c: R = Et; R^1 = H
152d: R = Me; R^1 = Me
152e: R = Et; R^1 = Et
152f: R/R^1 = (-$CH_2(CH_2)_3CH_2$-)
152g: R/R^1 = (-$CH_2(CH_2)_2CH_2$-)

153a: R = Me; R^1 = H
153b: R = Et; R^1 = H
153c: R = Me; R^1 = Me
153d: R = Et; R^1 = Et
153e: R/R^1 = (-$CH_2(CH_2)_3CH_2$-)
153f: R/R^1 = (-$CH_2(CH_2)_2CH_2$-)

Fig. 80 Structure of fluorinated indazole derivatives **152–154**.

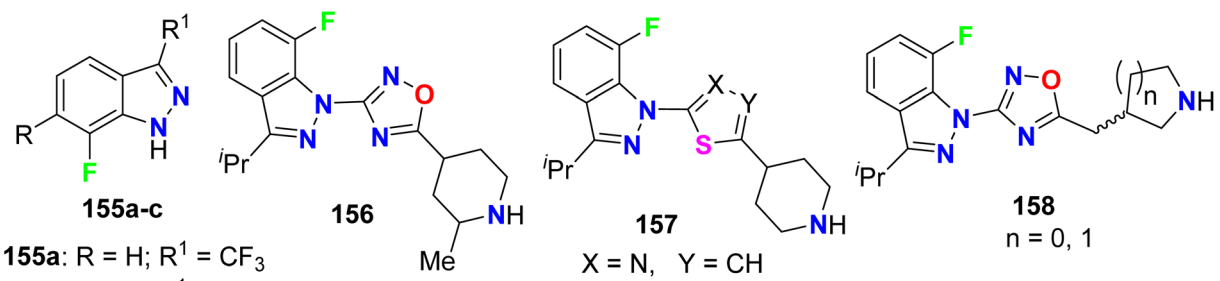

155a: R = H; R^1 = CF_3
155b: R = F; R^1 = Et
155c: R = F; R^1 = ^{i}Pr)

X = N, Y = CH
X = CH, Y = N

Fig. 81 Structure of fluorinated indazole derivatives **155–158**.

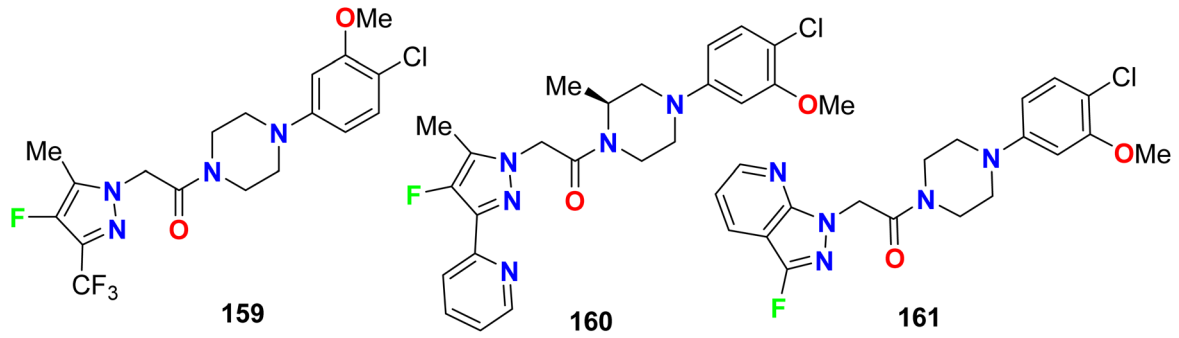

Fig. 82 Structure of piperazine-based 4-fluoropyrazole derivatives **159–161**.

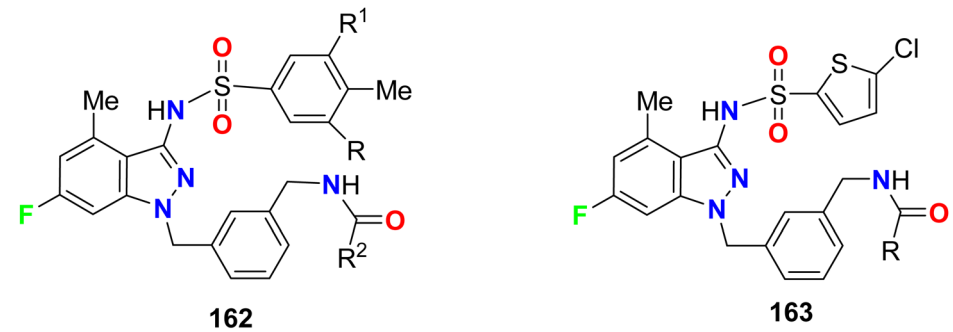

Fig. 83 Structure of piperazine-based 4-fluoropyrazole derivatives **159–161**.

most of the studied compounds had EC_{50} ranging between 3.7 nM and 53.0 nM. In addition, the intrinsic activities (IA) of the tested fluorinated indazoles varied between 26–125%, and the best result was for compound **155a** (IA = 125%).[137]

5.8. Chemokine receptor activity of fluorinated pyrazoles and indazoles

The piperazine-based 4-fluoropyrazole molecular hybrids **159–161** (Fig. 82), were synthesized and patented as antagonists of C–C chemokine receptor-1 (CCR1) and had *in vivo* anti-inflammatory activity. The chemotaxis assay showed good CCR1 antagonistic activity of both compounds **159** and **160** with IC_{50} < 0.5 μM but compound **161** had an IC_{50} value of 1.0 μM.[138–141]

The 6-fluorininated indazole scaffolds **162–163** (Fig. 83) were synthesized and evaluated as allosteric human CCR4 antagonists. The [^{35}S]GTPγS (*i.e.* guanosine 5′-*O*-[gamma-thio] triphosphate) binding assay, that measures the level of G-protein activation following agonist occupation of GPCR (G-

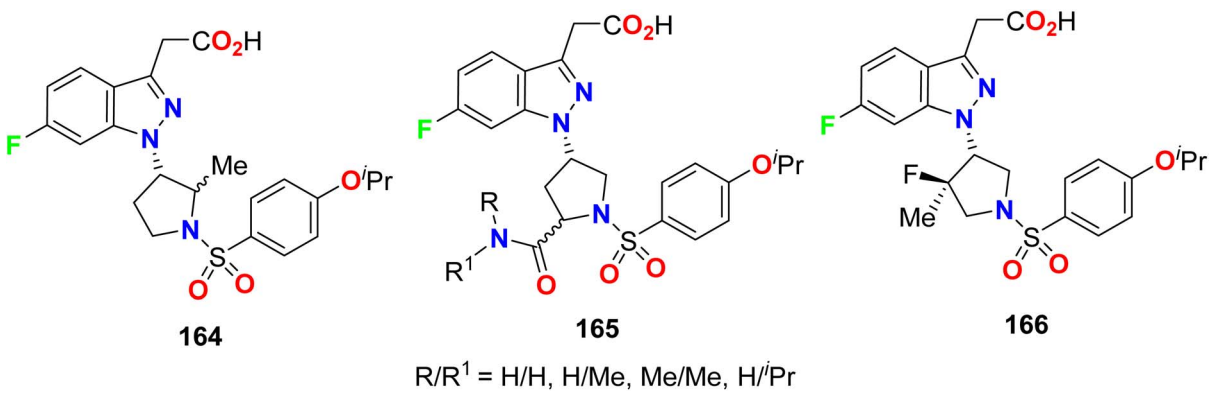

Fig. 84 Structure of 6-fluoro-1-pyrrolinyl-indazole derivatives **164–166**.

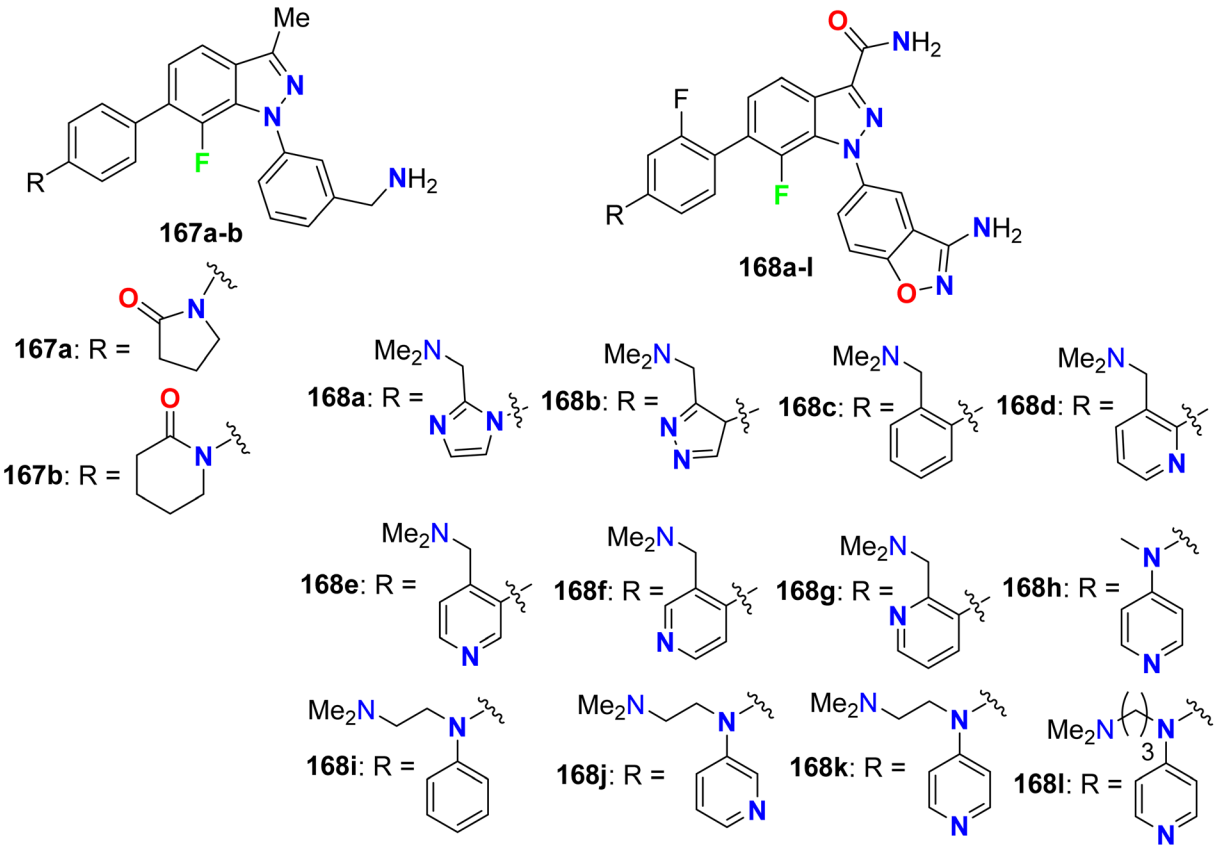

Fig. 85 Structure of 7-fluoroindazole derivatives **167a–b** and **168a–l**.

protein-coupled receptor), was studied *in vitro*. Compounds **162** and **163** demonstrated human CCR4 antagonistic activity in the range: 6.0 ≤ GTPγS pIC_{50} < 8.1.[142,143]

5.9. Prostaglandin-D2 receptor activity of fluorinated indazoles

The 6-fluoro-1-pyrrolinyl-indazole derivatives **164–166** (Fig. 84) were described and examined as antagonists of the Prostaglandin D2 (PGD2) receptor. The *in vitro* binding assay of human CRTH2 (chemoattractant receptor-homologous molecule expressed on T-helper type-2 cells) was measured, where activation of CRTh2 receptors occurs *via* prostaglandin D2 (PGD2). The results showed that most of the tested compounds displayed the high inhibitory activity of CRTH2 with K_i values <100 nM, especially compound **166** presented a K_i value of 2.8 nM for the CRTH2 receptor.[144,145]

5.10. Xa-factor inhibitory activity of fluorinated indazoles

A series of 7-fluoroindazole derivatives **167a–b** and **168a–l** were described as potent and selective inhibitors of factor Xa, that were useful as anticoagulant agents (Fig. 85). The 7-fluoroindazoles **167a–b** were highly active against factor Xa, where their potencies (fXa K_i) were 223 and 124 nM compared with their non-fluorinated analogues K_i > 14 400 and 6850 nM, respectively, and their selectivities of *versus* trypsin were about 4-fold and 10-fold, respectively. In addition, most of the 7-fluoroindazole series **168a–l** disclosed significant factor Xa potency (K_i) ranged between 1.4–15 nM, particularly compound **168b** was the most potent where the presence of 1*H*-pyrazole-moiety caused a great enhancement of the factor Xa K_i to be 1.4 nM. The SAR study revealed that the factor Xa inhibitory potencies of 7-fluoroindazole derivatives **167a** and **167bc** were about 60-fold greater ($\Delta\Delta G \approx 2.4$ kcal mol^{-1}) compared with their corresponding non-fluorinated indazoles. The structure of a factor Xa cocrystal having 7-fluoroindazoles proved the hydrogen bonding between the 7-fluoro atom and the N–H of Gly216 in the peptide backbone.[146]

5.11. PBR inhibition activity of fluorinated imidazo[1,2-*a*]pyridine

Synthesis of some fluorinated imidazo[1,2-*a*]pyridine heterocycles **169–170** (Fig. 86) were patented and evaluated for their binding affinity towards PBR (peripheral benzodiazepine receptor), where PBR is a mitochondrial protein participated in the cholesterol transport regulation from the outer to the inner mitochondrial membrane. The *in vitro* binding studies disclosed that compounds **169a**, **169b**, and **170** had good inhibition potencies of for the PBR binding site with IC_{50} values of 38 nM, 32 nm, and 800 nM, respectively.[147]

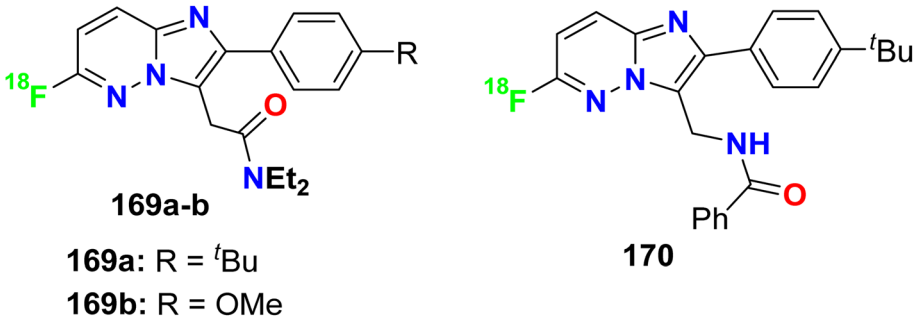

Fig. 86 Structure of fluorinated imidazo[1,2-*a*]pyridine heterocycles **169–170**.

6. Conclusions

In this review article, we collected all reports covering the biological activities of directly ring-fluorinated five-membered heterocycles and their benzo-fused systems. This review covered antiviral, anti-inflammatory, enzymatic inhibitory, antimalarial, anticoagulant, antipsychotic, antioxidant, anti-protozoal, histamine-H_3 receptor, serotonin receptor, chemokine receptor, prostaglandin-D2 receptor and PBR inhibition activities of the fluorinated heterocycles. Most of the reported fluorinated derivatives demonstrated potent antiviral activity such as *anti*-HIV-1, *anti*-HBV, hepatitis C virus (HCV), and inhibition of CVB4 virus with IC_{50} values better than the reference drugs. On the other side, the fluorinated azoles showed good anti-inflammatory inhibitory potency with good stability and selectivity for HNE over other serine proteases, with IC_{50} values of 0.1 μM. In addition, some fluorinated pyrazole-based heterocycles exhibited high inhibitory potency with IC_{50} values varied between 1 nM to 0.1 μM against PDK1 (pyruvate dehydrogenase kinase (1) for treating inflammatory diseases. In the case of enzymatic inhibitory activity, the tested derivatives of fluorinated azoles showed potent activity with IC_{50} that exceeded that of the reference drug. It is important to refer to some derivatives of fluorinated pyrazoles that were recommended as ideally safe and effective anticoagulants due to their promising thrombin inhibition with IC_{50} values ranging from 0.004 μM to 0.06 μM with ETP (TGA) varied between 2.3 μM and 46 μM. As a result, it is not surprising that fluorine is found in more than 20% of all medications on the market. The current review article is expected to be a valuable resource for researchers interested in medicinal chemistry and pharmaceutics looking into the possibility of synthesizing drug-like small fluorine molecules.

Data availability

This is a review article and there is no available data.

Conflicts of interest

The authors declare no conflicts of interest.

References

1 M. M. Heravi and V. Zadsirjan, *RSC Adv.*, 2020, **10**, 44247–44311.
2 E. Henary, S. Casa, T. L. Dost, J. C. Sloop and M. Henary, *Pharm.*, 2024, **17**, 281.
3 M. Inoue, Y. Sumii and N. Shibata, *ACS Omega*, 2020, **5**, 10633–10640.
4 C. Zhang, *ACS Omega*, 2022, **7**, 18206–18212.
5 J. Fried and E. F. Sabo, *J. Am. Chem. Soc.*, 1954, **76**, 1455–1456.
6 D. O'Hagan and J. Fluor, *Chem*, 2010, **131**, 1071–1081.
7 M. Inoue, Y. Sumii and N. Shibata, *ACS Omega*, 2020, **5**, 10633–10640.
8 T. T. Simur, T. Ye, Y. J. Yu, F. L. Zhang and Y. F. Wang, *Chin. Chem. Lett.*, 2022, **33**, 1193–1198.
9 *Fluorine in Heterocyclic Chemistry*, ed. V. Nenajdenko, Springer, 2014, vol. 1, 2.
10 *Fluorinated Heterocyclic Compounds: Synthesis, Chemistry and Applications*, ed. V. A. Petrov, Wiley, New York, 2009.
11 *Fluorinated Heterocycles*, ed. A. Gakh and K. L. Kirk, ACS, Washington, 2009.
12 V. P. Reddy, Organofluorine compounds in biology and medicine, *Chapter 9, Organofluorine Compounds as Anticancer Agents*, Elsevier, 2015, pp. 265–300.
13 N. A. Meanwell, *J. Med. Chem.*, 2018, **61**, 5822–5880.
14 S. Purser, P. R. Moore, S. Swallow and V. Gouverneur, *Chem. Soc. Rev.*, 2008, **37**, 320–330.
15 H. J. Bohm, D. Banner, S. Bendels, M. Kansy, B. Kuhn, K. Muller, U. Obst-Sander and M. Stahl, *ChemBioChem*, 2004, **5**, 637–643.
16 X. G. Hu and L. Hunter, *Beilstein J. Org. Chem.*, 2013, **9**, 2696–2708.
17 N. Sheikhi, M. Bahraminejad, M. Saeedi and S. S. Mirfazli, *Eur. J. Med. Chem.*, 2023, **260**, 115758.
18 W. K. Hagman, *J. Med. Chem.*, 2008, **51**, 4359–4369.
19 J. A. Olsen, D. W. Banner, P. Seiler, B. Wagner, T. Tschopp, U. Obst-Sander, M. Kansy, K. Muller and F. Diederich, *ChemBioChem*, 2004, **5**, 666–675.
20 J. A. Olsen, D. W. Banner, P. Seiler, U. O. Sander, A. D'Arcy, M. Stihle, K. Muller and F. Diederich, *Angew. Chem., Int. Ed.*, 2003, **42**, 2507–2511.

21 K. Muller, C. Faeh and F. Diederich, *Science*, 2007, **317**, 1881–1886.
22 P. Zhou, J. Zou, F. Tian and Z. Shang, *J. Chem. Inf. Model.*, 2009, **49**, 2344–2355.
23 Y. X. Du and X. P. Chen, *Clin. Pharmacol. Ther.*, 2020, **108**, 242–247.
24 B. K. Kim, J. Oh, S. Y. Kwon, W. Hyeok and H. Lee, *J. Hepatol.*, 2009, **51**, 829–834.
25 P. Fernandez-Calotti, R. Gamberale, M. Costas, J. S. Avalos, J. Geffner and M. Giordano, *Int. Immunopharmacol.*, 2006, **6**, 715–723.
26 Q. Meng, N. Liu, B. Huang, P. Zhan and X. Liu, *Expert Opin. Ther. Pat.*, 2015, **25**, 1477–1486.
27 D. C. Liotta and G. R. Painter, *Acc. Chem. Res.*, 2016, **49**, 2091–2098.
28 D. Ding, S. Xu, X. Zhang, X. Jiang, S. Cocklin, A. Dick, P. Zhan and X. Liu, *Expert Opin. Drug Discovery*, 2023, **18**, 5–12.
29 World Health Organization, "*International nonproprietary names for pharmaceutical substances (INN): recommended INN: list 62*", WHO Drug Information, 2009, 23, 3, p. 261.
30 R. J. Hamilton, *Tarascon Pocket Pharmacopoeia 2015 Deluxe Lab-Coat Edition*, Jones & Bartlett Learning, 2015, pp. 434–435.
31 L. H. Wang, J. Begley, R. L. St. Claire III, J. Harris, C. Wakeford and F. S. Rousseau, *AIDS Res. Hum. Retroviruses*, 2004, **20**, 1173–1182.
32 J. Y. Feng, J. Shi, R. F. Schinazi and K. S. Anderson, *FASEB J.*, 1999, **13**, 1511–1517.
33 N. A. Meanwell, O. B. Wallace, H. Fang, H. Wang, M. Deshpande, T. Wang, Z. Yin, Z. Zhang, B. C. Pearce, J. James, K. S. Yeung, Z. Qiu, J. J. K. Wright, Z. Yang, L. Zadjura, D. L. Tweedie, S. Yeola, F. Zhao, S. Ranadive, B. A. Robinson, Y. F. Gong, H. G. Wang, W. S. Blair, P. Y. Shi and R. J. Colonno, *Bioorg. Med. Chem. Lett.*, 2009, **19**, 1977–1981.
34 J. P. Begue and D. Bonnet-Delpon, *Bioorganic and Medicinal Chemistry of Fluorine*, Wiley, Hoboken. 2008.
35 E. A. Kitas, G. Galley, R. Jakob-Roetne, A. Flohr, W. Wostl, H. Mauser, A. M. Alker, C. Czech, L. Ozmen, P. David-Pierson, D. Reinhardt and H. Jacobsen, *Bioorg. Med. Chem. Lett.*, 2008, **18**, 304–308.
36 P. L. Kalar, S. Agrawal, S. Kushwaha, S. Gayen and K. Das, *Curr. Org. Chem.*, 2023, **27**, 190–205.
37 R. Chatterjee, R. Dandela and J. Fluor, *Chem*, 2023, **268**, 110133.
38 R. Szpera, D. F. Moseley, L. B. Smith, A. J. Sterling and V. Gouverneur, *Angew Chem. Int. Ed. Engl.*, 2019, **58**, 14824–14848.
39 M. D. Markus, *Chem. Soc. Rev.*, 2018, **47**, 5786–5865.
40 K. M. Dawood, *Tetrahedron*, 2004, **60**, 1435–1451.
41 K. M. Dawood and T. Fuchigami, *J. Org. Chem.*, 2004, **69**, 5302–5306.
42 K. M. Dawood and T. Fuchigami, *J. Org. Chem.*, 2001, **66**, 7691–7695.
43 K. M. Dawood, H. Ishii and T. Fuchigami, *J. Org. Chem.*, 2001, **66**, 7030–7034.
44 T. Fuchigami, S. Higashiya, Y. Hou and K. M. Dawood, *Rev. Heteroatom Chem.*, 1999, **19**, 67–78.
45 M. G. Campbell and T. Ritter, *Org. Process Res. Dev.*, 2014, **18**, 474–480.
46 A. A. Abbas, T. A. Farghaly and K. M. Dawood, *RSC Adv.*, 2024, **14**, 19752–19779.
47 A. A. Abbas and K. M. Dawood, *Expert Opin. Drug Discovery*, 2022, **17**, 1357–1376.
48 K. M. Dawood, T. A. Farghaly and M. A. Raslan, *Curr. Org. Chem.*, 2020, **24**, 1943–1975.
49 K. M. Dawood and A. A. Abbas, *Expert Opin. Ther. Pat.*, 2020, **30**, 695–714.
50 H. Behbehani, K. M. Dawood and T. A. Farghaly, *Expert Opin. Ther. Pat.*, 2018, **28**, 5–29.
51 D. M. Mohamed, N. A. Kheder, M. Sharaky, M. S. Nafie, K. M. Dawood and A. A. Abbas, *RSC Adv.*, 2024, **14**, 24992–25006.
52 J. Wu, W. Yu, L. Fu, W. He, Y. Wang, B. Chai, C. Song and J. Chang, *Eur. J. Med. Chem.*, 2013, **63**, 739–745.
53 Y. Liu, Y. Peng, J. Lu, J. Wang, H. Ma, C. Song, B. Liu, Y. Qiao, W. Yu, J. Wu and J. Chang, *Eur. J. Med. Chem.*, 2018, **143**, 137–149.
54 D. B. Smith, G. Kalayanov, C. Sund, A. Winqvist, T. Maltseva, V. J. P. Leveque, S. Rajyaguru, S. L. Pogam, I. Najera, K. Benkestock, X. X. Zhou, A. C. Kaiser, H. Maag, N. Cammack, J. A. Martin, S. Swallow, N. G. Johansson, K. Klumpp and M. Smith, *J. Med. Chem.*, 2009, **52**, 2971–2978.
55 M. I. Kharitonova, K. V. Antonov, I. V. Fateev, M. Y. Berzina, A. L. Kaushin, A. S. Paramonov, S. K. Kotovskaya, V. L. Andronova, I. D. Konstantinova, G. A. Galegov, V. N. Charushin and A. I. Miroshnikov, *Synthesis*, 2017, **49**, 1043–1052.
56 S. Martínez-Montero, S. Fernández, Y. S. Sanghvi, E. A. Theodorakis, M. A. Detorio, T. R. Mcbrayer, T. Whitaker, R. F. Schinazi, V. Gotor and M. Ferrero, *Bioorg. Med. Chem.*, 2012, **20**, 6885–6893.
57 P. Das, S. Boone, D. Mitra, L. Turner, R. Tandon, D. Raucher and A. T. Hamme, *RSC Adv.*, 2020, **10**, 30223–30237.
58 P. Jones, D. C. Pryde and T. D. Tran, *WO Pat.*, PCT WO 2007093901, 2007.
59 J. D. Oslob, R. S. McDowell, R. Johnson, H. Yang, M. Evanchik, C. A. Zaharia, H. Cai and L. W. Hu, *WO Pat.*, PCT WO 2014008197, 2014.
60 L. R. Roberts, J. Bryans, K. Conlon, G. McMurray, A. Stobie and G. A. Whitlock, *Bioorg. Med. Chem. Lett.*, 2008, **18**, 6437–6440.
61 L. H. Jones, G. Allan, O. Barba, C. Burt, R. Corbau, T. Dupont, T. Knöchel, S. Irving, D. S. Middleton, C. E. Mowbray, M. Perros, H. Ringrose, N. A. Swain, R. Webster, M. Westby and C. Phillips, *J. Med. Chem.*, 2009, **52**, 1219–1223.
62 Y. Gai, Y. S. Or, Z. Wang, *WO Pat.*, PCT WO 2009076173A2, 2009.
63 F. Piscitelli, A. Coluccia, A. Brancale, G. La Regina, A. Sansone, C. Giordano, J. Balzarini, G. Maga, S. Zanoli, A. Samuele, R. Cirilli, F. L. Torre, A. Lavecchia,

E. Novellino and R. Silvestri, *J. Med. Chem.*, 2009, **52**, 1922–1934.
64 G. La Regina, A. Coluccia, A. Brancale, F. Piscitelli, V. Gatti, G. Maga, A. Samuele, C. Pannecouque, D. Schols, J. Balzarini, E. Novellino and E. Silvestri, *J. Med. Chem.*, 2011, **54**, 1587–1598.
65 G. La Regina, A. Coluccia, F. Piscitelli, A. Bergamini, A. Sinistro, A. Cavazza, G. Maga, A. Samuele, S. Zanoli, E. Novellino and M. Artico, *J. Med. Chem.*, 2007, **50**, 5034–5038.
66 K. S. Yeung, Z. Qiu, Q. Xue, H. Fang, Z. Yang, L. Zadjura, C. J. D'Arienzo, B. J. Eggers, K. Riccardi, P. Y. Shi, Y. F. Gong, M. R. Browning, Q. Gao, S. Hancel, K. Santone, P. F. Lin, N. A. Meanwell and J. K. Kadow, *Bioorg. Med. Chem. Lett.*, 2013, **23**, 198–202.
67 K. S. Yeung, Z. Qiu, Z. Yin, A. Trehan, H. Fang, B. Pearce, Z. Yang, L. Zadjura, C. J. D'Arienzo, K. Riccardi, P. Y. Shi, T. P. Spicer, Y. F. Gong, M. R. Browning, S. Hancel, K. Santone, J. Barker, T. Coulter, P. F. Lin, N. A. Meanwell and J. F. Kadow, *Med. Chem. Lett.*, 2013, **23**, 203–208.
68 K. S. Yeung, Z. Qiu, Z. Yang, L. Zadjura, C. J. D'Arienzo, M. R. Browning, S. Hansel, X. S. Huang, B. J. Eggers, K. Riccardi, P. F. Lin, N. A. Meanwell and J. F. Kadow, *Bioorg. Med. Chem. Lett.*, 2013, **23**, 209–212.
69 N. Zhang, X. Zhang, J. Zhu, A. Turpoff, G. Chen, C. Morrill, S. Huang, W. Lennox, R. Kakarla, R. Liu, C. Li, H. Ren, N. Almstead, S. Venkatraman, F. G. Njoroge, Z. Gu, V. Clausen, J. Graci, S. P. Jung, Y. Zheng, J. M. Colacino, F. Lahser, J. Sheedy, A. Mollin, M. Weetall, A. Nomeir and G. M. Karp, *J. Med. Chem.*, 2014, **57**, 2121–2136.
70 G. Cihan-Üstündağ, E. Gürsoy, L. Naesens, N. Ulusoy-Güzeldemirci and G. Çapan, *Bioorg. Med. Chem.*, 2016, **24**, 240–246.
71 J. T. Randolph, C. A. Flentge, P. Donner, T. W. Rockway, S. V. Patel, L. Nelson, D. K. Hutchinson, R. Mondal, N. Mistry, T. Reisch and T. Dekhtyar, *Bioorg. Med. Chem. Lett.*, 2016, **26**, 5462–5467.
72 D. Dressen, A. W. Garofalo, J. Hawkinson, D. Hom, J. Jagodzinski, J. L. Marugg, M. L. Neitzel, M. A. Pleiss, B. Szoke, J. S. Tung and D. W. Wone, *J. Med. Chem.*, 2017, **50**, 5161–5167.
73 C. Gibson, T. Tradler, K. Schnatbaum, J. Pfeifer, E. Locardi, D. Scharn, M. Paschke, U. Reimer, U. Richter, G. Hummel, U. Reineke, *WO Pat.*, PCT WO 2008116620, 2008.
74 C. Gibson, K. Schnatbaum, T. Tradler, J. Pfeifer, D. Scharn, U. Reimer, U. Richter, G. Hummel, U. Reineke, E. Locardi, M. Paschke, *WO Pat.*, PCT WO 2010031589, 2010.
75 C. Bolea, *WO Pat.*, PCT WO 2010079239, 2010.
76 M. Sakagami, H. Hashizume, S. Tanaka, T. Okuno, H. Yari, K. Tonogaki, N. Kouyma, *WO Pat.*, PCT WO 2009131096, 2009.
77 G. D. Glick, A. R. Hurd, C. B. Taylor, C. A. Vanhuis, *WO Pat.*, PCT WO 2012078874, 2012.
78 W. Mingchun and L. Qingyi, *CN Pat.*, CN 116655536A, 2023.
79 L. Rooney, A. Vidal, A. M. D'Souza, N. Devereux, B. Masick, V. Boissel, R. West, V. Head, R. Stringer, J. Lao and M. J. Petrus, *J. Med. Chem.*, 2014, **57**, 5129–5140.
80 J. Nan, J. Liu, G. Lin, S. Zhang, A. Xia, P. Zhou, Y. Zhou, J. Zhang, J. Zhao, S. Zhang, C. Huang, Y. Wang, Q. Hu, J. Chen, M. Xiang, X. Yang and S. Yang, *J. Med. Chem.*, 2023, **66**, 3460–3483.
81 L. Crocetti, I. A. Schepetkin, A. Cilibrizzi, A. Graziano, C. Vergelli, D. Giomi, A. I. Khlebnikov, M. T. Quinn and M. P. Giovannoni, *J. Med. Chem.*, 2013, **56**, 6259–6272.
82 H. Fujiwara, S. Mizumoto, Y. Kubo, H. Nakada, S. Hagiwara, Y. Baba, T. Tamura, H. Kuniyoshi, T. Masuko and M. Yamamoto, *JP Pat.*, JP 2013136535, 2013.
83 F. Padilla, N. Bhagirath, S. Chen, E. Chiao, D. M. Goldstein, J. C. Hermann, J. Hsu, J. J. Kennedy-Smith, A. Kuglstatter, C. Liao, W. Liu, L. E. Lowrie, K. C. Luk, S. M. Lynch, J. Menke, L. Niu, T. D. Owens, C. O-Yang, A. Railkar, R. C. Schoenfeld, M. Slade, S. Steiner, Y. C. Tan, A. G. Villasenor, C. Wang, J. Wanner, W. Xie, D. Xu, X. Zhang, M. Zhou and M. C. Lucas, *J. Med. Chem.*, 2013, **56**, 1677–1692.
84 A. R. Hurd, D. J. Skalitzky, C. B. Taylor, P. L. Toogood and C. A. Van Huis, *WO Pat.*, PCT WO 2013185045, 2013.
85 L. N. Casillas, S. J. Chakravorty, A. K. Charnley, P. Eidam, P. A. Haile, T. V. Hughes, J. U. Jeong, J. Kang, S. A. Lakdawala, L. K. Leister, R. W. Marquis, N. A. Miller, D. J. Price, C. L. Sehon, G. Z. Wang and D. Zhang, *WO Pat.*, PCT WO 2011120025, 2011.
86 V. K. Patel and S. Swanson, *WO Pat.*, PCT WO 2005073217, 2005.
87 K. B. Goodman, H. Cui, S. E. Dowdell, D. E. Gaitanopoulos, R. L. Ivy, C. A. Sehon, R. A. Stavenger, G. Z. Wang, A. Q. Viet, W. Xu, G. Ye, S. F. Semus, C. Evans, H. E. Fries, L. J. Jolivette, R. B. Kirkpatrick, E. Dul, S. Khandekar, T. Yi, D. K. Jung, L. L. Wright, G. K. Smith, D. J. Behm, C. P. Doe, R. Bentley, E. Hu and D. Lee, *J. Med. Chem.*, 2007, **50**, 6–9.
88 D. Lee and K. B. Goodman, *WO Pat.*, PCT WO 2005082890, 2005.
89 C. A. Sehon, G. Z. Wang, A. Q. Viet, K. B. Goodman, S. E. Dowdell, P. A. Elkins, S. F. Semus, C. Evans, L. J. Jolivette, R. B. Kirkpatrick, E. Dul, S. S. Khandekar, T. Yi, L. L. Wright, G. K. Smith, D. J. Behm, R. Bentley, C. P. Doe, E. Hu and D. Lee, *J. Med. Chem.*, 2008, **51**, 6631–6634.
90 N. D. Smith, S. P. Govek, M. Kahraman, J. D. Julien, J. Y. Nagasawa, K. L. Douglas, C. Bonnefous and A. G. Lai, *WO Pat.*, PCT WO 2013142266, 2013.
91 S. Usui, T. Takada and Y. Nishio, *JP Pat.*, JP 2014166961, 2014.
92 M. Calderini, M. Wucherer-Plietker, U. Graedler and C. Esdar, *WO Pat.*, PCT WO 2011006567, 2011.
93 B. S. Sathe, V. A. Jagtap, S. D. Deshmukh and B. V. Jain, *Int. J. Pharm. Sci.*, 2011, **3**, 220–222.
94 B. D. Varpe and S. B. Jadhav, *Int. J. Pharm. Invest.*, 2021, **11**, 189–194.
95 A. J. Ayoub, G. A. El-Achkar, S. E. Ghayad, L. Hariss, R. H. Haidar, L. M. Antar, Z. I. Mallah, B. Badran, R. Grée, A. Hachem, E. Hamade and A. Habib, *Int. J. Mol. Sci.*, 2023, **24**, 10399.

96 T. Fuchigami, *Phosphorus, Sulfur Relat. Elem.*, 1997, **120**, 343–344.
97 Z. Wang, C. Yi, K. Chen, T. Wang, K. Deng, C. Jin and G. Hao, *Eur. J. Med. Chem.*, 2022, **228**, 114025.
98 P. Limpachayaporn, B. Riemann, K. Kopka, O. Schober, M. Schäfers and G. Haufe, *Eur. J. Med. Chem.*, 2013, **64**, 562–578.
99 H. Wang, Y. Wang, S. Liu, Y. Mai, X. Zong, H. Gao, R. Hu, X. Jiang and Y. Y. Yeung, *Adv. Synth. Catal.*, 2019, **361**, 5334–5339.
100 S. Crosignani, S. Cauwenberghs, F. Deroose and G. Driessens, *WO Pat.*, PCT WO2015067782, 2015.
101 M. Chochkova, B. Stoykova, G. Ivanova, A. Ranz, X. Guo, E. Lankmayr, T. Milkova and J. Fluor, *Chem*, 2013, **156**, 203–208.
102 Q. Meng, B. Zhao, Q. Xu, X. Xu, G. Deng, C. Li, L. Luan, F. Ren, H. Wang, H. Xu and Y. Xu, *Bioorg. Med. Chem. Lett.*, 2012, **22**, 2794–2797.
103 K. Sato, H. Sugimoto, K. Rikimaru, H. Imoto, M. Kamaura, N. Negoro, Y. Tsujihata, H. Miyashita, T. Odani and T. Murata, *Bioorg. Med. Chem.*, 2014, **22**, 1649–1666.
104 S. Nomura, Y. Yamamoto, Y. Matsumura, K. Ohba, S. Sakamaki, H. Kimata, K. Nakayama, C. Kuriyama, Y. Matsushita, K. Ueta and M. Tsuda-Tsukimoto, *ACS Med. Chem. Lett.*, 2014, **5**, 51–55.
105 X. Li, D. Bai, H. Dong, Y. Chen and F. He, *WO Pat.*, PCT WO2023116862 A1, 2023.
106 A. Lantermann, E. L. P. Chekler, D. Blom, K. M. Couto, B. A. Lefker and D. B. Kitchen, *WO Pat.*, PCT WO2023049438A1, 2023.
107 G. Semple, C. Averbuj, P. J. Skinner, T. Gharbaoui and Y. J. Shin, *WO Pat.*, PCT WO 2004032928, 2004.
108 B. Pelcman, A. Sanin and P. Nilsson, *WO Pat.*, PCT WO 2006032851, 2006.
109 B. Pelcman, A. Sanin, P. Nilsson, T. Boesen, S. B. Vogensen, H. Kromann and T. Groth, *WO Pat.*, PCT WO 2007045868, 2007.
110 S. N. Haydar, H. Bothmann, C. Ghiron, L. Maccari, I. Micco, A. Nencini and R. Zanaletti, *WO Pat.*, PCT WO 2010009290, 2010.
111 A. A. Trabanco-Suarez, H. J. M. Gijsen, M. L. M. Van Gool, J. A. Vega Ramiro and F. Delgado-Jimenez, *WO Pat.*, PCT WO 2012117027, 2012.
112 C. Gege, O. Kinzel, C. Steeneck, G. Kleymann and T. Hoffmann, *WO Pat.*, PCT WO 2014023367, 2014.
113 K. Ahn, M. Boehm, S. Cabral, P. A. Carpino, K. Futatsugi, D. Hepworth, D. W. Kung, S. Orr and J. Wang, *WO Pat.*, PCT WO 2013150416, 2013.
114 C. Zhou, W. Zou, Y. Hua and Q. Dang, *WO Pat.*, PCT WO 2013040790, 2013.
115 Q. Dang, C. Zhou, W. Zou and Y. Hua, *WO Pat.*, PCT WO 2013043624, 2013.
116 S. K. Dodd, P. Furet, R. M. Grotzfeld, D. B. Jones, P. Manley, A. Marzinzik, X. F. A. Pelle, B. Salem and J. Schoepfer, *WO Pat.*, PCT WO 2013171639, 2013.
117 P. Furet, R. M. Grotzfeld, D. B. Jones, P. Manley, A. Marzinzik, X. F. A. Pelle, B. Salem and J. Schoepfer, *WO Pat.*, PCT WO 2013171642, 2013.
118 R. M. Claramunt, C. Lopez, C. Perez-Medina, M. Perez-Torralba, J. Elguero, G. Escames and D. Acuna-Castroviejo, *Bioorg. Med. Chem.*, 2009, **17**, 6180–6187.
119 T. M. Ballard, Z. K. Groebke, E. Pinard, T. Ryckmans and H. Schaffhauser, *WO Pat.*, PCT WO 2015044072, 2015.
120 S. B. Hoyt, J. A. Taylor, C. London, Y. Xiong and A. J. Cooke, *WO Pat.*, PCT WO 2014099833, 2014.
121 I. P. Buchler, M. J. Hayes, S. G. Hegde, S. L. Hockerman, D. E. Jones, S. W. Kortum, J. G. Rico, R. E. Tenbrink and K. K. Wu, *WO Pat.*, PCT WO 2009106980, 2009.
122 S. Lin, L. Xu, E. Metzger, E. R. Parmee and S. D. Debenham, *WO Pat.*, PCT WO 2010098994, 2010.
123 G. Henkel, M. Liu and T. Neuberger, *WO Pat.*, PCT WO 2009145814, 2009.
124 R. M. Claramunt, C. López, A. López, C. Pérez-Medina, M. Pérez-Torralba, I. Alkorta, J. Elguero, G. Escames and D. Acuña-Castroviejo, *Eur. J. Med. Chem.*, 2011, **46**, 1439–1447.
125 A. Kousaxidis, A. Petrou, P. Rouvim, P. Bodo, M. Stefek, I. Nicolaou and A. Geronikaki, *J. Mol. Struct.*, 2023, **1271**, 134116.
126 A. Mallia, M. Nguyen, J. Sloop, N. Forlemu and J. Undergrad, *Chem. Res.*, 2023, **22**, 22.
127 K. M. Short, M. A. Estiarte, S. M. Pham, D. C. Williams, L. Igoudin, S. Dash, N. Sandoval, A. Datta, N. Pozzi, E. Di Cera and D. B. Kita, *Eur. J. Med. Chem.*, 2023, **246**, 114855.
128 J. O. Witt, A. L. McCollum, M. A. Hurtado, E. D. Huseman, D. E. Jeffries, K. J. Temple, H. C. Plumley, A. L. Blobaum, C. W. Lindsley and C. R. Hopkins, *Bioorg. Med. Chem. Lett.*, 2016, **26**, 2481–2488.
129 S. N. Mistry, J. Shonberg, C. J. Draper-Joyce, C. Klein Herenbrink, M. Michino, L. Shi, A. Christopoulos, B. Capuano, P. J. Scammells and J. R. Lane, *J. Med. Chem.*, 2015, **58**, 6819–6843.
130 M. Marcinkowska, M. Kołaczkowski, K. Kamiński, A. Bucki, M. Pawłowski, A. Siwek, T. Karcz, B. Mordyl, G. Starowicz, P. Kubowicz, E. Pękala, A. Wesołowska, J. Samochowiec, P. Mierzejewski and P. Bienkowski, *Eur. J. Med. Chem.*, 2016, **124**, 456–467.
131 T. E. Ali and R. M. Abdel-Rahman, *J. Sulfur Chem.*, 2014, **35**, 399–411.
132 J. F. Ge, Q. Q. Zhang, J. M. Lu, M. Kaiser, S. Wittlin, R. Brun and M. Ihara, *MedChemComm*, 2012, **3**, 1435–1442.
133 R. Aslanian, X. Zhu, H. A. Vaccaro, N. Y. Shih, J. J. Piwinski, S. M. Williams and R. E. West, *Bioorg. Med. Chem. Lett.*, 2008, **18**, 5032.
134 C. Ojeda-Gómez, H. Pessoa-Mahana, P. Iturriaga-Vásquez, C. D. Pessoa-Mahana, G. Recabarren-Gajardo and C. Méndez-Rojas, *Arch. Pharm.*, 2014, **347**, 174–184.
135 Y. Xiong, J. S. K. Choi, B. M. Smith, S. Strah-Pleynet and B. Teegarden, *WO Pat.*, PCT WO 2008054748, 2008.
136 H. M. Elokdah, A. A. Greenfield, K. Liu, R. E. McDevitt, G. R. McFarlane, C. Grosanu, J. R. Lo, Y. Li,

A. J. Robichaud and R. C. Bernotas, *US Pat.*, US 20070037802, 2007.

137 K. Mizuno, J. Ikeda, T. Nakamura, M. Iwata, H. Otakaand and N. Goto, *JP Pat.*, JP 2014133739, 2014.

138 A. Pennell, J. Aggen, J. J. Wright, S. Sen, B. McMaster, D. Dairaghi, W. Chen and P. Zhang, *US Pat.*, US 20050256130, 2005.

139 A. Pennell, J. Aggen, J. J. Wright, S. Sen, B. McMcmaster, D. Dairaghi, W. Chen and P. Zhang, *US Pat.*, US 20060106218, 2006.

140 P. Zhang, A. M. K. Pennell, J. K. J. Wright, W. Chen, M. R. Leleti, Y. Li, L. Li, Y. Xu, M. M. Gleason, Y. Zeng and K. L. Greenman, *US Pat.*, US 20080058341, 2008.

141 P. Zhang, A. M. K. Pennell, J. K. Wright, W. Chen, M. R. Leleti, Y. Li, L. Li, Y. Xu, M. M. Gleason, Y. Zeng, K. L. Greenman, *WO Pat.*, PCT WO 2008147822 A1, 2008.

142 N. P. Barton, H. Hobbs, S. T. Hodgson, Y. M. L. Lacroix, P. A. Procopiou, CC.chemokine receptor 4 antagonists, *WO Pat.*, WO 2012025473, 2012.

143 P. A. Procopiou, J. W. Barrett, N. P. Barton, M. Begg, D. Clapham, R. C. Copley, A. J. Ford, R. H. Graves, D. A. Hall, A. P. Hancock, A. P. Hill, H. Hobbs, S. T. Hodgson, C. Jumeaux, Y. M. L. Lacroix, A. H. Miah, K. M. L. Morriss, D. Needham, E. B. Sheriff, R. J. Slack, C. E. Smith, S. L. Sollis and H. Staton, *J. Med. Chem.*, 2013, **56**, 1946–1960.

144 K. Hata, M. Masuda, H. Nakai, D. Taniyama, H. Tobinaga, A. Hato and M. Fujo, *WO Pat.*, PTC WO 2013061977, 2013.

145 K. Hata, M. Masuda, H. Nakai, D. Taniyama, H. Tobinaga, A. Hato and M. Fujo, *JP Pat.*, JP 2014224104, 2014.

146 Y. K. Lee, D. J. Parks, T. Lu, T. V. Thieu, T. Markotan, W. Pan, D. F. McComsey, K. L. Milkiewicz, C. S. Crysler, N. Ninan, M. C. Abad, E. C. Giardino, B. E. Maryanoff, B. P. Damiano and M. R. Player, *J. Med. Chem.*, 2008, **51**, 282–297.

147 A. Katsifis, C. J. R. Fookes, T. Q. Pham, I. D. Greguric, M. F. P. S. Mattner, *WO Pat.*, PCT WO 2008022396A1, 2008.